THE UREA PROCESS FOR UO_2 PRODUCTION

PROEFSCHRIFT

TER VERKRIJGING VAN DE GRAAD VAN DOCTOR IN DE TECHNISCHE WETENSCHAPPEN AAN DE TECHNISCHE HOGESCHOOL TE DELFT OP GEZAG VAN DE RECTOR MAGNIFICUS IR. H. J. DE WIJS, HOOGLERAAR IN DE AFDELING DER MIJNBOUWKUNDE, VOOR EEN COMMISSIE UIT DE SENAAT TE VERDEDIGEN OP WOENSDAG 1 JULI 1964 DES NAMIDDAGS TE 4 UUR

DOOR

MARIE EGIDIUS ANTONIUS HERMANS
scheikundig ingenieur

geboren te Brunssum (L.)

W. D. MEINEMA N.V. - DELFT

DIT PROEFSCHRIFT IS GOEDGEKEURD DOOR DE PROMOTOREN
PROF. DR. J. H. DE BOER EN PROF. DR. J. J. WENT

Aan mijn ouders

Aan mijn vrouw

The investigations described in this thesis have been carried out in the KEMA-laboratories at Arnhem, Netherlands, under the auspices of the Euratom-RCN-KEMA Reactor Development Group

CONTENTS

INTRODUCTION

A nuclear homogeneous suspension reactor requires a fuel with quite specific properties. This is especially true when the principle of fission recoil separation is used for a continuous removal of the fission products [1].

As the work described here is part of the development of the KEMA Suspension Test Reactor (KSTR) at Arnhem, a description of the main principles of this reactor is given first [2]. The main purpose of this reactor will be to investigate the applicability of aqueous fuel suspensions to nuclear power reactors. Therefore it will be more or less an instrument to study a process. The KSTR is meant to be a 250 kW suspension reactor operating at a total pressure of 60 atms and with a maximum temperature of about 250 °C. The main circuit will consist of the reactor vessel with a volume of 16 to 20 liters, a canned rotor pump and a heat exchanger. Through this primary system a suspension will be circulated. The reactor vessel will be surrounded by a BeO-graphite reflector, to reduce the critical volume and to flatten the flux. Some important details of the reactor are enumerated below:

1. The combined system of moderator and fuel will be composed of an aqueous suspension of a uranium compound (4 volume per cent of $UO_2 \cdot ThO_2$ in light water). The temperature of the reactor will be controlled by the concentration of the fuel. For this purpose fuel can be collected outside the primary circuit by means of a side stream which can be passed through a hydrocyclone with a collecting vessel underneath. Material can also be introduced into the main system from this latter vessel.
2. The fission products originating from the fission of the uranium nuclei poison the reactor by neutron absorption. It is therefore advantageous to remove them as completely as possible. The kinetic energy of the heavy fission fragments is such that their range in UO_2 is about 5 microns, as was demonstrated in a preceding near critical experiment [3]. However, at the time when the preparation of the fuel for this experiment was started, the range was assumed to be 10 microns, as stated in literature [4].

If all the particles are smaller than this range and homogeneously distributed in the water phase, all the fission products will leave the UO_2 in first instance. The suspension should, therefore, be well dispersed to prevent the trapping of fission fragments in neighbouring particles and to preserve the maximum

separation yield. This high degree of dispersion can be attained in a colloid chemically stable suspension.

Preliminary experiments seemed to indicate that for 13 micron particles, still 90 percent of the fission products leave the particles [5, 6]. This size was therefore accepted as the upper limit for the fuel particles during the first stages of development.

3. Because the fuel has to be separated in a hydrocyclone, 4 microns was chosen as the lower limit of the particle size in order to obtain a good separation efficiency. Recently it was demonstrated in high temperature loops that even 2 microns is acceptable.
4. Although ultimately ThO_2 with 15 percent highly enriched uranium oxide will be used in the KSTR, in order to be able – in a future power reactor – to convert ^{232}Th into the fissile ^{233}U, it was necessary to start the project with UO_2 enriched to 20 percent ^{235}U. The degree of enrichment was dictated by the requirement to work at the same volume concentration (4 percent) which is desirable for a large power reactor. The highest enrichment of uranium at that time available was 20%. This is too low to prepare the 15% $UO_2 \cdot 85\%$ ThO_2 fuel and still have the right concentration of ^{235}U.

UO_2 is preferred to UO_3 because in the latter case hydrothermal growth occurs at temperatures around 250 °C, as has been shown by experiments in our laboratory and elsewhere [7].

Such growth is inadmissable in view of the fission recoil separation required. The use of U_3O_8 as a fuel seemed unattractive because this might induce rather strict requirements for the oxygen overpressure in the system in order to prevent oxidation or reduction. In UO_2 no hydrothermal changes were observed. Oxidation, and thus phase transition, does not occur in an oxygen-free hydrogen atmosphere.

5. Apart from the reason given under 4, hydrogen has been chosen as a pressurizing gas to prevent boiling in the system, because it has several advantages:

a. the radiolytic decomposition of the water is expected to be suppressed by hydrogen, which means that a lower oxygen concentration can be expected to build up in the liquid. Thus the possibility of UO_2 oxidation might become less serious.
b. the radiolytic gas is diluted to such an extent that the composition of the total gas mixture (including the water vapour) is beyond the explosion limits.
c. though no exact data are available on the corrosion of stainless steel under the conditions of high temperature, high pressure and radiation, it is generally accepted that hydrogen may prevent stress corrosion to a large extent.

6. From early experiments it appeared that the hydrolyzable fission products (such as the Rare Earths) which leave the particles by recoil are converted into oxides or hydroxides at 250 °C. These attach themselves to any surface present, and in particular very strongly to the uranium oxide particles. A competing adsorber [5], therefore, is added to the suspension to reduce the adsorption onto the UO_2. For this purpose specially treated active carbon has been suggested. The carbon (containing the fission products) will be separated from the UO_2 in an elutriator or a special hydrocyclone, where it will leave with the overflow stream and will be fed to an evaporator. From this it will be discarded as waste after concentration.
7. The fission products that are soluble at the working pH, remain in the water phase, and will therefore be fed to the evaporator with the same stream which carries the carbon.
8. The volatile and gaseous fission products will be stripped from the suspension directly after leaving the reactor vessel. The hydrogen mentioned under 4 will also serve this purpose. A decay vessel, providing an outside volume, will cause the concentration of these fission products inside the reactor to be relatively small, thus decreasing the poisoning level. A schematic diagram of the KSTR is presented in FIG. 1.

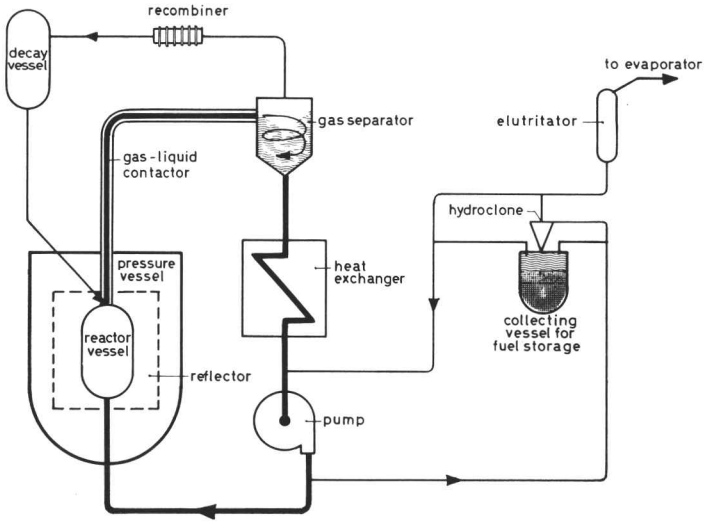

FIG. 1 Schematic diagram of the main system of the Kema Suspension Test Reactor.

In the development of the KSTR four stages may be distinguished:

1. The rheological behaviour of the suspension in different components of the system and especially in the reactor vessel was studied in full size plexiglas models.

2. A subcritical assembly at low temperature (20–80 °C) was completed early in 1958 [8, 9]. In principle it contains the full size core vessel of the KSTR, a collecting device and full instrumentation to measure and control temperature, flow velocity, fuel concentration and neutron flux.

Either of two external neutron sources can be used for the subcritical experiments:

a. a radium-beryllium neutron source;
b. a linear accelerator tube, providing the fast deuterium ions for the neutron generating (*d*, *d*) reaction.

The fuel consists of a 2 volume percent suspension of uranium dioxide, 20 percent enriched in ^{235}U. This subcritical assembly has been constructed for carrying out reactor kinetic measurements and to study the influence of rheological properties on the reactor behaviour. The assembly can be and has been used very near to criticality ($k > 0.995$).

3. In the third stage, high temperature – high pressure loops are being used for evaluating and testing reactor components and for the investigation of corrosion, erosion and attrition of the suspension system.
4. Finally, the KSTR will be constructed using the data obtained in former stages. It is intended to test the reactor as a subcritical assembly at high temperature and high pressure, first with UO_2 as a fuel and then with compound particles of ThO_2 and UO_2. At a higher specific power density only the $UO_2 \cdot ThO_2$ compound particles will be used as a fuel because under these conditions caking might occur with UO_2. Furthermore the $UO_2 \cdot ThO_2$ fuel is the important one, because only with the ^{232}Th–^{233}U cycle the breeding point can be used in a large homogeneous reactor. The first two stages, as mentioned under 3 above, have now been finished, loop experiments are going on, and the KSTR is in its construction phase.

The aim of the construction of the KSTR is to obtain a tool for physicists and chemists to investigate the behaviour and the use of suspensions as reactor fuels under power reactor conditions and to study possible methods for the removal of corrosion and fission products in such a reactor system.

For the experiments with the subcritical assembly and the loops, UO_2-powders with the following specific properties were required:

1. The particle size should be limited to a range between 4 and 13 microns. At a later stage these figures may be made somewhat lower, as the separation efficiency of the hydrocyclone is high enough, and because a further gain in the recoil separation effect is both possible and desirable.
2. To minimize the erosion of the circuit, the particles should have a more or less spherical shape or at least they should have a smooth outer surface.
3. The specific surface area of the particles should be small in view of the possible adsorption of fission products. A specific area of less than 0.1 m^2

per gram was chosen. This value corresponds to the geometric surface area of spheres of 6 microns diameter.

4. The fuel particles should be able to withstand pumping under reactor conditions for extended periods of time without considerable attrition or fracturing occurring.
5. Expectedly, the fuel must be exposed to sufficiently high temperatures during its preparation, in order to decrease the chance of caking.
6. A process ought to be used which requires no, or at the utmost a very simple recycle for rejected material, especially because only a limited amount of enriched uranium was available for our subcritical experiments. This is necessary for reasons of efficiency and health precaution.
   In enriching the content of the fissile ^{235}U in natural uranium, use is made of the difference in diffusion rate of the different isotopes of uranium. To this purpose the gas UF_6 diffuses through Teflon membranes. During this diffusion process the hazardous α-emitting isotope ^{234}U, which is present in natural uranium in very small quantities, is more enriched than ^{235}U. The health precautions to be taken are mainly caused by the increased amount of ^{234}U isotope, present in enriched uranium.

The purpose of the work described in this thesis was:

1. to develop a process for preparing UO_2-powder of the required specifications;
2. to study the size distribution of the powders as a function of process variables;
3. to investigate the chemical reactions involved.

Although the work was primarily directed towards application of the process for the Suspension Reactor Project, some of the results are of a more general interest, either in the field of nuclear fuels and of uranium chemistry, or outside the uranium field. Examples of the latter are the particle growth by controlled flocculation discussed in CHAPTER II and the hydrolytic reactions during the precipitation described in CHAPTER VI. Both phenomena occur most certainly with other cations, and they can be applied to achieve certain technical objectives.

In the field of nuclear fuel the urea process has the distinct advantage that extremely reproducible products are obtained, provided that the conditions are chosen judiciously. Therefore a better understanding of the process was required than was available at that time. From this point of view again, the work described in this thesis seems to be fully justified.

CHAPTER I

THE PREPARATION OF UO_2

I.1 Introduction

Because of the great importance of UO_2 as a nuclear fuel, extensive studies have been made of its preparation, especially regarding the technological aspects of possible production methods. The structural and physical properties of UO_2 powders depend largely on their method of preparation. Hence, the method of preparation is chosen with a view on the way the UO_2 will be used. However, only a very limited amount of work has been carried out elsewhere on powders for aqueous fuel suspensions.

UO_2 can be prepared from uranium metal or uranium hydride by controlled oxidation with steam or air, or by the reduction of U(VI) compounds with hydrogen or with ammonia, or electrolytically. Methods starting from uranium metal or uranium hydride were considered to be unsatisfactory because the elaborate metal production process would complicate the fuel preparation. They will not be discussed here.

The starting materials generally used for the UO_2 preparation are:
1. higher uranium oxides or their hydrates;
2. uranium peroxide;
3. ammonium diuranate;
4. uranyl oxalate.

These materials are reduced to UO_2 – sometimes after calcination – at temperatures ranging from 500 °C to 1000 °C. They can be sintered or fused if required.

In the past years, an electrolytic reduction method has been developed for preparing UO_2 monocrystals from a UO_2Cl_2 melt [10, 11].

A survey of the various preparation methods will now be given in more detail.

I.2 Methods of preparation

I.2.1 Preparation of UO_2 by the reduction of higher oxides

The reduction of U_3O_8 or UO_3 (hydrates) is generally performed with hydrogen [12], ammonia [13] or a mixture of hydrogen and nitrogen [14].

Depending on the reactivity of the required powder, the reduction temperatures vary between 500 °C and 1000 °C.

The oxides to be reduced can be:

1. U_3O_8. This is obtained by calcination of any uranium compound in air at about 700 °C.
2. UO_3. Though this compound results from calcination of many uranium compounds at about 300 °C in air, it is generally prepared by denitration of uranyl nitrate hexahydrate [15, 16].
   This latter salt melts in its own hydration water at 78 °C and decomposes at higher temperatures. At about 300 °C in air a fairly pure UO_3 is obtained which, however, contains some residual nitrate and water. Most commercially available UO_2 is produced by reduction of such UO_3. Particle size and particle form are strongly influenced by small variations in the denitration method.
3. UO_3 hydrates. UO_3 hydrates can be grown hydrothermally in sizes ranging from fourty to several hundred microns. After reduction with hydrogen at 1700 °C, they yield a very dense UO_2 (pseudomorphic with UO_3 hydrate) which is used in matrix type fuel elements [17].

I.2.2 Preparation of UO_2 via uranium peroxide

As it seems to be an open question whether the peroxide is a simple UO_4 hydrate or a $UO_3 \cdot H_2O_2$-hydrate, it is considered separately here.

When a hydrogen peroxide solution is added to a uranyl nitrate solution, maintaining the pH at about 2 to 3, a yellow precipitate is formed: the (hydrated) uranium peroxide [18]. The overall reaction can be written

$$UO_2(NO_3)_2 + H_2O_2 + nH_2O \rightarrow UO_4 \cdot nH_2O + 2\,HNO_3$$

The acid formed has to be neutralized by ammonia. The filterability of the precipitate depends strongly on the concentrations, pH and temperature of the precipitation. The peroxide product decomposes and evolves oxygen above 60 °C. Generally the reduction is carried out after calcination to UO_3 at 300–400 °C [19].

I.2.3 Preparation of UO_2 via ammonium diuranate

It should clearly be stated that it is very doubtful whether material known as ammonium diuranate and obtained with any of the methods described in the literature has the composition $(NH_4)_2U_2O_7$. Results from the work described in this thesis lead to the opinion that a dihydrated UO_3 results in which part of the water may have been replaced by ammonia. The standard indication "ADU" for any uranium precipitate obtained with any form of ammonia may indicate the uncertainty about the real composition of the product. When

ammonium hydroxide is added to a uranyl solution, a precipitate is obtained if the conditions of pH, concentration and temperature are correct. The composition of the precipitate depends essentially on the ultimate pH in the process [20].

Three methods of adding ammonia are used:

1. NH_3 or NH_4OH is added directly as such. The precipitate consists of irregular particles showing a crystalline habit. The size distribution is usually very wide.
2. Urea can be added as an ammonia donor [21]. A relatively low pH and an increased temperature cause the urea to hydrolyse, according to

$$CO(NH_2)_2 + 3\,H_2O \rightarrow 2\,NH_4OH + CO_2\uparrow$$

   Simultaneously the pH rises to the point of precipitation. The precipitate consists of polycrystalline spherical particles of 70 to 150 microns.
3. Ammonium carbonate can be used as a donor [22]. The ammonium uranyl carbonate formed in solution decomposes at increased temperatures and "ADU" is precipitated. Again polycrystalline spherical particles are obtained which are very uniform in size.

The products prepared by these methods are calcined and reduced with hydrogen or ammonia gas.

I.2.4 Preparation of UO_2 via uranyl oxalate

By combining stoichiometric amounts of partly neutralized uranyl nitrate and oxalic acid solutions at 90 °C uranyl oxalate is precipitated. The precipitate consists of small hexagonal crystals with a diameter of a few microns in a very close size range.

I.3 Technical methods used for UO_2 production

The large-scale methods in use for production or preparation of UO_2 powders are all modifications of one of the laboratory methods described above. These techniques can be divided into four groups, according to the specific use made of their products in reactor technology.

I.3.1 UO_2 powders for uranium metal fabrication

As UO_2 is an intermediate product in producing uranium metal, much technological work has been done to obtain it in the most suitable form for the next stage in the process, converting it into "green salt" (UF_4). Nearly all the uranium oxide of the natural isotopic uranium composition (called "natural" uranium) for this purpose is prepared by denitration of uranyl hexahydrate

to UO_3 and reduction to UO_2. In the United States this process has proved to be cheap and to yield a reliable product. Several technical variations are known:

1. By far the largest amounts of UO_3 have been prepared by batch denitration in stainless steel pots with powerful agitators [23]. A disadvantage of this method is the inhomogeneity of the product. The properties of the UO_3 obtained depend on the place where it is formed, *i.e.* on the pot wall, at the stirrer blades or somewhere in the bulk. The UO_2 obtained by reduction of the UO_3 shows corresponding variations. This inhomogeneity gives rise to many problems in the production of UO_2 fuel elements, for which those powders are also used.
2. In 1956 in the United States a plant came into operation based on continuous denitration [24]. The uranyl nitrate hexahydrate is fed into a horizontal heated trough. The contents are stirred and transported by a rotating agitator. The UO_2 powders resulting from the reduction of UO_3 consist of spheroids with an average diameter of 150 microns.
3. The latest production development since 1957 uses fluidized bed denitration in air [25]. A uranyl nitrate solution is sprayed onto UO_3 particles in a hot fluid bed. The particles thus produced show a laminar, onion like structure. They are 150–200 microns in diameter and spherical.

If enriched uranium has to be produced, the starting material is gaseous UF_6 supplied from the diffusion plant. The gas is hydrolyzed to ADU by feeding it into an ammonium hydroxide solution [26]. The crystallite size of the powder is controlled by the reaction rate.

In England the uranium metal production started with the precipitation of ADU [27]. Another process, using a fluidized bed denitration as a first step was chosen more recently [28]. A hydrogen peroxide precipitation is included in the process only for the purification of the starting uranyl solution. In France [29] and Belgium [30] the uranium peroxide was used as the first precipitate in the production of uranium metal. However, ADU-precipitation is preferred now [31].

I.3.2 UO_2 powders for ceramic elements

An ADU precipitate is usually employed as a starting material [32, 33] because of the good sintering behaviour of UO_2 obtained by low temperature reduction of such a precipitate. The precipitate can be obtained by the reaction of gaseous or dissolved ammonia with a warm uranyl solution. If a high reaction rate is chosen and if the reduction temperature of the product is low, a material is obtained ("ceramic grade" UO_2) which can be easily compacted and sintered. In the United States, UO_2 prepared by denitration is also used for

ceramic elements. At Aktiebolaget Atomenergi (Sweden) urea is used as an ammonia donor in a precipitation from homogeneous solution [21]. An "ADU" powder is obtained with spherical particles of 50 to 100 microns, consisting of crystallites a few microns in size. After calcination and reduction, a UO_2 product results which has very desirable properties in UO_2 pellet production [34].

I.3.3 UO_2 powders for dispersed and swaged fuel elements

For solid dispersed fuel elements hard, dense "pigment grade" UO_2 powders are used [35]. They are prepared by a slow reaction between ammonia and a uranyl solution, and reduction of the product at 1700 to 1800 °C. They are mixed with suitable metal powders and sintered into elements.

Another type of a UO_2 dispersion in metal is the matrix type element, where "sintered UO_2" is incorporated as a fuel in metal by rolling [36]. A coarse dense UO_2 powder of the ADU type is used. It is prepared by a fast reaction of uranyl ions with ammonia. The reduction is carried out at 1700–1800 °C.

The same "sintered UO_2" is used as a fuel in swaged elements, where a metal tube is filled with the UO_2 powder under vibration in order to obtain a high compaction. After the tube has been closed it is narrowed and elongated by circular hammering to reach a high bulk density of the powder inside the tube. A density of 95% of the theoretical one can be attained in a reproducible way.

Alternatively, electrolytically produced UO_2 has been proposed as a fuel material for swaged elements [11].

I.3.4 UO_2 powders for use in aqueous suspension reactors

No UO_2 powders have previously been prepared specially for use in an aqueous suspension reactor. However, attempts have been made to produce U_3O_8 or UO_3 powders which might be used as such, and which could be converted into UO_2 powders with similar physical properties.

The methods which were developed are all denitration techniques. A suitable uranyl solution is sprayed into a hot chamber where the water evaporates from the droplets and where the salt decomposes to UO_3 or U_3O_8. The off-gases, containing the particles, are scrubbed in a circulating stream of water or pass a COTTRELL precipitator. The only difference between the denitration processes is the method of heating the decomposition chamber. This can be done by dissolving the uranyl nitrate salt in acetone and igniting the acetone in the combustion chamber [37], by spraying an aqueous solution into an electrically heated chamber [38] or (for reasons of economy) to heat the chamber internally by the combustion of natural gas [39]. All products consist of particles of 1 micron or less.

I.4 Preparation of UO_2 powders for the KEMA subcritical assembly

No commercially available UO_2 powder was found which met the specifications stated in the INTRODUCTION, nor could an adequate method of preparation be obtained from the literature.

In order to avoid intricate classification procedures in the subsieve particle size range considered, it seemed highly preferable to develop a preparation technique by which particles of the right size range could be produced directly. Such particles could, however, be of any shape as modification methods like pneumatic grinding or superficial (or complete) melting might be used in a later stage of the process in order to smooth them. Similar methods are used for other high-melting materials.

It has been shown from previous work that a large number of uranium compounds exhibits pseudomorphic transitions during processes like calcination, reduction and sintering and, except for a certain degree of shrinkage, no alteration in the shape takes place. Therefore preference was given to a method where particles of the right shape could be obtained during the first step of the preparation.

I.4.1 The urea precipitation method

Precipitation from a homogeneous solution provides a method to prepare uranium containing powders of spherical form, as has been shown by Swedish investigations [21]. It was hoped that this precipitation technique, if thoroughly controlled, might lead to powder dimensions with a very narrow particle size distribution. The principle of this method is that the reagent (in this case ammonia) is not added directly to the uranyl nitrate solution, but is generated from a compound which can be added to the solution without causing precipitation. Urea is used as such an ammonia donor. Its rate of hydrolysis depends on the temperature of the solution and, to a lesser extent, on the pH. Good homogeneity assures that ammonia is formed evenly throughout the system. Due to the formation of ammonia, the pH of the solution rises slowly to a point where spontaneous nucleation occurs throughout the liquid. If the generation of ammonia can be controlled in such a way that any further nucleation is prevented, and if every particle has the same chance of growth, the result will be a precipitate with a very narrow size distribution. The ultimate size, in this case, is determined by the number of nuclei, which in turn depends on the reaction rate and the total amount of uranium present in the system.

These considerations were accepted as being valid in any case of precipitation from a homogeneous solution. They also led to the decision to study this technique for the preparation of the fuel for the suspension reactor. This work resulted in a new process which was used to produce the 20% enriched UO_2 for the subcritical assembly.

Procedure *

Due to health safety regulations the enriched uranyl nitrate solution was processed in batches of about 100 grams of 20% enriched uranium. All solutions used were first filtered to remove nuclei which could cause unwanted precipitation. One litre of a solution of uranyl nitrate and nitric acid (containing 0.40 mol uranium and 1.32 mol nitrate) were run into a 3 litre round bottom flask.

50 ml of a 25% ammonium hydroxide solution was then added to increase the pH to 2.6–3.0. The solution was vigourously stirred by a vibrational stirrer with a set amplitude, and heated to a temperature of 95 °C. At this temperature 500 ml of a warm solution, containing 250 grams of urea, was added. The temperature was kept at 95 °C throughout the complete process.

After about 50 minutes the precipitation started, and it was complete in another hour. The pH of the solution did not exceed 6.0. The precipitate was immediately filtered off, washed with cold water and dried with acetone or alcohol. The yield of the precipitation was better than 99.5%.

The dry precipitate was then fed to an electric furnace where it was reduced with hydrogen at 800 °C. The specific surface area of the product was reduced to the required value of less than 0.1 m^2/gram by sintering at 1250 °C in wet hydrogen. During both heat treatments the powder was slowly transported by vibration of the furnace tube in order to prevent serious agglomeration as far as possible.

Properties of the products

The resulting precipitate (mainly consisting of $UO_3 \cdot 2H_2O$) contained 68% U, 4.6% CO_2, 2.3% NH_3 and about 1% of urea.** The water content was 9–10%. The particles had a gel-like appearance (Fig. 2) and showed only a very diffuse X-ray pattern. The real density [40] of the precipitate was 4.2 and the bulk density 1.9. The particle size distribution, as determined by the settling velocity according to Stokes' law, was strictly geometric.

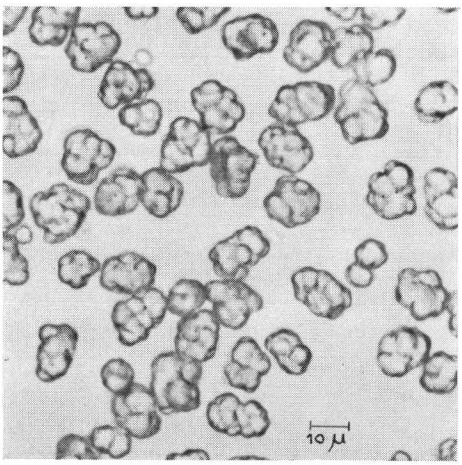

Fig. 2 Amorphous precipitate in the urea process.

* The valuable assistance of Mr. G. H. T. van Osch in the development of this process is gratefully acknowledged.

** The analytical procedures are presented in the appendix.

When the weight frequency of such a powder is plotted versus the logarithm of the particle size, a Gaussian probability curve is obtained. This distribution can therefore be described with two parameters: the geometric mean diameter d_g (50 weight percent of the powder being smaller than this size) and the geometric standard deviation σ_g (the size ratio between the 84% and 50% or the 50% and 16% limits). The cumulative weight curve of this size distribution is a straight line in a so called log-probability grid [41].

The geometric mean diameter d_g of the precipitate from the above described process was 15.2 microns * and the standard deviation σ_g was equal to 1.2.

After reduction at 800 °C in hydrogen and sintering at 1200 °C in wet hydrogen ** some agglomeration was observed which resulted in a rather wide particle size distribution ($d_g = 12.9\ \mu$, $\sigma_g = 1.33$). However, after a short period of pumping in the subcritical experiment, the agglomerates were broken down into the original particles. The size distribution was again geometric with a value of d_g of 10.6 μ and a value of σ_g of 1.2. The weight size distribution for both the sintered and the redispersed UO_2 fuel is shown in FIG. 3 (curves a and b respectively).

Because of the urgency of the subcritical experiments, the UO_2 powder thus produced was accepted as a fuel material before any improvement could be made, even though the particle size was still higher than required and the particles were not completely spherical. Electron micrographs showed, however, that the surface of the particles was smooth and without crystal edges.

A spectrographic analysis of the starting material and the final UO_2 fuel is given in TABLE I.1.

TABLE I.1 Spectrographic analysis of the starting material and the final UO_2 from the urea process.

	Starting material (ppm)	Final product (ppm)
Chromium	2	9
Iron	8	17
Manganese	2	5
Sodium	21	19
Silicon	> 30	> 50
Aluminium	> 75	22
Antimony	4	10
Molybdenum	2	0.4
Magnesium	> 40	8

* In CHAPTER II.3 we will see that this figure is dependent on the amplitude of the stirrer. The amplitude chosen for this preparation proved to be a very good one.

** This method has been in use in our laboratory since early 1954. The method has become common practice now and is called steam sintering [42].

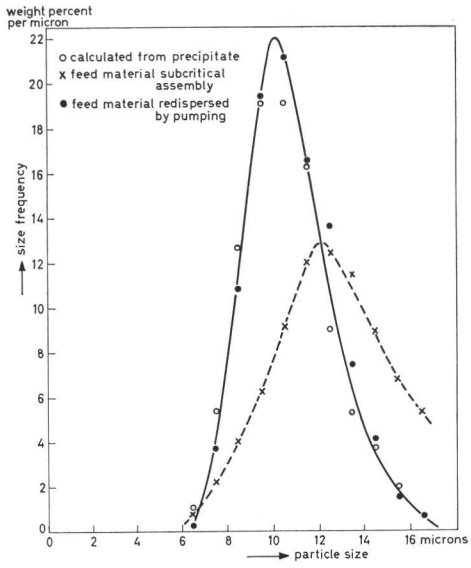

FIG. 3 Particle size distribution of UO_2 prepared with the urea process.

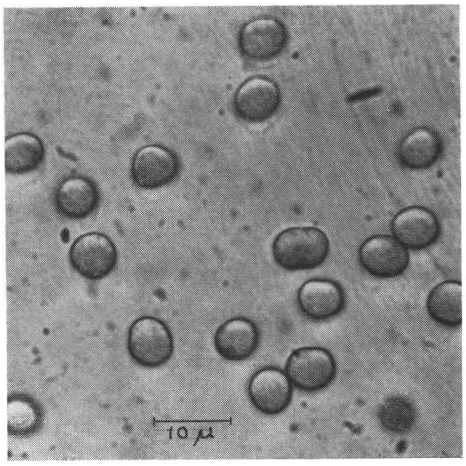

FIG. 4 Precipitate of the sulphate process.

I.4.2 The sulphate precipitation method

During the investigations of the urea precipitation method mentioned above, another procedure was discovered which showed a strong resemblance with a precipitation from homogeneous solution. From a clear solution of partly hydrolyzed uranyl nitrate a basic ammonium uranyl sulphate was precipitated by a slow hydrolytic reaction.

Procedure

2 grams of solid ammonium nitrate were added to 50 ml of an aqueous uranyl nitrate solution containing 10.5 grams of uranium and 79 milliequivalents of nitrate. After this had dissolved 34 ml of 1 N ammonia was added at a temperature of 20 °C. When the solution was not completely clear, it was filtered. Subsequently 5 grams of solid ammonium sulphate were added. A few seconds after the complete dissolution of the sulphate, a yellow precipitate began to form. This precipitate consisted of nearly spherical particles, very uniform in size. Progressing hydrolysis caused a slow decrease of the pH to about 2.9 and at the same time particle growth occurred by further precipitation. After one hour the precipitate was filtered off and dried.

A slight disadvantage of this process was its low yield. Only about 35% of the total uranium content was precipitated. The reprocessing, however, of the spent solution is rather simple.*

* Recently the process has been improved by Ir. F. J. KOCKEN from our laboratory. The particles have a better shape and the yield is higher than 80% now.

After preheating the precipitate at 150 °C, the sulphate was extracted by leaching with 2 N ammonium hydroxide at 45 °C. The suspension was again filtered and the precipitate dried. After reduction and sintering a satisfactory powder for use as a suspension fuel was obtained.

Properties of the product

The precipitate consisted of nearly spherical particles of a very narrow size distribution around 12 microns (FIG. 4) the density being 4.25. X-ray analysis showed a pattern, very similar to that of zippeite, which according to TRAILL [43] has a formula $(UO_2)_3\,(SO_4)_2\,(OH)_2 \cdot 8H_2O$ (Analysis: 60.5% U, 16.3% SO_4^{2-}) The chemical composition of our product, however, was definitely different: 65% U, 14% SO_4^{2-}, 2.7% NH_4^+.

After reduction and sintering a UO_2 powder was obtained with the same particle shape as the precipitate and with a sharp size distribution, the mean diameter being 8 microns and with a geometric standard deviation of 1.13.

CHAPTER II

THE PARTICLE SIZE DISTRIBUTION IN THE UREA PROCESS

II.1 Introduction

The particle size distribution of the UO_2 powder obtained by the urea process (described in CHAPTER I) influences the recoil separation efficiency that can be obtained in the suspension reactor. There are two reasons why it appeared to be necessary to investigate which parameters determine this size distribution:

1. The product should be prepared with a good reproducibility.
2. In the future it might be necessary to produce powders with other size ranges.

This holds both for suspension fuels and for powders used in the production of oxide fuel elements. Therefore a better insight in the phenomena governing the particle size distribution obtained in the process under consideration, may result in a better technological performance.

In this chapter the principle of the size distribution measurement and the characterization of the distribution will be discussed first. In practice a slightly different method of evaluating the size distribution data is used of which it is proved theoretically that correct results are obtained.

The mechanism proposed for the particle formation in the urea process is in accordance with the experimental results.

II.2 General considerations of size measurement and size distribution.

II.2.1 Measurement of the size distribution

Because it is the sedimentation velocity and not the absolute size of the particles that is most important in the hydrodynamic behaviour of the suspension it seemed to be appropriate to characterize the particles by their Stokes diameter assuming a spherical shape. Therefore a sedimentation method was chosen for the determination of the particle size distribution. Due to the small size of the samples required and to the simplicity of the measurement, the photo-extinction method [44] was used. The measuring apparatus was a Leitz sedimentometer constructed according to the principles of TELLE [45, 46].

A spherical particle settling under gravity in a stagnant liquid has, according to Stokes' law, a final vertical velocity

$$v = \frac{g \times d_p^2 \times \Delta\varrho}{18\eta} \quad \ldots\ldots\ldots\ldots\ldots\ldots\ldots\ldots\ldots\ldots \quad (1)$$

where g = acceleration of gravity; d_p = diameter of the particle; $\Delta\varrho$ = difference in density between solid (ϱ_s) and liquid (ϱ_l); η = viscosity of the liquid.

Usually g is expressed in cm/sec^2, d_p in cm, $\Delta\varrho$ in g/cm^3, and η in Poise. In that case v is obtained in cm/sec.

If the particle is not spherical, one can define a "Stokes diameter", which is the diameter of a spherical particle of the same density and which settles at the same rate as the particle measured. The word "diameter" for a particle will be taken in this sense henceforth. The physical meaning of it depends on the degree of roundness of the particle under consideration.

Consider a suspension of nonuniform particles, homogeneously distributed throughout the liquid and at such a concentration that no interaction takes place between the particles in their motion.* When settling starts in such a system, each particle will fall according to Stokes' law after a short period of acceleration. Particles of the same size thus fall at the same rate, and therefore they move at constant relative distances. The same holds for other sizes, but the settling rate is different. Consequently, the concentration of particles of a certain size d_p at a certain distance h below the liquid level remains constant until a time

$$t = \frac{h}{v(d_p)} \quad \ldots\ldots\ldots\ldots\ldots\ldots\ldots\ldots\ldots\ldots \quad (2)$$

when all particles of size d_p will have passed by. At time t the concentration of particles at a distance h below the liquid level is equal to the total initial concentration of all particles smaller than d_p.

When the size distribution is denoted $F(x)$ (where $\int_0^\infty F(x) \cdot dx = 1$), expressed in relative weight per unit size, and the initial concentration of the suspension at $t = 0$ is C_0, the concentration at a depth h at time t will be

$$C(h, t) = C_0 \times \int_0^{d_p} F(x) \cdot dx \quad \ldots\ldots\ldots\ldots\ldots\ldots \quad (3)$$

The relative concentration at the same depth and the same time is

$$Q(h, t) = \frac{C(h, t)}{C_0} = \int_0^{d_p} F(x) \cdot dx \quad \ldots\ldots\ldots\ldots\ldots\ldots \quad (4)$$

The change in relative concentration at this place with time is

---

* It has been generally agreed that particle interference in free settling occurs at concentrations above 0.5 percent by volume. However, this interference may even not be neglected until the concentration is under 0.05 percent by volume [47].

$$\frac{\partial Q}{\partial t} = \frac{\partial}{\partial t} \int_0^{d_p} F(x) \cdot dx$$

or
$$\frac{\partial Q}{\partial t} = F(d_p) \times \frac{\partial d_p}{\partial t} \quad \ldots\ldots\ldots\ldots\ldots\ldots\ldots\ldots \quad (5)$$

According to (1) and (2) d_p is equal to

$$d_p = K \sqrt{\frac{h}{t}} \quad \ldots\ldots\ldots\ldots\ldots\ldots\ldots\ldots \quad (6)$$

where

$$K = \sqrt{\frac{18\eta}{g \times \Delta\varrho}}$$

and thus

$$\frac{\partial d_p}{\partial t} = -\frac{K}{2} \times \sqrt{\frac{h}{t^3}} \quad \ldots\ldots\ldots\ldots\ldots\ldots\ldots\ldots \quad (7)$$

Substituting (7) into (5) results in

$$\frac{\partial Q}{\partial t} = -\frac{K}{2} \sqrt{\frac{h}{t^3}} \times F(d_p)$$

or
$$F(d_p) = -\frac{2}{K} \sqrt{\frac{t^3}{h}} \times \frac{\partial Q}{\partial t} \quad \ldots\ldots\ldots\ldots\ldots\ldots\ldots\ldots \quad (8)$$

The size distribution of a powder dispersed in a liquid can thus be derived from concentration changes at a certain level during settling of a homogeneous suspension. Another equivalent method is to measure concentration gradients at a certain time. An equation similar to (8) can be derived as follows:
from equation (4) one arrives at

$$\frac{\partial Q}{\partial h} = \frac{\partial}{\partial h} \int_0^{d_p} F(x) \cdot dx$$

or
$$\frac{\partial Q}{\partial h} = F(d_p) \times \frac{\partial d_p}{\partial h} \quad \ldots\ldots\ldots\ldots\ldots\ldots\ldots\ldots \quad (9)$$

From equation (6) it follows that

$$\frac{\partial d_p}{\partial h} = \frac{K}{2} \times \frac{1}{\sqrt{ht}} \quad \ldots\ldots\ldots\ldots\ldots\ldots\ldots\ldots \quad (10)$$

Substituting (10) into (9) results in

$$\frac{\partial Q}{\partial h} = \frac{K}{2 \times \sqrt{ht}} \times F(d_p)$$

or
$$F(d_p) = \frac{2}{K} \times \sqrt{ht} \times \frac{\partial Q}{\partial h} \quad \ldots\ldots\ldots\ldots\ldots\ldots\ldots\ldots \quad (11)$$

In practice both methods are combined. The change in concentration is than first measured at a certain height as a function of time, and after about half an hour, when only small particles are left in suspension, the concentration gradient is measured.

There are several methods to measure the concentration in a suspension. From these, the light extinction method was chosen because it does not disturb the settling system in any way, and because only small samples are required. The measurement is carried out by measuring the extinction of a beam of light passing through the suspension. The relation between the solids concentration and the light extinction in such a case can be derived as follows:

Let us consider a system in which the suspension particles are randomly distributed throughout the liquid, and let us neglect scattering of the light.

A beam of light (intensity I_0) with a cross sectional area A traverses a cell of length l (measured in the direction of the beam) containing a suspension with a concentration of C grams of solids per c.c. (FIG. 5). Within this cell an

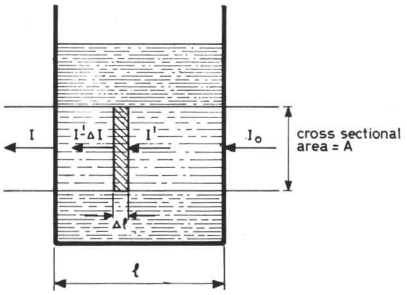

FIG. 5 Extinction of a light beam.

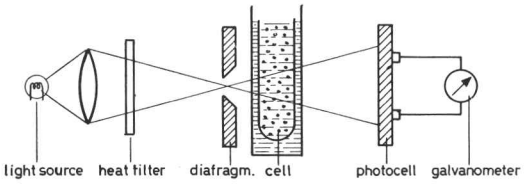

FIG. 6 Schematic diagram of the Leitz Sedimentometer.

element of suspension with length Δl in the direction of the beam, and with the same cross sectional area A as the light beam is considered. We suppose that no overlapping of particles occurs in this element in the direction of the light beam. If furthermore no light is absorbed in the pure liquid and the light extinction is solely caused by the fact that the particles present in the beam obscure the light completely in an area equal to their projected area, the total amount of light leaving a certain plane in the liquid, perpendicular to the beam, can therefore be expressed either as the product of the original intensity and a decreased area, or as the product of the original area and an apparent decreased intensity. For a light intensity I' falling on the element of the suspension, and with an apparent decrease to $(I'-\Delta I')$

$$I' \times (A-\Delta A) = A \times (I'-\Delta I') \quad \ldots\ldots\ldots\ldots\ldots\ldots \quad (12)$$

where ΔA is the projected area of all particles in the element under consideration.

Thus $$\Delta A = \frac{A}{I'} \times \Delta I' \quad . \quad . \quad . \quad . \quad . \quad . \quad . \quad . \quad . \quad . \quad . \quad . \quad . \quad . \quad . \quad . \quad . \quad . \quad . \quad (13)$$

If the total projected area of one gram of the powder is S_p, the projected area ΔA in an element of volume $A \times \Delta l$ is

$$\Delta A = C \times S_p \times \Delta l \times A \quad . \quad . \quad . \quad . \quad . \quad . \quad . \quad . \quad . \quad . \quad . \quad . \quad . \quad . \quad . \quad . \quad . \quad . \quad . \quad (14)$$

Eliminating ΔA from (13) and (14) results in

$$\frac{\Delta I'}{I'} = C \times S_p \times \Delta l \quad . \quad . \quad . \quad . \quad . \quad . \quad . \quad . \quad . \quad . \quad . \quad . \quad . \quad . \quad . \quad . \quad . \quad . \quad . \quad (15)$$

Integrating for the total distance l which the light beam traverses in the liquid one obtains

$$-\int_{I_0}^{I} \frac{\mathrm{d}I}{I} = C \times S_p \times \int_{0}^{l} \mathrm{d}l$$

or $$\ln \frac{I_0}{I} = C \times S_p \times l \quad . \quad . \quad . \quad . \quad . \quad . \quad . \quad . \quad . \quad . \quad . \quad . \quad . \quad . \quad . \quad . \quad . \quad . \quad . \quad (16)$$

Changing to the common logarithm and replacing $l \times \log e$ by the constant α one arrives at the expression for the extinction E:

$$E = \log \frac{I_0}{I} = \alpha \times C \times S_p \quad . \quad . \quad . \quad . \quad . \quad . \quad . \quad . \quad . \quad . \quad . \quad . \quad . \quad . \quad . \quad . \quad . \quad . \quad . \quad (17)$$

Thus, for a homogeneously dispersed powder of known size distribution for which S_p is known also, and in the absence of scattering, the concentration can be derived by measuring the extinction ($\log I_0/I$) in a cell of known thickness.*

Let us now consider a suspension at a distance h below the surface, at a time t after settling has started. The largest particles at this level have then a diameter d_p, which depends on h and t. The contribution of these particles to the extinction can be written as

$$\Delta E = \alpha \times \Delta C \times S_p \quad . \quad . \quad . \quad . \quad . \quad . \quad . \quad . \quad . \quad . \quad . \quad . \quad . \quad . \quad . \quad . \quad . \quad . \quad . \quad (18)$$

where S_p is the projected surface area per gram in the direction of the beam, of

---

* In the directions for use supplied with the Leitz-sedimentometer, the light absorption $(I_0 - I)/I_0$ is used for the calculation of the size distribution instead of the extinction. This is unacceptable for the region of extinction where the apparatus is used. For the size distribution shown in FIG. 7 the measured mean diameter decreases by over half a micron if the light absorption is measured instead of the light extinction.

the particles of size d_p and where ΔC is their relative concentration. S_p can be written as

$$S_p = \frac{K_1}{d_p}$$

where K_1 is a constant containing a geometrical factor and the density of the particles.

Equation (18) now converts to

$$\Delta E = \alpha \times K_1 \times \frac{\Delta C}{d_p}$$

or in terms of relative concentration changes

$$\Delta E = \frac{1}{K_2} \times \frac{\Delta Q}{d_p}$$

or $$\Delta Q = K_2 \times d_p \times \Delta E$$

where K_2 is another constant.

According to equations (8) and (11) we need to know for our measurements the relations $\partial Q/\partial t$ and $\partial Q/\partial h$.

Starting with $\partial Q/\partial t$ we have

$$\frac{\partial Q}{\partial t} = K_2 \times d_p \times \frac{\mathrm{d}E}{\mathrm{d}d_p} \cdot \frac{\partial d_p}{\partial t}$$

Substitution of equation (7) results in

$$\frac{\partial Q}{\partial t} = -\frac{K \times K_2}{2} \times d_p \times \sqrt{\frac{h}{t^3}} \times \frac{\mathrm{d}E}{\mathrm{d}d_p}$$

and introduction of this equation into (8)

$$\mathrm{F}(d_p) = K_2 \times d_p \times \frac{\mathrm{d}E}{\mathrm{d}d_p} \quad \ldots\ldots\ldots\ldots\ldots\ldots \quad (19)$$

Similarly $\partial Q/\partial h$ can be introduced into (11):

$$\frac{\partial Q}{\partial h} = K_2 \times d_p \times \frac{\mathrm{d}E}{\mathrm{d}d_p} \times \frac{\partial d_p}{\partial h}$$

$$\frac{\partial Q}{\partial h} = \frac{K \times K_2}{2} \times d_p \times \frac{1}{\sqrt{ht}} \times \frac{\mathrm{d}E}{\mathrm{d}d_p}$$

$$\mathrm{F}(d_p) = K_2 \times d_p \times \frac{\mathrm{d}E}{\mathrm{d}d_p}$$

which, of course, is the same result as that of equation (19). The curves of

extinction versus time (at a constant h) or versus heighth (at a constant t) are converted into tables of extinction versus particle diameter d_p at time t and height h. From these $F(x)$ can be calculated easily.

In the derivation of the equations it was assumed that the particles were completely opaque and that no scattering occured. However, below about 3 microns scattering does occur as is evident from calibration curves. A correction for this phenomenon at small sizes is made in that dE/dd_p is multiplied by an empirical factor, which is larger than the normal one. The extra correction factor that accounts for scattering is 1.00 for 3 microns, 1.06 for 2 microns, 1.60 for 1 micron and 10.0 for 0.1 micron.

Another important conclusion can be drawn from equation (19). This can be written as

$$F(d_p) = K_2 \times \frac{dE}{d \ln d_p} \quad \ldots\ldots\ldots\ldots\ldots\ldots\ldots\ldots \quad (20)$$

Both K_2 and d_p are dependent on the density of the powder particles. K_2 is unimportant in the calculation of the size distribution, because

$$\int_0^\infty F(x) \cdot dx = 1$$

by definition. The introduction of the wrong value for the density of the powder results in the multiplication of d_p with a constant factor over the whole size range. However, this does not change the values obtained for $dE/d \ln d_p$. It is therefore possible to calculate the size distribution of a powder by measuring the light extinction of a settling suspension of this powder with time and at different heighths even when the wrong value for the density of the powder is introduced into the equations. The size axis must then be normalized at the end by multiplication with a factor. This procedure is restricted to those cases where no scattering occurs and thus where particles smaller than 3 microns are absent. This holds for the amorphous precipitates to be described in this thesis. For the sake of convenience the size distributions have been calculated with the density of UO_2. The corresponding factors for conversion of the size axis are calculated further on in this chapter.

Finally it should be remarked that the light extinction method is not used any more for particle size analysis of our fuel powders. For quantitative colloid chemical studies up to 250 °C a new apparatus has been developed by Drs. J. KALSHOVEN of our laboratory which produces on a recorder the cumulative size distribution curve of the powder in a few minutes.

Apparatus

The measuring device of the Leitz Sedimentometer, shown diagrammatically

in FIG. 6, consists of a light fed from an extremely constant voltage source, an optical system including lenses, a dark blue heat filter, a horizontal slit of 0.5, 1.0 or 1.5 mm width and a photo cell with a galvanometer to indicate the intensity of the light. The glass cell containing the suspension is placed just behind the slit and can be kept at a constant temperature by a thermostat. The complete optical system and the photocell can be moved up and down so that measurements can be taken at any level. The complete apparatus is enclosed in a light proof housing.

Procedure

The particles were dispersed in a liquid chosen such that no flocculation of the particles occurred during the complete measurement. For the precipitates under investigation both dry n-butylalcohol and 0.01 N ammonia were used. If necessary, the powder was screened and only the fraction below 60 microns was dispersed.

After the cell had been filled with the pure dispersing liquid and the apparatus had been closed, the light beam was interrupted by means of a shutter and the galvanometer scale was corrected to its zero point. In this way the background caused by small leaks in the apparatus was taken into account. The shutter was then removed and the current through the galvanometer was adjusted to full scale deflection (200 mm). This point indicates zero extinction and automatically corrects for the light absorption in the dispersing liquid.

The cell was then filled to the mark with a suspension of the powder to be investigated in the dispersing liquid at such a concentration that an extinction of about 0.5 was obtained in the well mixed suspension. The position of the light beam was adjusted (normally 10 cm below the liquid level) the cell was shaken to disperse the particles, and replaced in the apparatus which was then closed. Starting from the moment the cell was placed in the apparatus ($t = 0$) the extinction was measured at intervals. After 30 minutes, the concentration gradient across the cell was measured by moving the measuring device from the lowest position upwards along distances of about 5 mm at a time and taking the readings of the extinction.

The extinction values were plotted against the logarithm of the time of sedimentation and against the height in the cell, and a smooth curve was drawn through these points. From the curves readings of the extinction were taken at points corresponding to different particle sizes. These points were calculated from equation (6). The decrease of the extinction for a certain size interval was multiplied by a given factor [45] to obtain a relative weight for this interval. By dividing this weight by the total of all the intervals, the weight frequency curve and the cumulative curve were constructed.

II.2.2 Characterization of the size distribution

It appeared that all the amorphous powders obtained by precipitation from a uranyl nitrate solution by the method described in this thesis have a distribution which follows the so called log-normal law [41]. This law very often governs the size distribution of powders obtained by comminution. The validity of this law for the amorphous precipitate was therefore less surprising when we discovered afterwards that one of the processes which influence the ultimate size distribution is the comminution of flocs.

Even more striking is that the law is followed in a very wide region (1 to 99 percent by weight). We believe that these very good statistics are reached because growth and comminution phenomena occur simultaneously, as will be shown in this chapter. According to the log-normal law the number of particles of size d_p in the frequency curve is given by

$$n = \frac{1}{\sqrt{2\pi}\log\sigma_g} \times e^{-\frac{(\log d_p - \log d_g)^2}{2\log^2\sigma_g}} \quad \ldots\ldots\ldots\ldots\ldots \quad (21)$$

where d_g is the geometric mean diameter (median) and σ_g the geometric standard deviation.

The weight frequency curve again follows the log-normal law. If the weight percent of particles being less than a given size is plotted against that size on a probability grid, whose second axis has a logarithmic scale, a straight line is obtained when the size distribution was a log-normal probability one.

In such cases the size distribution is completely determined by the parameters d_g and σ_g. Of these the geometric mean diameter d_g is defined by the fact that 50 percent of the sample by weight has a size smaller than d_g. The geometric standard deviation σ_g can be derived from formula (21). The result is that

$$\log\sigma_g = \sqrt{\frac{\Sigma[n(\log d_p - \log d_g)^2]}{\Sigma F(d_p)}} \quad \ldots\ldots\ldots\ldots\ldots \quad (22)$$

where $F(d_p)$ is the weight fraction of particles of size d_p.

It can be shown from statistical theory that 68% of a sample with a geometric size distribution, has a particle size between d_g/σ_g and $d_g \times \sigma_g$. Therefore the standard deviation can easily be obtained from the log-probability graph as

$$\sigma_g = \frac{84\%\text{ size}}{50\%\text{ size}} = \frac{50\%\text{ size}}{16\%\text{ size}}$$

As an example, graphs are given for the weight frequency (FIG. 7) and the cumulative weight distribution (FIG. 8) of the sintered UO_2 material prepared for the subcritical experiments. For this powder $d_g = 10.6\ \mu$ and $\sigma_g = 1.2$.

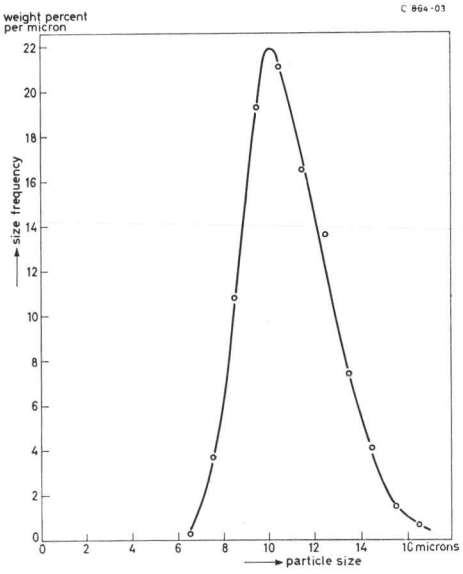

FIG. 7 Particle size distribution of UO_2 for the nearcritical experiments.

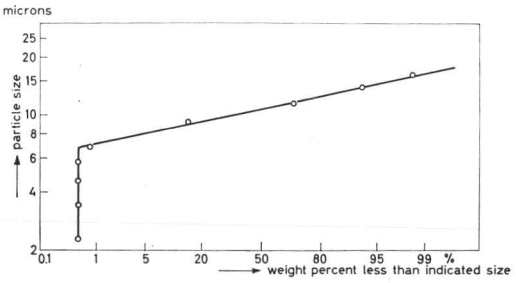

FIG. 8 Cumulative weight distribution of FIG. 7 on a log-normal probability grid. (d_g = 10.6 microns, σ_g = 1.2).

Concerning the size distribution, the most important powders are the amorphous precipitates and the UO_2 produced from them. They all follow quite strictly the log-normal law and they will therefore be characterized by their d_g and σ_g values. The other products, which are crystalline, generally deviate from this distribution law. As the complete size distribution is of no significance for the discussions presented, the powder will be characterized by a mean particle size below which the diameters of 50 percent of the powder by weight is found.

II.3 The determination of the weight frequency as applied for precipitates in the urea process

As the various experiments to be described were carried out in order to prepare a suitable sintered UO_2 fuel, it was not the size distribution of the precipitates that was of main interest, but that of the UO_2 which could be prepared from them by reduction and individual sintering without any intergrowth of the separate particles.

As it was advantageous to know at once whether a batch of precipitate could yield an acceptable batch of sintered UO_2, the size distribution of the precipitate itself was measured. Allowance can be made for the shrinkage of the particles during sintering and their change in density. It has been shown already in this chapter in a similar case, that the size axis in the particle size distribution graph has to be normalized then. The conversion factors for this normalization will be calculated now.

If we confine ourselves to a non-porous precipitate there are two particle sizes which should be known: the true size of the precipitate particle (d_s) and the true size of the non-porous UO_2 particle which can be obtained from it by reduction and sintering (D_t). Because the density of UO_2 is used in the calculation still another size is found before normalizing: that of the dense UO_2 particle (D_s) which has the same settling velocity as the precipitate particle. In FIG. 9 this notation is shown schematically. The important ratio's are d_s/D_s and D_t/D_s.

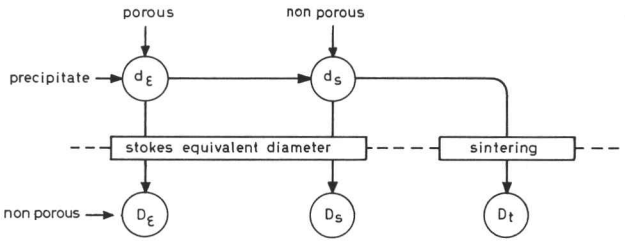

FIG. 9 Schematic presentation of the particle sizes used in the calculations.

Consider a spherical particle of the precipitate with a diameter d_s, density ϱ_s and containing a weight percentage x of uranium. In order to calculate the diameter, it is considered to be a dense UO_2 particle with a diameter D_s, but with the same settling velocity as the precipitate particle. Therefore

$$\frac{g \times d_s^2 \times \Delta\varrho_s}{18\eta} = \frac{g \times D_s^2 \times \Delta\varrho_{UO_2}}{18\eta} \quad \ldots\ldots\ldots\ldots\ldots \quad (23)$$

where $\Delta\varrho_s$ and $\Delta\varrho_{UO_2}$ are differences in density between the precipitate or the dense UO_2, and the dispersing liquid.

Thus

$$d_s = D_s \times \sqrt{\frac{\Delta\varrho_{UO_2}}{\Delta\varrho_s}} \quad \ldots\ldots\ldots\ldots\ldots\ldots\ldots \quad (24)$$

For precipitate particles in n-butanol this relation is

$$d_s = 1.70 \times D_s$$

Additionally it is necessary to know the relation between the diameter D_s as determined and the true diameter D_t of the dense UO_2 particle that can be prepared from the precipitated particle (diameter d_s) by reduction and sintering.

The total uranium content in both particles is equal:

$$\frac{1}{6}\pi \times D_t^3 \times \varrho_{UO_2} \times \frac{238}{270} = \frac{1}{6}\pi \times d_s^3 \times \varrho_s \times \frac{x}{100} \quad \ldots\ldots \quad (25)$$

$$D_t = d_s \times \sqrt{\frac{\varrho_s}{\varrho_{UO_2}} \times \frac{270}{238} \times \frac{x}{100}} \quad \ldots\ldots\ldots\ldots \quad (26)$$

Or, substituting d_s from (24):

$$D_t = D_s \times \sqrt{\frac{\Delta\varrho_{UO_2}}{\Delta\varrho_s}} \times \sqrt[3]{\frac{\varrho_s}{\varrho_{UO_2}} \times \frac{270}{238} \times \frac{x}{100}} \quad \ldots\ldots\ldots \quad (27)$$

For a given system therefore

$$D_t = \text{constant} \times D_s \quad \ldots\ldots\ldots\ldots\ldots\ldots \quad (28)$$

In equation (28) D_s is obtained from Stokes' law by using the density of UO_2 instead of that of the precipitate. However, the ratio between the real diameter (D_t) and the measured one (D_s) is constant.

For the real values of an amorphous precipitate in n-butanol ($\varrho_s = 4.2$; $\varrho_{UO_2} = 10.6$; $\varrho_{liquid} = 0.8$ and $x = 68.5\%$) the relation is

$$D_t = D_s \times 1.15$$

The correct figure for the diameter of the sintered UO_2 particle (D_t) therefore is obtained by multiplying the figure (D_s) given by the analyst by 1.15.

Equation (27) leads to the result that a variation of 2% in the uranium content (x) causes a change of less then 1% in the result and a variation of 5% in the density of the particle (ϱ_s) a change of 1.5%. Both variations are well within acceptable limits of accuracy.

In conclusion it can be stated that by introducing the density of UO_2 into the equations, size distributions for the amorphous precipitates are obtained which are too small in size by a factor of 1.70. If one wants to predict the size distribution of the ultimate dense UO_2 particles obtained from the amorphous precipitate the size resulting from the calculation must be multiplied by 1.15. The above only holds in the absence of particles smaller than 3 microns or when the relative size distribution is restricted to diameters above 3 microns. When a log-normal distribution is present the introduction of the conversion factors results in a displacement of the straight line of the log-probability graph parallel to itself. This means that even without conversion, the right value of σ_g is found.

The influence of porosity

The porosity of the precipitate influences the particle size analysis of the UO_2 end product.

Consider a particle of the precipitate with a diameter d_ε (FIG. 9), a mean density ϱ_ε and a porosity ε, the latter being defined as the void fraction of the particle. By eliminating the porosity completely a particle of a diameter d_s, a density ϱ_s and a uranium content of $y\%$ will result, and this particle can be sintered into a dense UO_2 particle with a diameter D_t and a density ϱ_{UO_2}. The Stokes equivalent diameters of dense UO_2 particles for d_ε and d_s are D_ε and D_s respectively. The density of the dispersing liquid is ϱ_l.

1. Pores filled with the dispersing liquid

The ratio to be calculated is

$$\frac{D_t}{D_\varepsilon} = \frac{D_t}{d_s} \times \frac{d_\varepsilon}{D_\varepsilon} \times \frac{d_s}{d_\varepsilon} \quad \ldots \ldots \ldots \ldots \ldots \ldots \quad (29)$$

a. The total uranium content for the particles d_s and D_t is the same, hence:

$$\frac{1}{6} \times \pi \times d_s^3 \times \varrho_s \times \frac{y}{100} = \frac{1}{6} \times \pi \times D_t^3 \times \varrho_{UO_2} \times \frac{238}{270} \quad \ldots \quad (30)$$

$$\frac{D_t}{d_s} = \sqrt[3]{\frac{\varrho_s}{\varrho_{UO_2}} \times \frac{y}{100} \times \frac{270}{238}} \quad \ldots \ldots \ldots \ldots \quad (31)$$

b. The settling velocity for d_ε and D_ε are equal, hence:

$$\frac{g}{18\eta} \times d_\varepsilon^2 \times (\varrho_\varepsilon - \varrho_l) = \frac{g}{18\eta} \times D_\varepsilon^2 \times (\varrho_{UO_2} - \varrho_l) \quad \ldots \ldots \quad (32)$$

where

$$\varrho_\varepsilon = (1-\varepsilon) \times \varrho_s + \varepsilon \times \varrho_l \quad \ldots \ldots \ldots \ldots \quad (33)$$

Thus

$$\frac{d_\varepsilon}{D_\varepsilon} = \sqrt{\frac{\varrho_{UO_2} - \varrho_l}{(1-\varepsilon)(\varrho_s - \varrho_l)}} \quad \ldots \ldots \ldots \ldots \quad (34)$$

c. The total amount of solid material is equal for d_ε and d_s, hence:

$$\frac{1}{6} \times \pi \times d_s^3 = \frac{1}{6} \times \pi \times d_\varepsilon^3 \times (1-\varepsilon) \quad \ldots \ldots \ldots \quad (35)$$

$$\frac{d_s}{d_\varepsilon} = \sqrt[3]{1-\varepsilon} \quad \ldots \ldots \ldots \ldots \ldots \quad (36)$$

From equations (29), (31), (34) and (36) it follows that

$$\frac{D_t}{D_\varepsilon} = \sqrt{\frac{\varrho_{UO_2} - \varrho_l}{\varrho_s - \varrho_l}} \times \sqrt[3]{\frac{\varrho_s}{\varrho_{UO_2}} \times \frac{y}{100} \times \frac{270}{238}} \times \sqrt[6]{\frac{1}{1-\varepsilon}} \quad \ldots \quad (37)$$

Other important relations like D_ε/d_s can easily be derived from the above formulas.

2. Pores empty

Though this condition seems to be very unlikely, it might occur if the wetting of the porous particle under consideration is bad or if there are closed pores.

a. D_t/d_s is given by equation (31);
b. equal settling velocity for d_ε and D_ε is given by equation (32) where $\varrho_\varepsilon = (1-\varepsilon) \times \varrho_s$

Thus

$$\frac{d_\varepsilon}{D_\varepsilon} = \sqrt{\frac{\varrho_{UO_2} - \varrho_l}{\varrho_s \times (1-\varepsilon) - \varrho_l}} \quad \ldots\ldots\ldots\ldots\ldots\ldots \quad (38)$$

c. d_s/d_ε is given by equation (36).

From equations (29), (31), (38) and (36) it follows that

$$\frac{D_t}{D_\varepsilon} = \sqrt{\frac{\varrho_{UO_2} - \varrho_l}{\varrho_s \times (1-\varepsilon) - \varrho_l}} \times \sqrt[3]{\frac{\varrho_s}{\varrho_{UO_2}} \times \frac{y}{100} \times \frac{270}{238}} \times \sqrt[3]{1-\varepsilon} \quad \ldots \quad (39)$$

For the case of normal, amorphous precipitates, values of D_t/D_ε calculated from equations (37) and (39) are given in TABLE II.1 and FIG. 10.

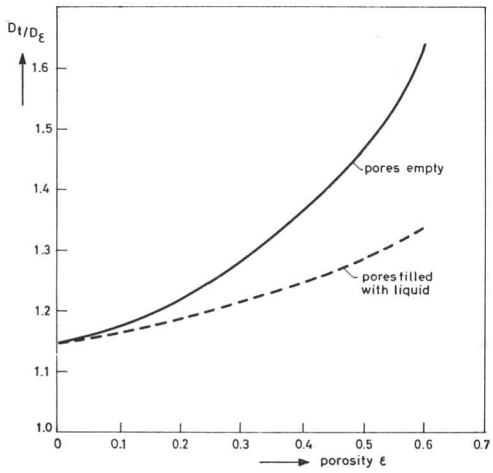

FIG. 10 Influence of the porosity on the measurement of a particle size distribution by settling.

TABLE II.1 The influence of the porosity on the size distribution measurement.

ε void fraction of particle	D_t/D_ε pores empty	D_t/D_ε pores filled with liquid	Remarks
0	1.15	1.15	y =68.5%
0.1	1.18	1.17	ϱ_s= 4.2
0.2	1.22	1.19	
0.3	1.30	1.22	
0.4	1.37	1.25	
0.5	1.47	1.29	
0.6	1.64	1.34	
0.1	1.20	1.18	y =68.5%
0.5	1.53	1.31	ϱ_s= 4.0
0.1	1.19	1.18	y =70 %
0.5	1.48	1.30	ϱ_s= 4.2

To demonstrate the influence of changes in ϱ_s and y, D_t/D_ε was also calculated for $\varepsilon = 0.1$ and 0.5 for $\varrho_s = 4.0$ (instead of 4.2) and once again for $y = 70\%$ (instead of 68.5%). The results are included in the table.

Here also, the conversion of projected area into weight fraction has no influence on the resulting size distribution as a constant factor is used provided that the porosity of all particles is the same.

From FIG. 10 it is seen that for a particle of 10 μ and a porosity of 10% an extra correction of 0.2 μ is needed. A change of 3% in uranium content or 5% in density of the solid precipitate cause another variation of 0.1 μ each.

In the case of porous particles the ratio between the real diameter of the particle d_ε and its equivalent Stokes UO_2-diameter D_ε is obtained from

$$\frac{g}{18\eta} \times d_\varepsilon^2 \times (\varrho_\varepsilon - \varrho_l) = \frac{g}{18\eta} \times D_\varepsilon^2 \times (\varrho_{UO_2} - \varrho_l)$$

Substitution of ϱ_ε from (33) results in

$$\frac{d_\varepsilon}{D_\varepsilon} = \sqrt{\frac{\varrho_{UO_2} - \varrho_l}{\varrho_s - \varrho_l}} \times \frac{1}{\sqrt{1-\varepsilon}} \quad \ldots\ldots\ldots\ldots\ldots\ldots \quad (40)$$

Under the described conditions, and with a porosity of 10%

$$\frac{d_\varepsilon}{D_\varepsilon} = 1.70 \times 0.95 = 1.61$$

The open porosity of the precipitates obtained during the investigations has been measured by water vapour condensation in the pores at a relative pressure of 0.98. It was found to be less than 3%. As deviations from the normal density ($\varrho_s = 4.2$) and the normal uranium content ($x = 68.5\%$) are very small, the size distribution of the final dense UO_2 product is found by multiplying the size obtained from the extinction measurements by 1.15. The real size distribution of the precipitate is obtained in the same way by multiplication of the measured size values by 1.70. Because we consider a log-normal distribution, the value of σ_g is unaltered. In this and in the next chapters particle sizes are always given as real size, determined in the way described above. Applied in this way, the method yields results which are in very close agreement with the much faster gamma absorptiometric method [48] developed later.

II.4 The influence of the stirring conditions on the mean particle size *

After it had been shown that it was possible to produce precipitates with the urea process which could be converted into UO_2 powders with the required properties, the experiments were directed towards the possibility of influencing the mean particle size.

Of the different products which could be obtained with the urea process, only the amorphous one met the requirements for the subcritical assembly. It could be prepared in the right size range and it had a very smooth surface without any sharp crystal edges. In the following only this precipitate will be discussed.

---

* The valuable assistance of Mr. T. C. Steemers is gratefully acknowledged for all the experimental work on the urea process.

As will be seen later, only limited variations of the temperature and the concentrations are possible for the amorphous precipitate, which is desired for the process. The variation in particle size obtained by a variation in the chemical conditions proved to be small (generally 10–15%). However, larger variations are possible, owing to other causes.

Originally, the reproducibility of the preparation of "natural" uranium oxide on a 10 grams scale was rather bad, but the production of 20% enriched UO_2 on a 100 grams scale gave fifty seven out of sixty batches with surprisingly small variations in size distribution. It was later proved, that this could be attributed to the completely fixed geometry of the apparatus, which in itself was necessary as a consequence of processing this hazardous radioactive material (See INTRODUCTION).

The degree of mixing during the reaction might be an important variable and therefore the effect of this on the size distribution in a fixed geometry of the precipitation apparatus was investigated.

II.4.1 Experiments with a vibrational stirrer

The precipitation was carried out in a 250 ml round bottom flask A (FIG. 11) provided with a vibrational stirrer C * with a frequency of 100 cycles. The flask was placed in a bath B kept at a constant temperature by circulating liquid from a thermostatic bath. The flask was made leak-tight so that the carbon dioxide evolved during the process could be measured in the gas burette E. Every part of the apparatus was fixed to a "Dexion" frame to ensure the same geometry in every experiment.

The stirrer D consisted of a conically perforated stainless steel plate with a diameter of 41.5 mm. The stirring action was controlled by a knob on the vibrator C, which limited the length of the stroke. The amplitude of the stirrer could be varied linearly between 0.25 and 2 mm and was checked by means of a simple perspex pointer (FIG. 12) attached to the shaft of the stirrer. This pointer consists of a isosceles triangle with a base of 3 mm (parallel to the shaft of the stirrer) and a height of 30 mm, subdivided in six equal lengths of 5 mm. When this pointer vibrates along its base, the long sides of the triangle appear to intersect at a point P, the position of which can be read from the horizontal scale. Each 5 mm mark on the pointer represents an amplitude of 0.5 mm. Thus FIG. 12 represents an amplitude of 1 mm.

Apart from the variation of the stirring action the experiments were carried out as described in CHAPTER I. Because the stirring was insufficient with an amplitude below 0.75 mm, experiments were carried out with amplitudes

* A Vibromischer, type E1 was used. This apparatus is manufactured by the A.G. für Chemie-Apparatebau (Switzerland).

TABLE II.2 The geometric mean particle diameter of the amorphous precipitate as a function of the amplitude of the stirrer.

Amplitude (mm)	Mean diameter d_g (microns)
0.75	18.0
1.00	16.7
1.25	16.0
1.50	14.6
1.75	13.6
2.00	12.8

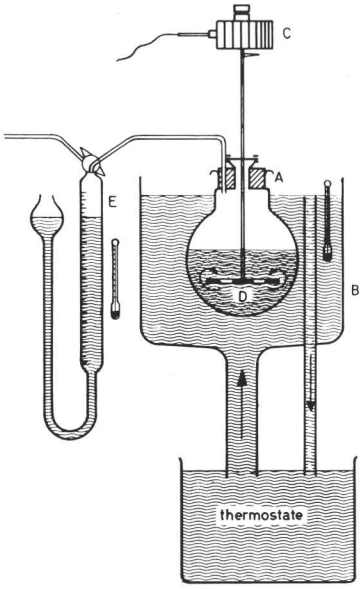

FIG. 11 Experimental set-up used for the urea process.

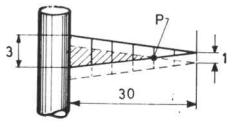

FIG. 12 Indicator of the amplitude for a vibrational stirrer. Measures in mm.

TABLE II.3 The geometric mean particle diameter of the amorphous precipitate as a function of the stirrer speed for a rotational stirrer.

Stirrer speed (r.p.m.)	Mean diameter d_g (microns)
200	40.0
300	39.1
500	33.0
700	25.6
900	22.8
1100	20.9
1300	19.4
1500	16.0

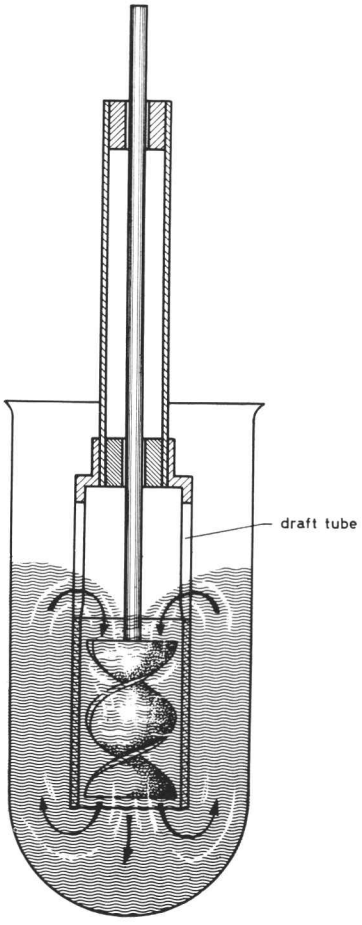

FIG. 13 Helical stirrer with draft tube.

between 0.75 and 2.00 mm. The results of these experiments are given in TABLE II.2.

The standard deviation (σ_g) was 1.2 in all cases.

II.4.2 Experiments with a rotational stirrer

As the stirrer speed influenced the mean particle size considerably, a few other methods of stirring were tested. From these experiments it was decided to use a stirrer consisting of a helix rotating in a draft tube through which the liquid was forced downwards. This stirrer is shown in FIG. 13.

The stirrer was placed in a cylindrical beaker with an inner diameter of 48.5 mm and containing 150 ml of liquid. The stirrer speed was measured with a stroboscope and proved to be very constant. The experimental procedure was the same as with the vibrational stirrer.

The mean particle size as a function of stirrer speed is given in TABLE II.3.

II.4.3 Discussion of results

The relation between the geometric mean diameter and the stirrer action proves to be simple. When one plots the inverse of d_g versus the amplitude (FIG. 14) or versus the stirrer speed (FIG. 15) a straight line is obtained. For the range of stirrer conditions investigated the mean diameter can therefore be found from

a. $$\frac{1}{d_g} = 1.83 \times 10^{-2} \times a + 0.0414 \quad \ldots\ldots\ldots\ldots\ldots\ldots \quad (41)$$

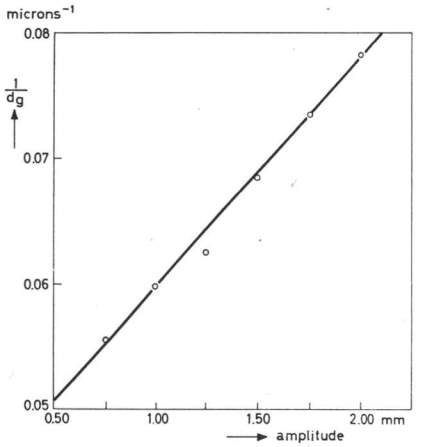

FIG. 14 Correlation between the inverse of the geometric mean diameter d_g of the amorphous precipitate and the amplitude of the vibrational stirrer.

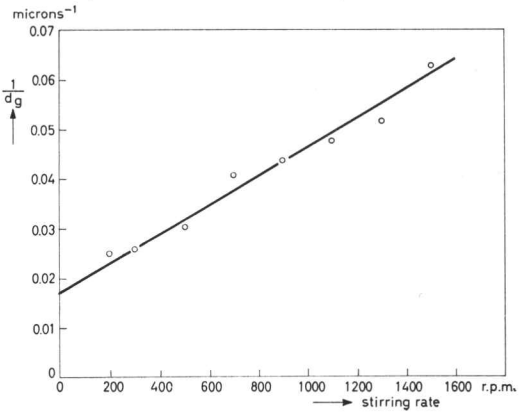

FIG. 15 Correlation between the inverse of the geometric mean diameter d_g of the amorphous precipitate and the rotational speed of a helical stirrer in a draft tube.

for the vibrational stirrer with an amplitude a, and

$$\text{b.} \qquad \frac{1}{d_g} = 2.92 \times 10^{-5} \times n + 0.0172 \quad . \quad . \quad . \quad . \quad . \quad . \quad . \quad . \quad . \quad . \quad . \quad . \quad . \quad . \quad . \quad (42)$$

for the rotational stirrer, where n is the rotational speed in r.p.m.

These results suggest that the shear rate in the field of the stirrer is determining the mean particle size. Although it must be possible to measure the effect in a system with a well defined shear rate (*e.g.* in a rotational viscometer) this experiment was not carried out due to experimental difficulties. Another method was chosen to obtain some qualitative information: a stirrer was used which was enlarged twice the original diameter. The distance between the stirrer and the draft tube however was kept the same. The idea was that at the same rotational velocity the shear rate would be twice the shear rate of the smaller stirrer. Four measurements were made in a vessel of 130 mm diameter, containing 1350 ml of liquid. The results are given in TABLE II.4.

These values are plotted in a graph of $1/d_g$ versus the rotational speed n in FIG. 16, curve a.

The equation of the straight line is

$$\frac{1}{d_g} = 5.56 \times 10^{-5} \times n + 0.0176 \quad . \quad . \quad . \quad . \quad . \quad . \quad . \quad . \quad . \quad . \quad . \quad . \quad . \quad . \quad . \quad (43)$$

TABLE II.4 The geometric mean particle diameter of the amorphous precipitate as a function of the stirrer speed for the enlarged rotational stirrer.

Stirrer speed (r.p.m.)	Mean diameter d_g (microns)
200	34.8
300	28.7
400	24.0
500	22.8

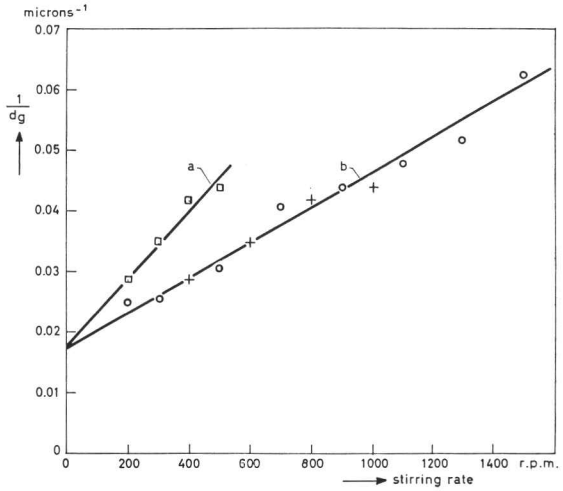

FIG. 16 Correlation between the inverse of the geometric mean diameter d_g of the amorphous precipitate and the rotational speed of two helical stirrers of different size.
a. diameter of the stirrer 60 mm;
b. diameter of the stirrer 30 mm.
The clearance between stirrer and draft tube was 1 mm in both cases.

From the equations (42) and (43) one sees that they represent two lines which meet the vertical axis in the same point. Furthermore the slope in (43) is roughly twice that of (42). Accordingly, the measurements represented in FIG. 15 are replotted in FIG. 16 as circles (curve b). The data of TABLE II.4 are included as squares (curve a). To compare the shear rates one should multiply the rotational speed of the points in curve a by 2. This has been indicated with crosses. The agreement is good enough to suppose that the shear rate is the important parameter which determines the mean particle size of the precipitate. In that case one would expect that the relation between the mean particle size d_g and the rotational speed n has the general form

$$\frac{1}{d_g} = \frac{2\pi rn}{\Delta r} \times C_1 + C_2 \quad \ldots \ldots \ldots \ldots \ldots \ldots \quad (44)$$

where r = radius of the stirrer; Δr = clearance between stirrer and housing; C_1 and C_2 = constants, which depend on viscosity, chemical conditions and geometry.

Contrary to the normal processes of nucleation and particle growth the mean particle diameter in the urea process appears to be controlled by the stirrer action. This might be caused by the occurrence of flocculation, the stirrer breaking down the flocs and controlling the floc size. This idea is supported by the appearance of the particles which look like "cauliflowers" (FIG. 2).

To verify this hypothesis a few experiments were carried out:

1. Direct microscopic observation revealed that during the process, a certain point is reached where a very strong flocculation of the particles occurs (FIG. 17). The precipitate, which is initially finely dispersed, agglomerates within a few minutes to equisized particles, which grow during the rest of the process.
2. The addition of 250 mg of gelatine or gum arabic to the system as a dispersant at low pH prevented flocculation. The end product then consisted of a very fine powder with a mean particle size of well below two microns. As there might be the possibility that colloidal additions hinder the growth of the particles by their presence upon the surface, another experiment was carried out with the addition of 1 ml of a 1% Separan 2610 * solution which acts as a flocculating agent. The mean particle size of the end product was only slightly higher than without addition. This was to be expected due to the presence already of large amounts of electrolyte. However, the experiment proved that the adsorption of some hydrophylic colloid need not prevent particle growth. Thus it is very likely that flocculation during the process strongly contributes to the growth of the particles.

---

* Manufactured by the Dow Chemical Company (U.S.A.).

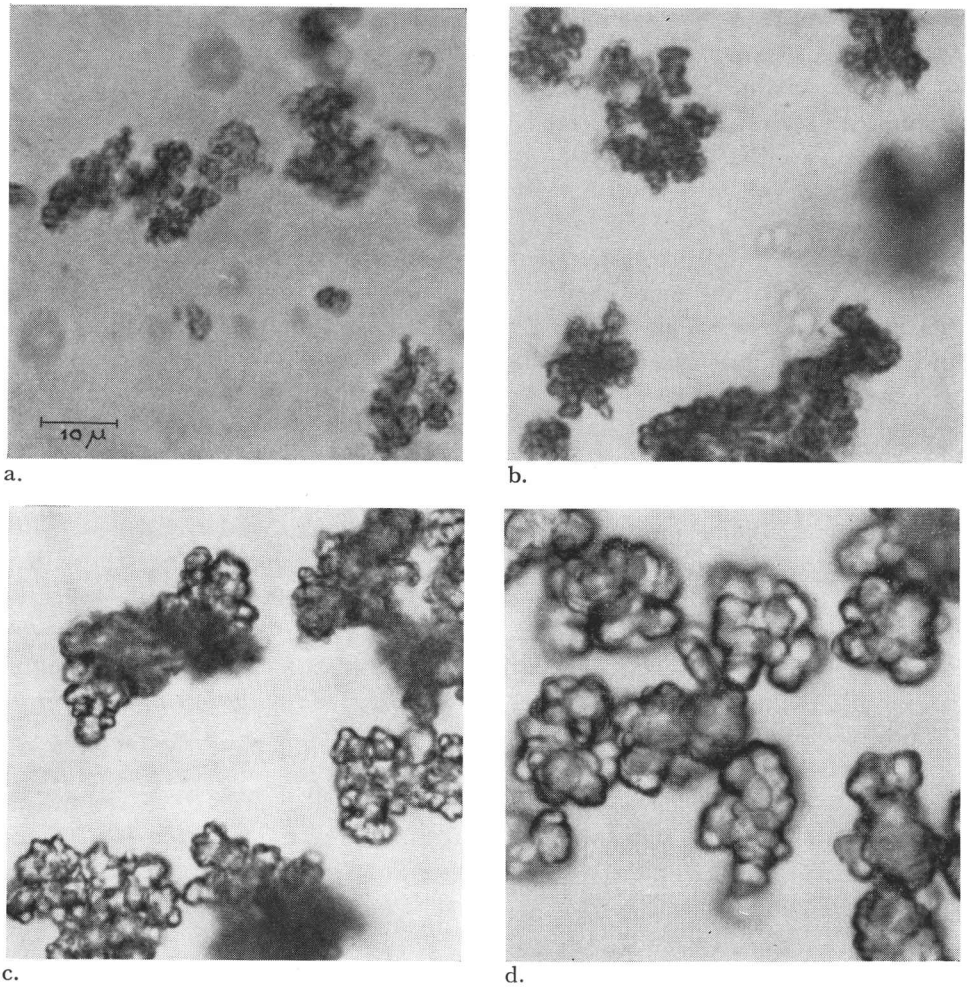

FIG. 17 Degree of flocculation of the amorphous precipitate in the urea process at different times after precipitation has started (5, 10, 20 and 50 minutes respectively).

II.4.4 Typical aspects of a too low or a too high stirrer speed

The phenomena described above occur only within certain limits of the stirring rate. However, at too low or too high stirrer speeds other mechanisms interfere with the process. As these mechanisms are different at low and at high stirring rates, both cases will be dealt with separately. Above the upper limit for the stirring speed a precipitate of crystalline form is obtained with an increase of particle size instead of a decrease. The reason for this change in particle habit will be discussed in CHAPTER IV. For the experiments given in TABLE II.3 a crystalline precipitate was obtained at 1700 r.p.m., with a $d_g = 36.5$ microns.

It is remarkable to see that with the rotational stirrer no amorphous precipitates with a d_g smaller than about 16 microns could be prepared, whereas this is certainly possible with the vibrational stirrer. It clearly shows the difference in applicability of different stirrers. In the case of the helical stirrer, the fact that a very deep vortex is drawn and only a thin layer of liquid is left at the inside of the draft tube exerts a great influence upon the process as will be shown later.

If the stirrer speed is too low the mean particle size decreases rapidly. The reason is, that settling occurs and that growth of the particles stops as soon as they are covered by the next layer of precipitate. In the supernatant liquid new nuclei are formed continuously. This could clearly be shown by carrying out an experiment without a stirrer: the mean particle size of the product was smaller than two microns. It might well be that, for similar reasons (differences in geometry and stirring characteristics) extrapolation of the d_g values of TABLES II.2 and II.3 to no stirring would result in products with different d_g values, although the chemical conditions are identical.

Another experiment to demonstrate this decrease in particle size caused by settling is to enlarge the volume of the liquid at a constant rotational velocity of the helical stirrer by using a reaction vessel with a larger diameter. Whereas for a vessel with a diameter of 48.5 mm the decrease in d_g is observed below 200 r.p.m., the same occurs at about 300 r.p.m. in a vessel with a diameter of 75 mm. Generally an increase in σ_g is observed at the same time.

According to the results reported under II.4 in this chapter the following mechanisms occur simultaneously in the formation of the amorphous particles in the urea process after the nucleation step:

1. Growth of the individual particles by deposition of uranium from the solution as a consequence of slowly increasing pH.

2. Growth of the particles by flocculation under colloid chemically unstable conditions. The deposition of uranium between the particles may provide sufficient strength to the agglomerates.

3. Limitation of the particle size by forces of the stirrer. The degree of dispersion depends on the bonding strength between the particles, their size and the forces of the stirrer. As the process is statistical, deviations will occur from the equilibrium size, which is determined by balancing the attraction and the disruption forces. Accordingly, the size distribution is represented as a probability curve.
   It is suggested to call the mechanism described above: particle growth by controlled flocculation.

A general experience of the work described was that the standard deviation in the size distribution of the precipitate was determined by the homogeneity of the mixing. A well defined stirring pattern without large variations in the circulation time of the particles should be chosen to obtain a low σ_g value. Settling of the precipitate in regions which are stagnant or have a low velocity increases the value of σ_g.

CHAPTER III

THE INFLUENCE OF THE CHEMICAL CONDITIONS ON THE PRECIPITATE IN THE UREA PROCESS

III.1 Introduction

The influence of the variation in the chemical conditions on the mean particle size of the amorphous precipitate proved to be smaller than might be expected from nucleation theories. The reason, as stated in CHAPTER II, is that precipitation occurs by controlled flocculation. On the other hand it was found that several different crystalline products could be obtained by using slightly differing process conditions. When in this chapter the distinction has to be made, such crystalline products are marked with an asterisk in the tables. In the graphs they are indicated by squares.

III.2 The influence of the chemical conditions on the particle size

The concentrations of uranium, urea and nitrate ion, and the temperature were taken as variables to be investigated. These experiments were mainly carried out to study the influence of deviations from the so called standard procedure. This procedure was used to produce the UO_2 fuel for the subcritical assembly and it was therefore chosen as the basis of the following experiments. Afterwards it was found that only the amplitude of the stirrer deviated slightly from the production conditions, but it was kept constant during the experiments to be described. The conditions were:

- a 250 ml round bottom flask was used as reaction vessel.
- 100 ml starting solution was used, being 0.4 molar in uranium and containing 132 milliequivalents nitric acid and 60 milliequivalents ammonia.
- 50 ml urea solution (500 gr/litre) were added.
- the reaction temperature was 95 °C.
- the system was stirred with a 100 cycles vibrational stirrer in a fixed position.
- the stirring plate diameter was 41.5 mm, the amplitude 1.65 mm and the liquid was forced downwards by the plate.

The experiment carried out under these conditions is cursified in the TABLES I to IV.

III.2.1 The influence of the uranium concentration

Using the standard procedure just described, the uranium concentration of

the starting solution was varied. In the experiment with the highest uranium content the nitrate ion concentration was slightly raised. The results of this series of experiments are given in TABLE III.1.

TABLE III.1 The influence of a variation of the uranium concentration on the mean particle size.

Concentration of the starting solution		Mean particle size d_g (microns)
uranium (g.atom/l)	nitrate ion (gram ions/l)	
0.3	1.32	13.3
0.3	1.32	11.1
0.4	*1.32*	*13.9*
0.5	1.32	14.3
0.6	1.32	14.6
0.8	1.43	14.6
0.8	1.64	12.2

III.2.2 The influence of the urea concentration

The total amount of urea added was varied using the standard procedure. The results are given in TABLE III.2. Care was taken that the final volume of the liquid was constant.

TABLE III.2 The influence of a variation of the urea concentration on the mean particle size.

Urea added (ml)	Mean particle size d_g (microns)	Urea added (ml)	Mean particle size d_g (microns)
20	30.1 *	45	12.9
25	30.9 *	*50*	*13.9*
25	12.2	55	13.1
25	25.0 *	60	12.2
32.5	13.8	65	19.2 *
40	14.3	70	16.7 *

III.2.3 The influence of the nitrate ion concentration

The results of variations of the nitrate ion concentration using the standard process are given in TABLE III.3. The extra nitrate ions were added as nitric acid. The pH was corrected with gaseous ammonia to avoid an increase in the volume of the liquid.

III.2.4 The influence of the temperature

The influence of the variation of the temperature on the mean particle size of the product obtained in the standard procedure is shown in TABLE III.4.

TABLE III.3 The influence of a variation of the nitrate ion concentration on the mean particle size.

Nitrate ion concentration of the starting solution (gram ions/l)	Mean particle size d_g (microns)
0.82	13.9
1.32	*13.9*
1.60	12.4
1.80	7.3 *
2.00	7.1 *

TABLE III.4 The influence of a variation of the reaction temperature on the mean particle size.

Temperature (°C)	Mean particle size d_g (microns)
87	14.1
92	14.1
92	13.1
93.5	13.9
95	*13.9*
95	12.2
96.5	15.0
97.5	14.8
98	13.9
108	21.1 *

III.2.5 The variation of the concentrations of uranium, urea and nitrate ion in a constant ratio

The concentrations of uranium, urea and nitrate ion were varied in a constant ratio at a process temperature of 95 °C. The results are shown in TABLE III.5. The total volume of the liquid was again kept constant.

TABLE III.5 The influence of a variation of the concentrations of uranium, urea and nitrate ion in a constant ratio on the mean particle size.

Starting solution		Urea solution (ml)	Mean particle size d_g (microns)
uranium (g.atom/l)	nitrate ion (gram ions/l)		
0.4	0.8	50	13.9
0.5	1.0	62.6	13.8
0.6	1.2	75	23.1 *
0.7	1.4	87.5	22.9 *
0.8	1.6	100	20.9 *
0.9	1.8	112.5	18.5 *

From the results obtained, it is clear that if there is an influence of the chemical conditions on the mean particle diameter of the precipitate, it is a minor one, except in those cases where a crystalline product is formed.

III.3 The influence of the chemical conditions on the type of product

Apart from the amorphous precipitate, at least three other types of products were obtained:

Type I (FIG. 18), resulted from a standard precipitation in which a low urea content was used. (TABLE III.2).

Type II (FIG. 19), was precipitated under standard conditions, when the urea content was high. (TABLE III.2).

Type III (FIG. 20), was obtained as the end product of a standard precipitation using a high nitrate ion content. (TABLE III.3).

Of course there are several interesting combinations of chemical conditions which might be investigated. In the one series of experiments which was carried out (TABLE III.5), urea and stoichiometric uranyl nitrate were used in a constant ratio but at different concentrations.

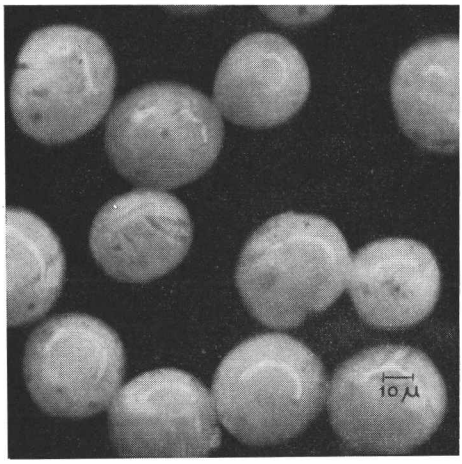

FIG. 18 Type I product.

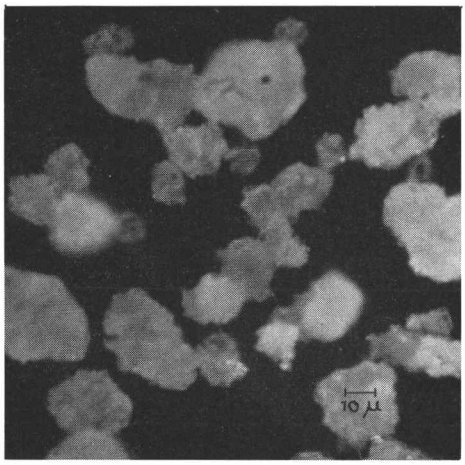

FIG. 19 Type II product.

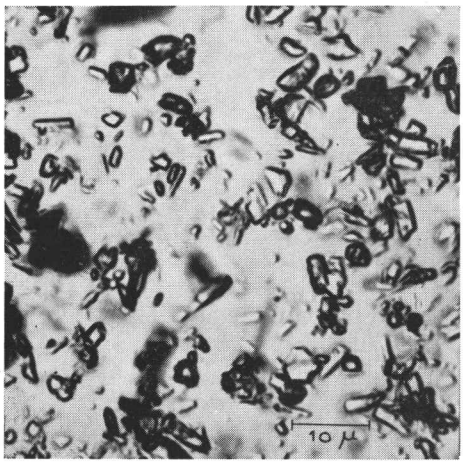

FIG. 20 Type III product.

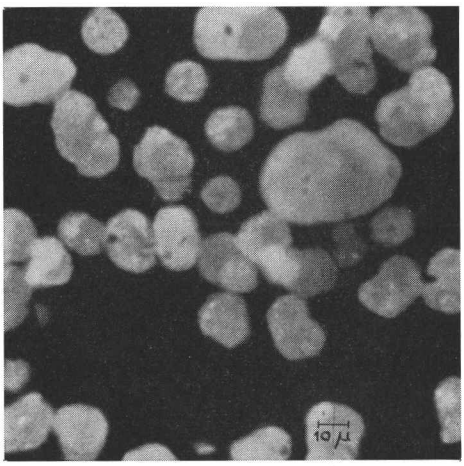

FIG. 21 Type V product.

At the higher concentrations the urea in itself promotes the formation of a type II material, whereas the nitrate concentration is favourable for a type III product. In the experiments it appeared that a type II material is formed. At high temperatures (TABLE III.4) a different material (FIG. 21) is obtained. It will be indicated as type V and it will be discussed further in CHAPTER VII.

Originally, types I, II and III, having distinctly different X-ray patterns, could not be identified, but later type II appeared to be identical with the urea-uranate of GENTILE [49]. The formula for this compound, as proposed by GENTILE is $H_2UO_4 \cdot 2CO(NH_2)_2$ with a theoretical composition of 56.1% U and 28.3% $CO(NH_2)_2$. Types I and III show a great resemblance in X-ray pattern, as they do in chemical composition. The average compositions * are given in TABLE III.6.

TABLE III.6 Average composition of the type A, I, II and III products in the urea process.

Type of product	% U	% NH_4^+	% CO_2	% Urea
A(morphous)	68.5	2.3	4.6	1
I	73	$>1.7^5$	–	–
II	57	–	–	27
III	73	$\leqslant 1.7^5$	–	–

Type I and III seem to consist essentially of $UO_3 \cdot 2H_2O$ (theoretically 73.9% U). In this, part of the water has been replaced by ammonia as will be shown in CHAPTER VII. Also the relation between types I and III will be discussed there in more detail, as will be their X-ray diffraction diagrams.

A remarkable conclusion from the data in TABLES III.1 to III.5 is that the mean particle size of type I and II precipitates is larger than that of type A (amorphous precipitate), probably because crystal growth is not liable to be effected by shear stresses as certainly are flocculation and agglomeration. However, the type III product, which is also crystalline, has a definitely smaller particle size than type A. This was one of the first indications for the fact that type III precipitates are formed by a simultaneous disintegration and crystallization of type A products during the process. If type III can only form from type A, the results of the experiments with high concentrations of uranium, urea and nitrate ion (TABLE III.5) can be understood, because no type A precipitate can occur at high urea concentrations and therefore no type III product is obtained.

* The analytical procedures are presented in the Appendix.

III.4 The evolution of carbon dioxide

In principle, the amount of ammonia generated by the hydrolysis of urea in the system can be measured by determining the amount of carbon dioxide evolved from the system, provided that there is no appreciable change in solubility of the carbon dioxide. In experiments carried out with a vibrational stirrer, the total amount of carbon dioxide was measured as a function of time by means of a gas burette connected to the precipitation vessel (FIG. 11).

The shape of the curves representing the amount of carbon dioxide evolved versus time proved to have a close relation with the type of precipitate. In FIG. 22 such curves are plotted for several different products. In this figure the beginning of the precipitation of the amorphous material is indicated by a circle, whereas the appearance of the crystalline products is marked by a square. The data for these experiments are given in TABLE III.7.

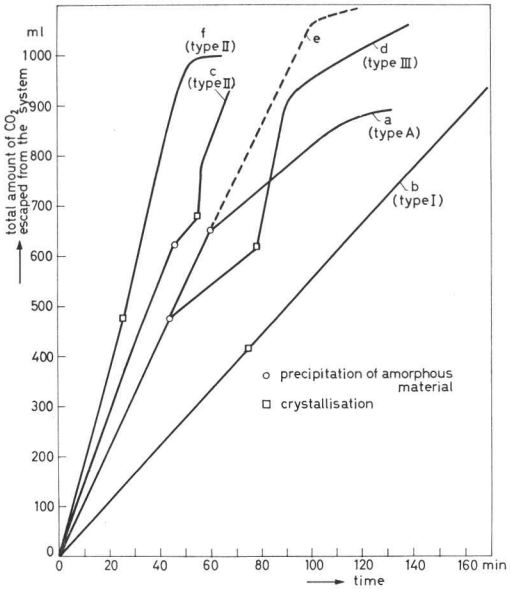

FIG. 22 CO_2 generation curves for the different products.

TABLE III.7 Some typical data of urea processes with different products.

Starting solution		Urea added (ml)	Initial rate of CO_2 generation (ml/min)	pH at time = 0	ml CO_2 until the moment of precipitation	Type of product	Curve in FIG. 22
moles U/l	m.Eq. NO_3^-/l						
0.4	1.32	50	10.9	2.32	650	A	a
0.4	1.32	25	5.5	2.78	415	I	b
0.4	1.32	65	14.3	2.30	620	II	c
0.4	2.00	50	10.9	2.68	475	III	d
0.7	1.40	87.5	18.7	2.50	480	II	f

starting solution: 100 ml
total volume: 150 ml
temperature: 95 °C

For the interpretation of the curves in FIG. 22 it should be realized, that during the complete process only 9 to 10 percent of the urea is decomposed. The decrease in the rate of evolution of carbon dioxide is, therefore, only a very slight one. For curve b however this decrease in rate was not observed.

Curve a, representing the precipitation of the amorphous product, shows a slightly decreasing rate of carbon dioxide generation until the first precipitate appears (59 min). At this point the rate of carbon dioxide generation suddenly decreases to less than half the preceding value, and at the end of the process when the pH has a value of about 6, it further decreases to zero.

At a low urea concentration the rate of carbon dioxide development is nearly constant (curve b) with possibly a slight increase from the moment the crystallization starts. A type I product is obtained.

Curve c – for relatively high urea concentrations – has a shape corresponding to that of curve a for the amorphous precipitate until a few minutes after the first precipitation. The precipitate then becomes crystalline and carbon dioxide is evolved at a rate considerably above the one at the moment of precipitation. After the carbon dioxide, withheld in the system during the precipitation, has escaped, the rate of generation of carbon dioxide before the precipitation is restored. The crystalline precipitate is of type II.

Precipitation of a type III product shows a carbon dioxide curve of the shape d, where an increase in the rate of gas evolution occurs in a later stage of a type A curve. As will be seen later, the delay in crystallization depends on the nitrate ion concentration.

Depending on chemical conditions, the break in curve c (high urea content) can disappear as is shown in curve f where the uranium and nitrate concentrations are also high.

Considering these curves up to the point of forming the first product the following conclusions can be drawn:

1. At a constant temperature the rate of generation of carbon dioxide is proportional to the concentration of urea and independent of the type of product which is formed in the process. The curves therefore show a slight curvature which accounts for the decrease in urea concentration during the process. In CHAPTER V however it will be shown that a large increase of the NH_4NO_3 content decreases considerably the rate of hydrolysis of urea.
2. Under the conditions used for the experiments, the hydrolysis of urea is independent of the pH. It can be described as a first order reaction. This is in agreement with measurements of SHAW and BORDEAUX [50] for the hydrolysis of urea in water and in 0.02 N H_2SO_4 solutions both at 95 °C. From the lower part of curve a a reaction constant $k = 1.91 \times 10^{-5}$ is found, compared to 2.20×10^{-5} as given by SHAW and BORDEAUX. Accordingly, the total

amount of carbon dioxide generated until time t (in minutes) at 95 °C can be derived from

$$CO_2 = 398.2 \times G \times (1 - e^{-1.146 \times 10^{-3} \times t}) \text{ ml}$$

where G is the initial weight of urea (in grams) in the system and 398.2 the number of ml of carbon dioxide of 20 °C which can be generated from 1 gram of urea. For the standard procedure (25 grams of urea in 150 ml solution) this relation is represented graphically as curve e in FIG. 22. It should be borne in mind that the experiments have not been carried out for the purpose of measuring the rate of hydrolysis of urea, and that consequently there is a slight uncertainty about the exact temperature.

3. The experiments listed in TABLE III.4 have been used to estimate the activation energy of the hydrolysis of urea as there might be the possibility of catalytic effects. The rate of carbon dioxide generation at $t = 0$ has been plotted versus the inverse of the absolute temperature in FIG. 23. From the slope of this curve an estimate of the activation energy E can be made. The line drawn represents an activation energy of 31.6 Kcal/mole. A more accurate calculation results in the ARRHENIUS plot of FIG. 24 from which an activation energy of 32.0 Kcal/mole and a frequency factor $f = 2 \times 10^{14}$/sec is deduced. SHAW and BORDEAUX [50] give a value of 32.7 Kcal/mole and $f = 5 \times 10^{14}$/sec. The agreement is again satisfactory and the conclusion is that an acceptable accuracy is obtained in determining the rate of hydrolysis of urea (and the amount of ammonia formed) by measuring in a simple way the total amount

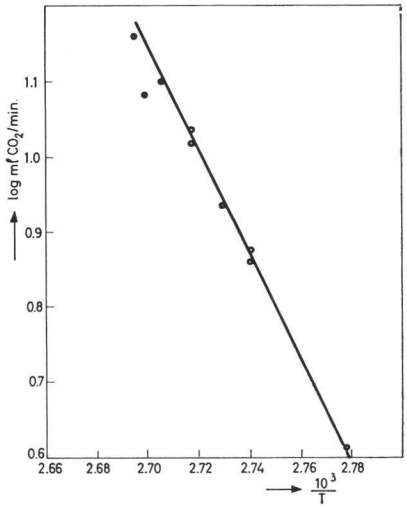

FIG. 23 Dependence of the rate of CO_2 generation on the temperature.

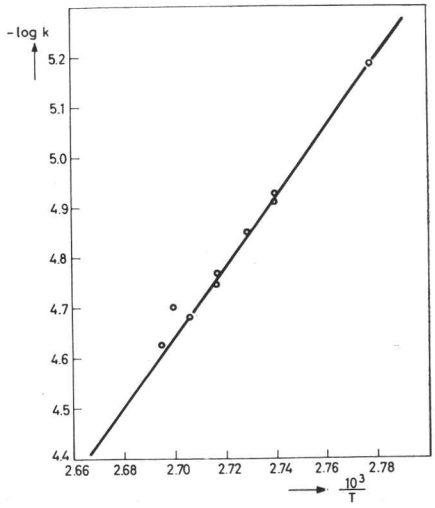

FIG. 24 Arrhenius plot for the hydrolysis of urea in the urea process.

of carbon dioxide evolved from the system. No catalytic activity could be deduced from these results.

4. The total volume of carbon dioxide generated at the moment that the first product is formed depends mainly on the starting pH of the solution and on the uranium concentration as may be seen from TABLE III.7. This implies that quantitative comparison of the curves of the generation of carbon dioxide measured at the same uranium concentration (a, b, c and d in FIG. 22) can only be made after the points of the appearance of the first product have been taken as a new origin.

Once precipitation has started, a discontinuous decrease of the rate of carbon dioxide evolution always indicates the incorporation of carbon dioxide in the precipitate, resulting in the formation of a type A product (curve a, FIG. 22). From this moment approximately half the amount of carbon dioxide escapes from the system. The rest is found quantitatively in the precipitate, thus proving that the hydrolysis of the urea has not changed. However, in the case of high nitrate ion concentrations (curve d) the precipitation of the type A product originally formed stops, as can be seen from a sudden increase in the rate of carbon dioxide evolution. This is even higher than can be expected from pure urea hydrolysis, and it indicates that carbon dioxide was expelled from the type A material which had already precipitated. The end product does not contain carbon dioxide any more and it has a crystalline structure (type III).

The rate of hydrolysis of the urea in the system proves to be almost equal to the rate of evolution of carbon dioxide before the point where the first product appears. This part of the curve can be extended (e), taking into account that the hydrolysis of the urea decreases rapidly at a certain pH, which marks the end of the process. By comparing this curve with the one measured during the process, information is obtained about changes in the product during the process. When an amorphous precipitate is formed the slope of the curve decreases suddenly to somewhat less than half the original slope, as already stated. We have seen that in a later stage of the process, this slope may increase again. If it becomes larger than the initial one this means that carbon dioxide is expelled from the already existing amorphous precipitate which crystallizes then, because the amorphous state can only exist in the presence of CO_2. This will be shown later on.

The degree to which this crystallization takes place can be calculated from the extra amount of carbon dioxide above the initial rate and from the known carbon dioxide content and the total amount of the precipitate present. In not a single experiment an indication was found, that the precipitation of a type A product was continued after crystallization had started.

In a few cases where an amorphous precipitate was found which crystallized in a later stage it was observed that the evolution of carbon dioxide increased

at the point of crystallization to exactly the initial rate. In the end product the total amount of amorphous precipitate was equal to the amount formed between the beginning of the precipitation and the beginning of the crystallization. This is in full agreement with the conclusion which should be drawn from the carbon dioxide curve, that the crystalline product was formed without interference with the existing amorphous precipitate.

Microscopically the crystallization of an amorphous precipitate can be observed easily by the occurrence of birefringency.

Some type II curves have a shape similar to those of a type III product, the only difference being that, in general, the time between the beginning of the precipitation and the crystallization is much shorter (curve c, FIG. 22).

A slight catalytic effect of the crystalline material might cause the increase of the carbon dioxide evolution right from the moment of crystallization (curve f). It might also explain the shape of curve b which is practically a straight one.

Summarising the usefulness of the carbon dioxide curves, it can be said that the method provides, by simple means, the possibility to check the precipitation process accurately. As the gas evolution before the precipitation can be predicted from the urea content and the temperature, it can be used as a check for leaks in the system. After the precipitation has started it provides instantaneous information about the type of precipitate and about changes in composition of the precipitate during precipitation. The accuracy of the method, as tested by calculation of the activation energy, appears to be good enough for obtaining a fast check on what is happening in the process.

III.5 The nature of the type A precipitate

The amorphous (type A) precipitate has not been described in the literature. Therefore some experiments were carried out to establish the identity of this product because a better knowledge of the precipitate seemed to be essential for a good understanding of the process.

TABLE III.8 Composition of some amorphous precipitates. a. lowest and b. highest carbonate content; c. standard procedure.

Sample	% U	% CO_2	% NH_4^+	mole CO_2 / gr.atom U	gram ion NH_4^+ / gr.atom U	gram ion NH_4^+ / mole CO_2
a	67.6	4.15	2.05	0.33	0.37	1.07
b	68.9	5.05	2.6	0.40	0.50	1.26
c	68.5	4.6	2.3	0.36	0.44	1.22

From X-ray diffraction work it appeared that the precipitate had an amorphous structure. The chemical analysis of the product however, provides more information. The composition is dependent on the process variables, but remains between rather narrow limits.

In TABLE III.8 the analyses of three samples are given.

Samples a and b represent the lower and upper limits in carbon dioxide and ammonia content obtained under extreme conditions in any amorphous product in the urea process * whereas c has the composition of precipitates in a standard procedure. All samples may contain up to 1% urea.

It is clear that the product is not a single compound, but a mixture or a compound with a variable composition, which can only exist within rather narrow limits of variation. A decrease of the carbon dioxide content to a value below about 4% causes crystallization of the precipitate even at room temperature. This could be demonstrated by dialysis and electrodialysis of the material. The compound thus obtained was crystalline and its composition was $UO_3 \cdot 2H_2O$ which – depending on the exact conditions – might contain some ammonia. The type A precipitate was therefore considered also to exist essentially of $UO_3 \cdot 2H_2O$, possibly with some ammonia. The crystallization of this compound might then be prevented by the presence of carbonate groups, which thus act as stabilizers of the amorphous form.

The question then arises in what chemical form the carbonate is present. It might be as an ammonium carbonate or as a bicarbonate, intimately mixed with the uranium compound, or directly attached to the uranyl groups.

BULLWINKEL [51], MCLAINE [52] and BLAKE [53] investigated the dissolution of UO_3, UO_2CO_3 and "ADU" in carbonate and bicarbonate solutions. They found that two mono-uranyl-carbonate complexes could be formed, a tri- and a dicarbonate:

$$UO_2(CO_3)_3^{4-} \text{ and } UO_2(CO_3)_2^{2-}$$

The equilibrium constants for the formation are [51]

for $UO_2^{2+} + 3CO_3^{2-} \rightleftharpoons UO_2(CO_3)_3^{4-}$ $K = 2 \times 10^{18}$

and for $UO_2^{2+} + 2CO_3^{2-} + 2H_2O \rightleftharpoons UO_2(CO_3)_2(H_2O)_2^{2-}$ $K = 4 \times 10^{14}$

From these constants it is evident that the complexes are very stable and that carbonate ions have a strong affinity for uranyl groups.

Accordingly we suppose that the type A precipitate consists of a skeleton of UO_2^{2+} groups to which OH^- ions, water molecules, probably some ammonia molecules and carbonate ions might be attached. The electrical neutrality might be preserved by exchangeable ammonium ions distributed throughout

* At room temperature amorphous precipitates with higher ammonia and carbon dioxide content can be obtained by the action of NH_3 and CO_2 on a uranyl nitrate solution.

the structure. A certain minimum ratio of carbonate to uranyl groups is required to block the crystallization in the structure. We suppose that the carbonate groups are attached directly to the UO_2^{2+} groups in the same way as in the uranyl carbonate complexes. Apart from the high equilibrium constants of formation of these complex uranyl carbonates there is another indication that a similar bond exists between the UO_2^{2+} and the CO_3^{2-} in the amorphous precipitate. When the ammonium – or uranyl carbonates are placed in a vacuum desiccator above sulphuric acid and concentrated NaOH, the samples loose ammonia and carbon dioxide rather fast. However, when the same experiment is carried out either with tetra ammonium uranyl tricarbonate or with the amorphous precipitate, no such loss is observed.

In the formation of the amorphous precipitate the urea has a very specific role, which according to our experiments can not be taken over by a combination of CO_2 and NH_3. It is known that urea forms a chemical compound with UO_3 and water, which was been called urea-uranate [49]. Through hydrolysis of the urea part, this compound can be converted into $UO_3 \cdot 2H_2O$ by boiling water [49]. We suppose that the occurrence of different products at varying urea concentrations of the starting solution is caused by the relatively slow rate of hydrolysis of this urea-uranate combination. If the conditions are such *e.g.* with a high concentration of urea, that the rate of formation of the solid is far higher than that of its hydrolysis, a crystalline di-urea-uranate $[(NH_2 \cdot CO \cdot NH_3^+)_2UO_4^{2-}]$ can be formed. It is our compound II, which has this composition and the according X-ray diagram. The rate of formation of this product is then sufficiently higher than the rate of hydrolysis of the "urea-uranate molecules". In this respect it should be borne in mind that a high rate of formation also means a short period during which the compound is in contact with the liquid, before it is covered by a subsequent layer. If however, with a low urea concentration the rate of formation of the solid compound is very low, the rate of hydrolysis of urea is sufficiently higher than the rate of crystallization and a CO_2-free crystalline product is obtained. The product is of the type I.

In intermediate cases, where the rate of solids formation and of hydrolysis of urea are of equal magnitude, the product contains partly hydrolyzed urea, it is of a variable composition and has an amorphous character.

III.6 The stability of the type A precipitate

There are two facts which might indicate that the type A precipitate is an unstable modification:

1. The precipitate is amorphous, and under certain conditions crystallization is observed.

2. Often small regions inside the particles are birefringent, showing the presence of crystallites which may grow.

It therefore seemed appropriate to investigate the stability of the type A precipitate in the presence of the crystalline types. Seeding experiments were carried out for this purpose. It will be shown in CHAPTER IV that the stirrer may exert an influence on the type of precipitate obtained, especially at high amplitudes or at high rotational speeds. To prevent the introduction of such effects into the experiments, a rotating stirrer of the type described in CHAPTER II (FIG. 13) was used at an intermediate speed of 600 to 700 r.p.m.

All further conditions were identical with those in the standard procedure, the total volume being 150 ml. Thirty minutes after the precipitation started 500 mgr of one of the crystalline types of precipitate was introduced as a dry powder. At that moment somewhat more than half the total amount of uranium had precipitated and, from the time the first precipitate appeared, the pH had increased by less than 0.2 pH units to nearly pH = 5. After complete precipitation the solid material was filtered, dried with acetone and analyzed.

The type I and III seeding materials contained about 1 and 1.5 mole percent of type II precipitate respectively, whereas the type II material contained 10 mole percent type A precipitate.

The results of the experiments are given in TABLE III.9. To see whether the small increase in uranium content caused by the introduction of seed material had a separate effect, a blank was included in which uranyl nitrate hexahydrate (UNH) crystals were introduced.

TABLE III.9 Seeding experiments at standard conditions.

	Composition of the end product			
Seeding material	% U	% NH_4^+	% CO_2	% urea
0.5 grams UNH	68.4	2.4[5]	4.8	1.0[5]
0.5 grams I	68.3	2.3[5]	4.7	1.6[5]
0.5 grams II	66.7	2.1	4.2	4.1
0.5 grams III	68.6	2.3[5]	5.0	1.0[5]

From the results it is seen that only by seeding the system with type II material a slight increase in the type II content was obtained. It seems, therefore, that the type A precipitate is the stable product under standard conditions. Further evidence that the type A product is not an unstable one can be derived from the observation that in many cases mixed precipitates are obtained due to a slight change in reaction conditions during the process.

In no case however, could a simultaneous growth of two types of product be proved. This does not mean, that it is impossible to grow several types successively. There are many examples of such a behaviour in this thesis.

CHAPTER IV

THE INFLUENCE OF THE STIRRER SPEED ON THE CRYSTALLIZATION OF THE AMORPHOUS PRODUCT

IV.1 Introduction

In CHAPTER II it was shown that the speed of the stirrer in the process for the production of the amorphous material has a great influence on the mean particle size of the product. The type of product obtained was determined by the chemical conditions of the process, as was discussed in CHAPTER III. However, it has been remarked incidentally in both chapters that, under certain conditions, a high stirrer speed resulted in the production of a crystalline product instead of the intended amorphous one.

This effect, which is the subject of this chapter, was quite remarkable, and it added a considerable complication to the original precipitation experiments. Additionally, it limits the range of particle sizes of the amorphous material which can be prepared with a given stirrer. This limitation depends on the type of stirrer, as can be seen by comparing the results of a vibrational and a rotational stirrer (CHAPTER II.4.1 and II.4.2).

In this chapter, experiments are discussed which led to the conclusion that the stirrer influences the chemical conditions in the system more or less mechanically, thereby favouring the production of crystalline products. As a result of these investigations, means were found to decrease, for amorphous products, the lower limit of the particle size imposed by the design of the stirrer.

IV.2 Preliminary experiments

A few preliminary experiments were carried out with different methods of stirring, and the products obtained were identified. Standard conditions were used in all cases: 100 ml of 0.4 M uranyl nitrate solution were adjusted to a pH of 2.7 by the addition of ammonia, heated to 95 °C, and then 50 ml 8.3 M urea solution of 95 °C was added.

Four vibrational stirrers were tested, only differing by their stirrer blade. They are shown in FIG. 25, and accordingly will be referred to as a, b, c and d respectively. The amplitude of all these stirrers, measured at their shaft, was the same (1.3 to 1.4 mm). The frequency of the stirrer was 100 cycles in all cases.

Three rotating stirrers were used, the helical stirrer described in CHAPTER II

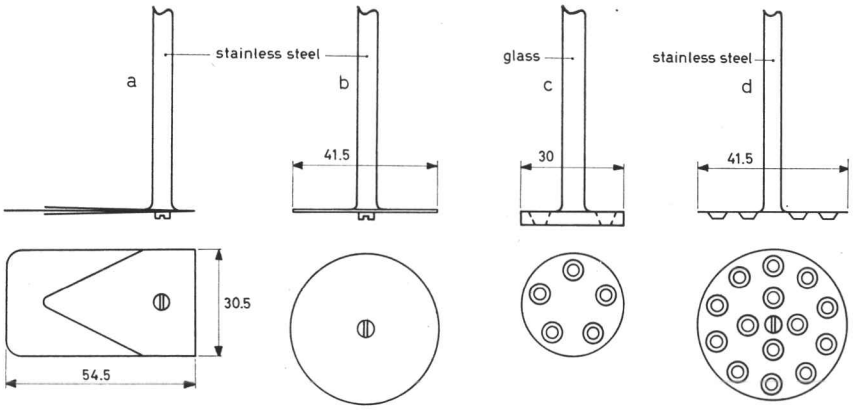

FIG. 25 Different types of stirrer blades used with the vibrational stirrer. Measures in mm.

(FIG. 13), a homogenizer * and a conventional propeller stirrer. The results of these experiments are given in TABLE IV.1.

TABLE IV.1 Habit of some products obtained under standard conditions with different stirrers.

Method of stirring		Type of product	Method of stirring		Type of product
Vibrational:			*Rotational:*		
stirrer blade	a	crystalline	Atomix Mill	(18000 r.p.m.)	crystalline
stirrer blade	b	$^2/_3$ amorphous, $^1/_3$ crystalline	Helix	(700 r.p.m.)	amorphous
			Helix	(1700 r.p.m.)	crystalline
stirrer blade	c	amorphous	Propeller	("low speed")	amorphous
stirrer blade	d	amorphous	Propeller	("high speed")	crystalline

From the results obtained with the rotational stirrer it is seen that under the same chemical conditions a high stirring speed promotes the production of a crystalline modification. The same seems to hold for the vibrational stirrers: type a is expected to cause the largest shear stresses because of the enlarged amplitude at the tip of the stirrer blade. Types c and d, through their pumping action, might well cause the lowest shear stresses.

The crystallization is more a question of shear stresses in the liquid than of pure mixing. With an Atomix Mill crystallization occurs even at a low stirrer speed where the mixing action is poor. This type of stirrer, however, is constructed to give high shear stresses in the liquid. We suppose that such a stirrer causes cavitation and bubble nucleation thereby lowering the carbon dioxide concentration in the liquid to such an extent that the total amount of uranyl

* A type 20St Atomix Mill was used, manufactured by Ing. Gerhard Lahl K.G. (Germany).

bound carbonate left in the solid is too low to stabilize the amorphous product. In other words, the stirrer lowers the degree of saturation of the liquid with respect to carbon dioxide and thus "extracts" carbon dioxide from the uranyl carbonate complexes.

IV.3 The stability region of the amorphous product for two different stirrers

In CHAPTER III, TABLE III.2, experiments were described which show the influence of the urea concentration on the type of precipitate obtained with a vibrational stirrer, the other conditions being standard. It was found that at intermediate urea concentrations the amorphous product was obtained whereas at a low and at a high concentration crystalline products (I and II respectively) occurred. This situation seemed to be an obvious example to study the influence of the stirrer over the region of stability of the type A precipitate.

For these experiments two vibrational stirrers were used with the same constant amplitude of the shaft: types a and d of FIG. 25. Except for the urea concentration, all conditions were standard again. The results are given in TABLE IV.2 and shown diagrammatically in FIG. 26.

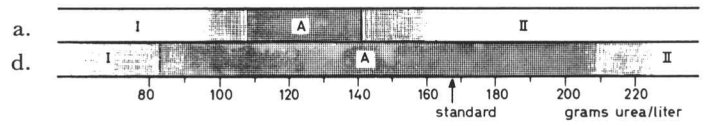

FIG. 26 Influence of the stirring rate on the region of stability of the amorphous precipitate.

TABLE IV.2 The influence of the type of stirrer on the product at different urea concentrations.

Urea concentration grams/litre	Type of product obtained: type of stirrer d	a
83	I(duplo A)	–
100	–	I+III
108	A	–
117	–	A
133	A	A
150	A	II+III
167	A	II
183	A	II
200	A	II
217	II	–

Although the shift in the lower limit of the stability range for the type A precipitate is not very significant, the reduction of the total range of stability obtained with stirrer a is remarkable. This can only be due to the influence of the stirrer.*

Similar phenomena are observed with rotational stirrers (*c.f.* IV.5). Because the mean particle size as well as the limit of crystallization are determined by the design and the speed of the stirrer, there is a minimum for the mean particle size for every stirrer. The minimum size may differ from one case to another. An example can be derived from FIG. 14 and 15, where it was shown that with the vibrational stirrer smaller amorphous particles could be produced than with the rotational one.

IV.4 The carbon dioxide content of the liquid

A direct check on the hypothesis that a stirrer running at a high speed lowers considerably the carbon dioxide content of the liquid, would be to measure that carbon dioxide content as a function of the stirrer speed. This procedure, however, is very complicated because, at the relatively low pH of the system (around pH = 5) and at the high temperature, the carbon dioxide content is very low, and at this high temperature 5–10 ml of carbon dioxide is generated per minute. During the time needed to draw a sample and cool it down, too large changes in the carbon dioxide content of the liquid occur unless very elaborate precautions are taken.

Therefore, it was preferred to demonstrate that the above described effect of crystallization can be provoked by lowering the carbon dioxide content of the liquid during the process by gas underpressure or by stripping. All the experiments were carried out under standard conditions and use was made of a normal vibrational stirrer (type d of FIG. 25) in the apparatus shown in FIG. 11. A water cooler was used to restrict the escape of water vapour. Normally, these conditions assure the precipitation of the amorphous material.

In the first experiment of this series, the gas inside the precipitation vessel was kept at a constant pressure of 44 cm water column below atmosphere. As a result an amorphous product was obtained which, however, contained about 10% of the type II material. The effect is significant.

A more efficient way of lowering the carbon dioxide concentration in the liquid is stripping with preheated air at a rate of 1 to 2 litres per hour. In that

* The reason why in some cases the type I and II products are accompanied by the type III material, was still unknown. In CHAPTER V arguments will be forwarded to show that both type A and type III products might occur in the region between types I and II. The question which one is formed would depend then on the carbon dioxide content of the liquid. This might explain the fact that III is always formed from A and that III is found in the type I and II products at the limits of the amorphous region.

case, the product consisted mainly of the type II material. In order to investigate whether the mere presence of extra gas in the system caused crystallization, carbon dioxide was used as the stripping gas for the liquid under the same conditions. The resulting product consisted mainly of type II precipitate.

Two further experiments were carried out then, under exactly the same conditions as those of the two previous ones, except that the stirrer was absent. If air was bubbled through the system, the final product was a type II precipitate. In the other experiment carbon dioxide was used instead of air and an amorphous precipitate was obtained.

From these four experiments it can be concluded that the stripping action of air on the system causes crystallization. The fact that for the combination of stripping with carbon dioxide and the vibrational stirrer crystallization is observed, indicates that also there extra carbon dioxide is removed from the system, thereby lowering the carbon dioxide content of the liquid. This is only possible if the liquid was supersaturated with carbon dioxide, because in that case the carbon dioxide introduced provides the necessary nuclei for the escape of more carbon dioxide from the system. A comparable observation was made in standard precipitations if the stirrer was stopped after the precipitation had

TABLE IV.3 Habit of the products obtained with different amplitudes of the stirrer and at different overpressures of carbon dioxide. (A = amorphous, II = type II product)

CO_2 overpressure (m W.C.)	Amplitude in mm						
	1.00	1.12[5]	1.25	1.50	1.75	2.00	2.50
0	A	II	II	II	–	II	–
1.05	–	–	A	II	–	II	–
1.30	–	A	–	–	–	–	–
1.50	–	–	A	–	–	–	–
1.55	–	–	–	II	–	–	–
1.68	–	A	–	–	–	–	–
1.70	–	–	–	II	–	–	–
1.75	–	A	–	–	–	–	–
1.80	–	–	–	A	–	–	–
1.86	–	–	–	A	A	A	A

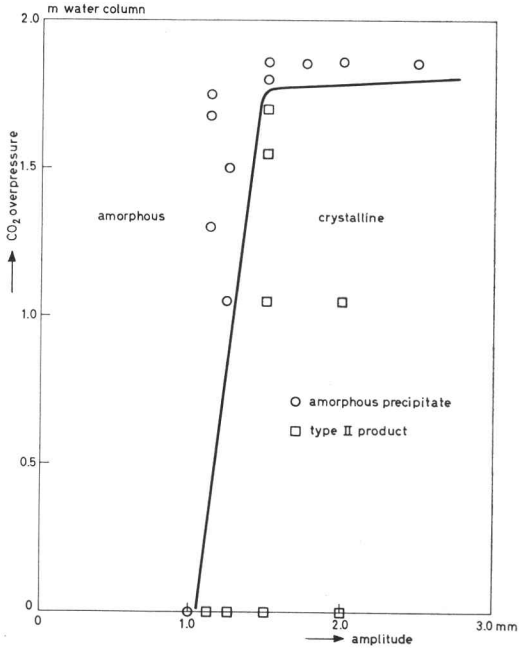

FIG. 27 Carbon dioxide overpressure required to prevent crystallization of the amorphous precipitate at different amplitudes of the stirrer.

started. Although the rate of hydrolysis of urea was constant, no carbon dioxide was evolved from the system. Especially in such cases where the stirrer was stopped for at least 5 to 10 minutes, a fast crystallization with a strongly increased evolution of carbon dioxide was observed, in some cases, on restarting the stirrer. If the extra amount of carbon dioxide accumulated in the liquid whilst the stirrer was stopped was large enough, it lowered on release the normal degree of supersaturation.

It is not yet understood why in these and the following experiments several different types of crystalline precipitates were obtained.

In the preceding pages, it has been shown that lowering the carbon dioxide content of the liquid has the same effect as a high stirring rate. It was therefore concluded that, apart from the shear stresses on the flocculating particles (discussed in CHAPTER II), the action of the stirrer is also that of decreasing the carbon dioxide concentration in the liquid.

A few other experiments were carried out to demonstrate that, on the other hand, an overpressure of carbon dioxide could compensate a too high stirring rate in the preparation of the amorphous product. For these experiments a type a vibrational stirrer (FIG. 25) was chosen. At an initial urea concentration of 137 grams/litre, the other conditions being standard, the amorphous precipitate was obtained with amplitudes up till 1.1 mm whereas above this limit a crystalline type II product was formed.* By applying an overpressure of carbon dioxide gas of nearly 2 meters water column, this transition point could be shifted from an amplitude of 1.1 mm to more than 2.5 mm.

These results, presented in TABLE IV.3 and in FIG. 27, in which amorphous precipitates have been indicated by circles, crystalline products by squares, are rather surprising on first sight. Although one might argue about the exact position of the curve, it is clear that there are two different regions. Below an overpressure of 1.80 m W.C. of carbon dioxide, the stirrer exerts a large influence on the system by extracting carbon dioxide. However at 1.80 m W.C. overpressure this influence becomes relatively small or even zero. The explanation might be that this overpressure is the equilibrium gas pressure for the minimum concentration of carbon dioxide in the liquid, required to precipitate an amorphous product. It is clear that at this overpressure cavitation cannot enlarge any more the extraction of carbon dioxide from the liquid.

Another example of this carbon dioxide compensation is found in the precipitation of type III material at high nitrate ion concentrations. The experiments given in TABLE IV.4 show that under standard conditions a crystalline product is obtained at a nitrate ion concentration of 1.2 gram ions per litre. However,

* In these experiments amorphous products containing less than 5% of a crystalline material were considered to be type A. All type II products contained less than 2% of the type A material.

even at 1.3 gram ions NO_3^-/l a nearly amorphous material is formed provided that a stirrer with a lower stirring rate is used. The same effect can be obtained with the vibrational stirrer (type d) by applying an overpressure of carbon dioxide to the system. These experiments show that the crystallization of the initially amorphous precipitate into a type III product at high nitrate ion concentrations may be due to a decrease of the carbon dioxide content of the liquid during the process.

TABLE IV.4 The influence of a carbon dioxide overpressure on the formation of a type III product.

Nitrate ion concentration (gram ions/litre)	Carbon dioxide overpressure (cm water column)	Type of stirrer	Composition of the product
1.2	0	vibrational (type d)	III
1.3	0	rotational at 700 r.p.m.	95% A + 5% II
1.2	90	vibrational (type d)	50% A + 50% II
1.2	200	vibrational (type d)	95% A + 5% II

IV.5 The carbon dioxide content of the solid

A decrease in the carbon dioxide content of the liquid may cause the formation of a crystalline product instead of an amorphous one. If the amorphous precipitate cannot exist unless enough uranyl bound carbonate is incorporated for stabilization, it is likely that crystallization will be caused by a decrease in concentration of the carbonate below a critical value. It should be expected that there is a direct relation between the carbon dioxide content of the liquid and that of the solid. Therefore, the influence of the stirring rate might well become evident from the carbonate content of the precipitate.

In the three series of experiments, carried out to investigate the influence of the stirrer speed on the mean particle size (CHAPTER II) the composition of the precipitate was determined as a function of that stirrer speed for the vi-

TABLE IV.5 The influence of the amplitude of a vibrational stirrer on the composition of the amorphous precipitate.

Amplitude (mm)	Analysis of the precipitate			
	% U	% CO_2	% NH_4^+	mole CO_2/mole U
0.7[5]	68.9	4.7[5]	2.4	0.373
1.0	68.7	4.7[5]	2.4[5]	0.374
1.2[5]	68.9	4.6	2.4[5]	0.361
1.5	68.9	4.6[5]	2.4	0.365
1.7[5]	69.0	4.6	2.4	0.361
2.0	69.2	4.6	2.4	0.359

TABLE IV.6 The influence of the speed of the small helical stirrer on the composition of the amorphous precipitate.

Stirrer speed (r.p.m.)	Analysis of the precipitate			
	% U	% CO_2	% NH_4^+	mole CO_2/mole U
0	69.1	4.9	2.6	0.384
200	68.2	4.9	2.5	0.388
300	68.4	5.0	2.4	0.395
350	68.9	4.9	2.5	0.385
500	68.5	4.8	2.3[5]	0.379
700	68.3	4.8	2.4	0.380
900	68.2	4.8	2.3[5]	0.381
1100	68.5	4.6[5]	2.3[5]	0.367
1300	67.9	4.7[5]	2.3[5]	0.378
1500	67.6	4.1[5]	2.0[5]	0.332
1700 *	60.9	0.2	0.4	0.018

* This sample was a type II precipitate with 20.7% urea.

brating and the two rotating stirrers respectively. All conditions were standard, the total volume of the liquid being 1350 ml for the enlarged helical stirrer and 150 ml for the other ones. TABLE IV.5 contains the results obtained with the type d vibrational stirrer (FIG. 25), TABLE IV.6 gives the same data for the small rotating helical stirrer with draft tube (FIG. 13), and TABLE IV.7 for the enlarged one.

TABLE IV.7 The influence of the speed of the enlarged helical stirrer on the composition of the amorphous precipitate.

Stirrer speed (r.p.m.)	Analysis of the precipitate			
	% U	% CO_2	% NH_4^+	mole CO_2/mole U
200	69.1	2.4[5]	4.98	0.390
300	68.9[5]	2.6	4.88	0.383
400	68.7	2.4	4.78	0.376
500	68.4	2.3[5]	4.68	0.370

In all cases the decrease in carbon dioxide content of the amorphous precipitate is evident although it is relatively small. The CO_2/U mole ratios are shown graphically in FIG. 28, 29 and 30 as a function of stirrer speed.

In CHAPTER II a linear relationship was suggested between the inverse of the mean particle diameter of the precipitate and the stirrer speed. From FIGURES 28 to 30 a decrease of the CO_2/U mole ratio in the precipitate with increasing stirrer speed is evident and a linear relationship seems acceptable. If both relationships are truely linear, a linear relationship must also exist between the inverse of the mean particle diameter and the CO_2/U mole ratio

in the precipitate. In FIG. 31 the experimental data are marked for all three stirrers and for all experiments. When the same relation between $1/d_g$ and the CO_2/U mole ratio is calculated from the straight lines drawn in FIG. 14, 15 and 16 on the one hand, and FIG. 28, 29 and 30 on the other hand, the lines shown

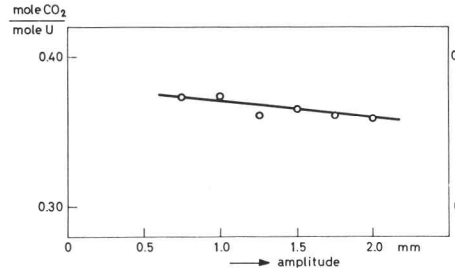

FIG. 28 CO_2/U mole ratio of the amorphous precipitate at different amplitudes of the vibrational stirrer.

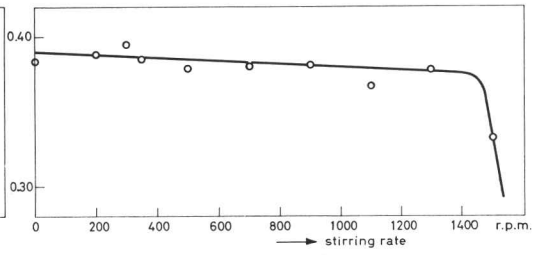

FIG. 29 CO_2/U mole ratio of the amorphous precipitate at different rotational speeds of the smaller helical stirrer.

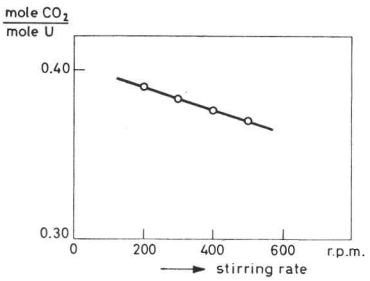

FIG. 30 CO_2/U mole ratio of the amorphous precipitate at different rotational speeds of the enlarged helical stirrer.

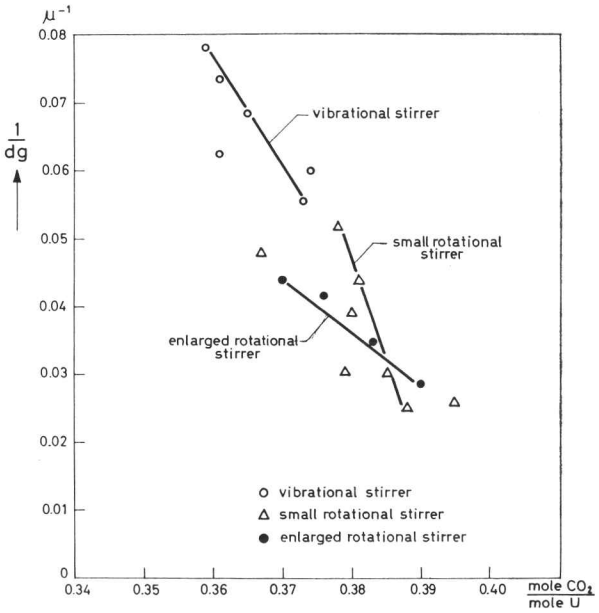

FIG. 31 Correlation between the inverse of the geometric mean diameter d_g and the CO_2/U mole ratio of the amorphous precipitate for three different stirrers.

in FIG. 31 are obtained. The agreement with the measurements is good for the enlarged helical stirrer, acceptable for the vibrational stirrer and bad for the small helical stirrer. The discrepancies may be due to inaccuracies of the chemical analysis and to the irreproducibility in the stirring conditions of the experiments, especially with those on a small scale. These difficulties could be over-

come to some extent by enlarging the experiments to a liquid volume of, for example, 1.5 litres and by using exactly the same geometry during each series of experiments.

Considering the lines drawn in FIG. 31, one might suppose that under the conditions used the relationship between $1/d_g$ and the CO_2/U mole ratio is the same for the vibrational and the small helical stirrer. At the higher values of $1/d_g$ the curve for the small helical stirrer is limited. There is a critical stirring rate above which crystallization occurs. This can not be caused by a too low overall CO_2/U ratio, but must be due to the design of the stirrer. The line for the enlarged helical stirrer might be somewhat different. The reason could be that the total volume of the liquid from which the carbon dioxide has to be extracted is 9 times larger than in the other series. The decrease of the carbon dioxide content of the liquid should be expected to be more sensitive to total volume than the mean particle diameter. To investigate this effect, additional experiments should be carried out with the same stirrers at different total volumes.

The experiments described demonstrate that the carbon dioxide content of the precipitate decreases with increasing stirrer speeds, thereby supporting the hypothesis that the stirrer speed controls, to some extent, the carbon dioxide content of the liquid.

IV.6 The influence of the temperature on the critical stirring rate

Another method to decrease the carbon dioxide content of the liquid is to increase the temperature. It is difficult to predict how other mechanisms in the process are effected by an increase in temperature and whether they might interfere with the pure solubility and saturation effect of the carbon dioxide.

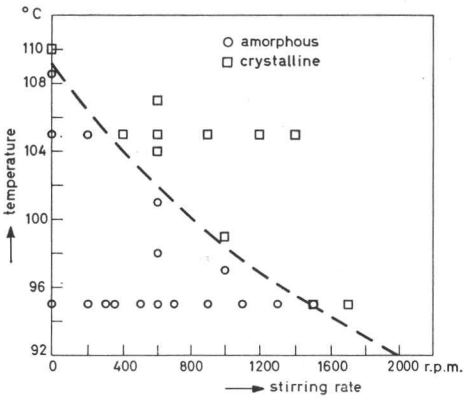

FIG. 32 Critical crystallization temperature of the amorphous precipitate at different rotational speeds of the smaller helical stirrer.

All the experiments which were carried out with the small helical stirrer under standard conditions, except for the temperature and the stirring rate, are collected in FIG. 32. The amorphous products again are indicated by circles and the crystalline ones by squares. A broken line indicates tentatively the separation between the occurrence of amorphous and crystalline products.

It should be pointed out that not all the crystalline precipitates in the diagram are of the same type. In CHAPTER VII it will be shown that there are some small differences. From the graph it is seen that the critical stirring rate decreases with an increasing temperature. Also this effect might be ascribed to a decrease in the carbon dioxide content of the liquid and thus to a decrease in uranyl bound carbonate in the precipitate. This may be partly compensated by the increase in evolution of carbon dioxide as a consequence of the increased rate of hydrolysis of urea at higher temperatures.

CHAPTER V

THE CHEMISTRY OF THE CRYSTALLIZATION

V.1 Introduction

In the preceding chapters several aspects have been discussed of the crystallization of initially amorphous precipitates. Such a crystallization occurs when the standard process is carried out at an increased nitrate content. In that case a type III product is formed. The time elapsed between the points of precipitation and crystallization appeared to be reproducible. It has been shown in CHAPTER IV that the crystallization can be suppressed by applying an overpressure of carbon dioxide on the system, but the reason why, at a certain point during the precipitation, all the carbon dioxide contained in the precipitate is expelled in a few minutes, was still an open question.

In this chapter experiments are therefore described which were carried out to study the delayed crystallization of the amorphous precipitate into a type III product at increased nitrate ion concentrations. It will be shown, that a sudden decrease of the pH causes the dissolution and the reprecipitation of the amorphous material. During this transition the incorporated carbon dioxide is expelled from the particles. An increase of the precipitation rate during the decrease of the pH was found and this demonstrated that a "retarded" hydrolysis of the uranyl ions is the cause of the sudden change in pH. The time of delay of crystallization was found to depend on the ammonium ion concentration and on the stirring rate. A theory is proposed to account for the phenomena observed.

From the results obtained it is possible to estimate the degree of hydrolysis of uranium in solution during the crystallization of a type III product.

V.2 The pH during the precipitation and the crystallization

One of the most fascinating observations reported in the preceding chapters, is the crystallization of an initially amorphous precipitate when the standard process is carried out at an increased nitrate ion content. The time delay between the appearance of the first precipitate and its crystallization into a type III product proved to be rather reproducible. This crystallization was observed by the birefringency of the newly formed product and by the expulsion of carbon dioxide from the precipitate.

We supposed, that the carbon dioxide was removed from the system because

of a sudden increase of the H^+ formation to such an extent, that a decrease of the pH is observed. We found similar effects in titration curves of uranyl salts with ammonia. Those will be discussed in CHAPTER VI. Therefore it seemed also appropriate to investigate the change of the pH during the formation of the different products in the urea process.

In order to determine pH effects in the solution during the process, samples had to be drawn at intervals, because fouling of the glass electrode by the deposition of solids prevented direct pH measurements in the system. The samples were cooled down rapidly, filtered or centrifuged and the pH was determined at room temperature. In order to apply this procedure, the volume of the liquid had to be increased such that the removal of the samples did not affect the system too much. On the other hand, the increase of the scale influenced the chemical conditions because the stirring rate and thus the extraction of carbon dioxide from the liquid could not be increased accordingly. We supposed, however, that even with this restriction, the basic phenomena could be studied.

FIG. 33 up to 36 inclusive show pH curves typical for the formation of the amorphous precipitate and the type I, II and III products respectively. All conditions, unless stated otherwise, were standard, except for the total volume. The stirrer used was the vibrational one with a perforated stirrer plate. In the figures the letters P and C indicate the points where the amorphous (Precipitation) or crystalline (Crystallization) product appears.

Unfortunately, the carbon dioxide generation curves could not be determined in these experiments at the same time. Separate measurements, how-

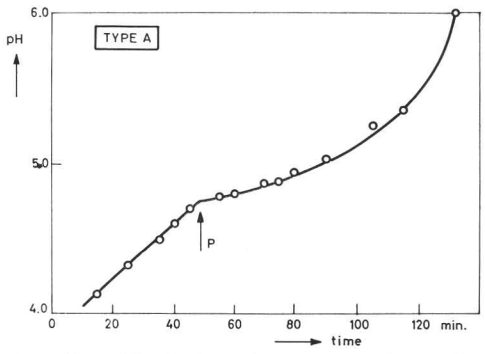

FIG. 33 pH during the preparation of a type A precipitate. Standard conditions.

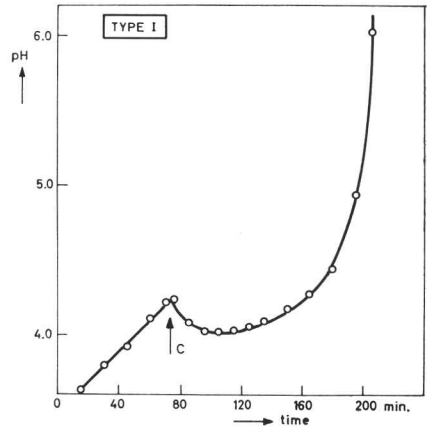

FIG. 34 pH during the preparation of a type I product. The urea concentration is 50% less than standard.

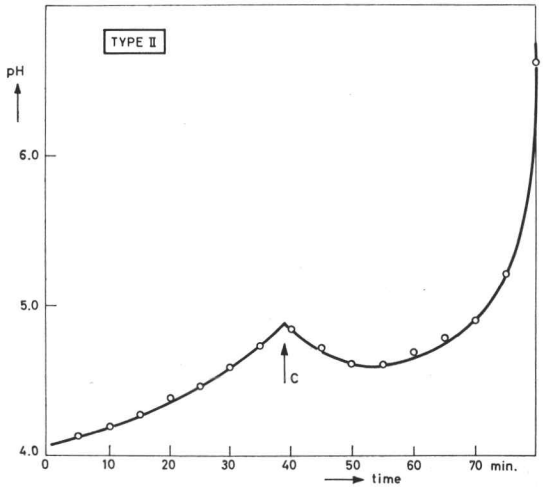

FIG. 35 pH during the preparation of a type II product. The urea concentration is 40% in excess of standard.

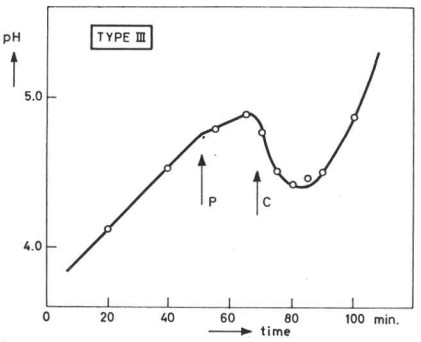

FIG. 36 pH during the preparation of a type III product. The nitrate ion concentration is 36% in excess of standard.

ever, showed that for the preparation of a type III product the increase of the carbon dioxide generation coincided with the decrease of the pH, shown in the graphs. By comparing the four pH curves the following information has been obtained:

1. The curve for the amorphous product is essentially different from the ones for the crystalline products in that it shows no decrease of the pH throughout the process.
2. In the curves for the crystalline products the pH starts to decrease at the point of crystallization (C). The type I and II products are crystalline at once,* whereas the type III product is formed from initially amorphous precipitate (P), thereby giving rise to a time delay between precipitation and crystallization.
3. The pH at which the first solid is formed seems to depend mainly on the urea concentration in the liquid, and consequently would not differ for the type A and type III curves (pH = 4.75).
4. The rate of decrease of the H^+ concentration before a solid is formed may be slightly higher for a type III than for a type A product, whereas this is certainly the case just after the appearance of the solid.

The first question arising from these observations is: Why does the decrease of the pH occur in most of these processes?

---

* This is not always true. In FIG. 22 curve c, the formation of a type II product from an amorphous precipitate is shown.

There are several reasons which might be considered:

1. In the process, urea is hydrolyzed and carbon dioxide is expelled at a rather constant rate. At the same time the uranium hydrolyzes also. The first process will cause a continuous increase of the pH. On the other hand, the hydrolysis of uranium produces H^+ ions. A decrease of the pH might therefore occur when the rate of hydrolysis of uranium suddenly increases considerably.
2. We found that the type III and the type I products consist of a $UO_3 \cdot 2H_2O$ in which part of the H_2O has been replaced by NH_3 (CHAPTER VII). A stepwise increase of the NH_3 content of a $UO_3 \cdot 2H_2O$ like product during the process will result in a relative decrease of the OH^- concentration. If sufficient NH_3 is taken up by the lattice, a decrease of the pH might result. However, this explanation seems unlikely as in the case of a type I product the decrease is observed at a moment when only a very small amount of solid is present. Moreover, such an exchange can not be expected in a type II product.
3. A third possibility is that an exchange takes place of ions adsorbed onto the surface of the precipitate with ions in the liquid. Here the same objection holds more or less as in the second explanation.

Of these possibilities the increased rate of hydrolysis of the uranium seemed most likely. In that case, however, it must be possible to detect the effect by determining the precipitation and crystallization rates. For although the decrease of the pH in itself is negligible in this well-buffered system, the amount of H^+ ions delivered is considerable. During the crystallization of the amorphous precipitate the carbon dioxide incorporated in the material is expelled. This requires 2 gramions H^+ per mole of CO_2. These 2 gramions H^+ have been formed by the hydrolysis of an equivalent amount of uranyl ion. Let us suppose that the sequence of hydrolysis can be represented by

$$UO_2^{2+} \rightarrow U_2O_5^{2+} \rightarrow U_3O_8^{2+} \rightarrow U_3O_8(OH)^+ \rightarrow UO_3^* \qquad [54]$$

It might then be that the $U_3O_8(OH)^+$ ions have to provide the H^+ ions by their hydrolysis. This again would mean that for one extra mole of carbon dioxide leaving the system six moles of UO_3 are precipitated. Therefore, measuring the rate of precipitation, especially for a process with a type III product, seemed to be most promising.

V.3 The rate of precipitation

The measurements of the rate of precipitation were carried out on the same scale as the pH measurements. Samples were drawn at intervals, and after

* In CHAPTER VI a notation will be presented, which tries to describe the actual structure of the ions more accurately. Until then the normal notation will be used.

filtration the uranium content of the filtrates was determined. For type A, II and III products the curves are shown in FIGURES 37, 38, 39 together with their pH curves. (The experiments are identical with those described under V.2.)

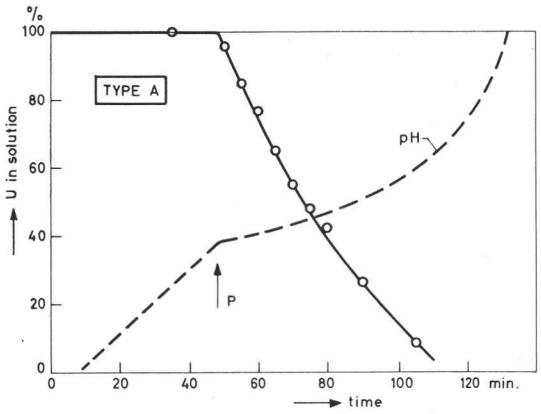

FIG. 37 Rate of solids formation during a type A process. The broken line represents the according pH curve. Standard conditions.

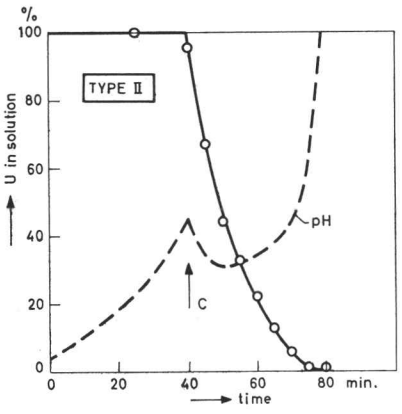

FIG. 38 Rate of solids formation during a type II process. The broken line represents the according pH curve. Urea concentration 40% in excess of standard.

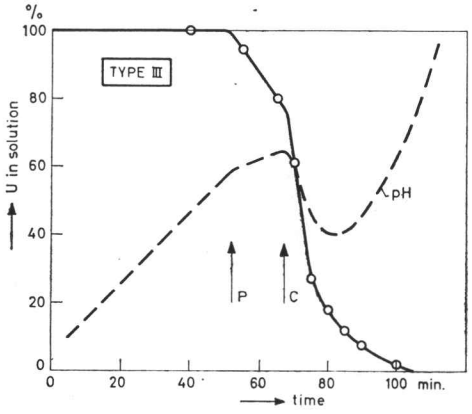

FIG. 39 Rate of solids formation during a type III process. The broken line represents the according pH curve. Nitrate ion concentration 36% in excess of standard.

FIG. 39 shows clearly that the crystallization, where the CO_2 escapes from the particles already formed, coincides with an increase of the rate of precipitation. In our opinion this is a strong support for the hypothesis that an increase of the rate of hydrolysis of the dissolved uranium causes the pH to fall. Consequently most of the H^+ ions produced are taken up by the amorphous precipitate to expel the carbon dioxide. The UO_3 now crystallizes into a NH_3

containing $UO_3 \cdot 2H_2O$, probably after a short dissolution. Depending on the form in which the carbonate is present ($UO_2(CO_3)_2^{2-}$ or $UO_2(CO_3)_3^{4-}$) 1 to 1.33 gramions H^+ are required to remove one mole of carbon dioxide from the amorphous precipitate and to transform the associated uranium into UO_3 hydrate.

Another interesting observation can be made by comparing the FIGURES 37 and 39 for the amorphous and the type III product respectively. The only difference in the chemical conditions between the two processes is that for the type III product the nitrate ion concentration of the solution is 1.2 gramions per litre whereas this is 0.8 in the other case. The rate of evolution of carbon dioxide during the process is equal. Nevertheless the initial rate of precipitation is higher for the amorphous product than for the type III one, although in the latter case also a type A product is formed before the crystallization (*cf.* TABLE V.1).

TABLE V.1 Concentration changes of $[H^+]$ and [U] in the liquid for different products. (P = point of precipitation, C = point of crystallization).

Conditions deviating from standard	Type of product	Rate of increase of $[OH^-]$ in the solution (gram ion/l min)				Rate of decrease of [U] in the solution (%/min)	
		just before P	just after P	just before C	just after C	after P	after C
	A (Fig. 37)	8.3×10^{-7}	1.9×10^{-7}	–	–	2.2	–
50% urea less	I (,, 34)	–	–	8.1×10^{-7}	-18.0×10^{-7}	–	
40% urea extra	II (,, 38)	–	–	12.2×10^{-7}	-8.9×10^{-7}	–	5.3
36% NO_3^- extra	III (,, 39)	8.6×10^{-7}	4.0×10^{-7}	2.6×10^{-7}	-22.8×10^{-7}	1.72	6.3[5]

Taking into account the fact that the increase of the pH during this period is faster for the type III process than for the amorphous, this indicates that the rate of hydrolysis of the uranium has decreased for some reason. There is no question of supersaturation, because seeding such a solution with type III crystals does not initiate a crystallization. Moreover, it was observed that a very small amount of such crystals has already formed a considerable time before the crystallization starts. It appears therefore, that there are circumstances in the liquid which prevent, to some extent, the hydrolysis of the uranium. If now these circumstances change during the process hydrolysis may occur at an increased rate and the system will change towards stable conditions. This again results in a decrease of the pH and in a higher precipitation rate (FIG. 39). In the FIGURES 34 and 38 this situation occurs just before the crystallization starts and consequently the pH decreases there towards stable conditions. A type A process (FIG. 37) might then be considered as a process

in which this fast hydrolysis can be prevented throughout the whole process. In order to check this, an experiment was carried out in which, under standard conditions, an amorphous precipitate was formed. Forty five minutes after the first precipitate had appeared, the system was cooled down rapidly to 20 °C and the subsequent changes of the pH were measured. The pH versus time curve of this experiment is shown in FIG. 40.* The slight increase of the pH after cool-down might be due to a too low cooling rate. It will be shown, however, in CHAPTER VI that similar phenomena occur during titrations of carbon dioxide containing uranyl solutions at room temperature. Another typical result of the experiment in FIG. 40 is that the subsequent decrease of the pH

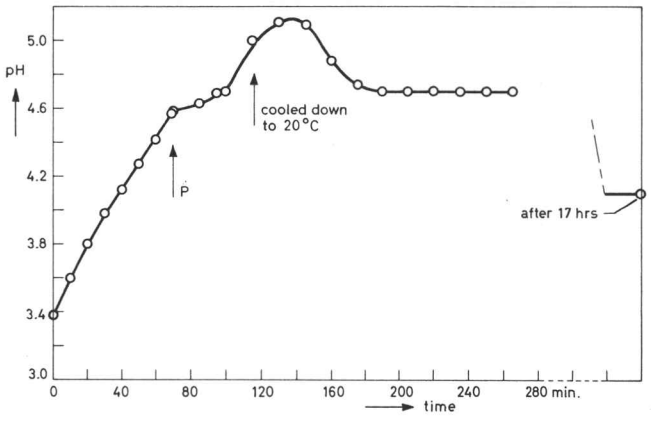

FIG. 40 pH during a type A process in which the liquid is cooled down to 20 °C 45 minutes after the precipitation has started.

takes place in two steps, the first one to pH = 4.7, the second to pH = 4.1. Also this effect was found for the first time during experiments on the hydrolysis of uranyl salts at room temperature. It will further be discussed in CHAPTER VI.

A method to overcome the difficulties that the system has to be cooled down in order to prevent further hydrolysis of urea, is to replace the urea by gaseous ammonia and carbon dioxide. The system was kept at 95 °C during the complete experiment and a fast decrease of the pH in two steps was observed after stopping the gas supply.

We have seen that a fast hydrolysis can be prevented in a type A process, that it can be withheld for some time in a type III process and in some cases in a type II process (FIG. 22, curve c). The reason has to be sought in the composition of the solution during the process, because the mere presence of type III crystals in the amorphous precipitate of a type III process does not cause the

* All the pH readings have been taken at room temperature.

decrease of the pH. It does only indicate that the moment of crystallization is nearing. We suppose that this at the same time indicates that the composition of the solution is becoming more favourable for crystallization. The question why in certain cases conditions are reached which allow or favour crystallization, is still unanswered.

In the next paragraph experiments will be discussed which were carried out to study the time of delay of crystallization for type III products in dependence of various conditions.

V.4 The time delay of the crystallization in the type III process

It has been argued that in a type III process the composition of the solution changes during the process from one that suppresses the hydrolysis of the uranium to one that allows or even favours it. One might expect to find this change reflected in a change of the chemical composition of the precipitate. From analyses, however, within our limits of accuracy no definite difference could be established between the composition in the amorphous region of a type III process, and that of a true type A precipitation. Both show a slight increase of the NH_3 and CO_2 content towards the end of the process, as has to be expected. It might be that for a type III product these NH_3 and CO_2 contents are somewhat higher than for an amorphous material.

Another approach might be that we investigate what changes in the conditions are able to shift the point of crystallization with regard to the point of precipitation. When such a shift occurs we know that the significant parameter in the system has changed.

The data obtained prove that the carbon dioxide content of the system is the decisive factor for the occurrence of crystallization. This conclusion has been drawn from the following observations:

1. In CHAPTER IV (TABLE IV.4) the influence of a carbon dioxide overpressure on a type III process was shown. When the pressure increases first a type II product is obtained, but at 200 cm water column, 95% of the precipitate is of the type A. The crystallization of the amorphous precipitate can therefore be prevented by a sufficient overpressure of carbon dioxide.
2. The influence of the stirring rate was demonstrated in more detail in a series of three experiments (a, b and c) only differing by the intensity of the stirring. The precipitation rate and the pH during the process were measured at the same time. The intensity of stirring decreased in the order a to c. In the same order, an increasing amount of type A material was found in the end product. The results of these experiments are shown graphically in the FIGURES 41 and 42.

From the pH curves we concluded that the period between precipitation and

crystallization decreases with an increasing intensity of stirring and that the decrease of the pH at the point of crystallization becomes larger at the same time. Furthermore, at high stirring speeds the rate of increase of the pH before the point of crystallization is well above that of a normal type A process, but for curve c it has become nearly equal.

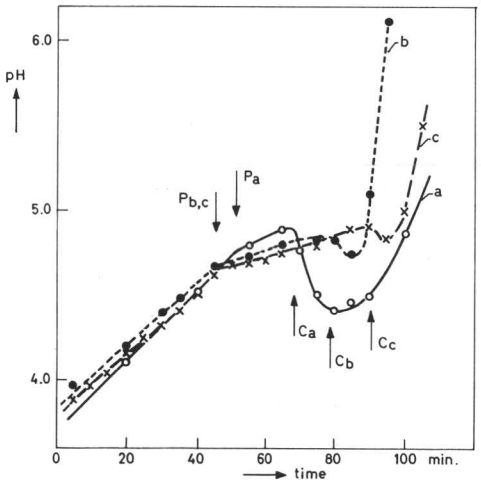

FIG. 41 pH during a type III process at different stirring rates. The rate of stirring decreases in the order a to c.

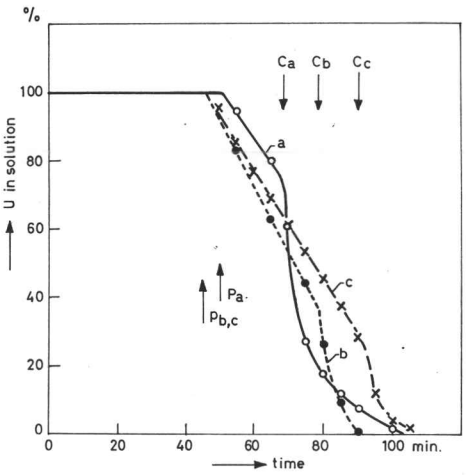

FIG. 42 Rate of solids formation for the experiments shown in FIG. 41.

3. The influence of the total volume is parallel to the influence of the intensity of stirring. An increase of the volume has the same effect as a decrease of the stirring rate.

It is evident from the above that carbon dioxide is the agent which retards or even blocks the transition of the amorphous precipitate into the crystalline type III product. In the normal type III process, however, the effect is produced by the presence of extra ammonium nitrate, the concentration of which influences, as will be shown, the time delay of crystallization. Two questions arise then, whether the effect is specific for ammonium nitrate and how the ammonium nitrate concentration influences the carbon dioxide concentration of the system.

1. The specificity of the NH_4^+ ion.

Four experiments were carried out to investigate whether the NH_4^+, the NO_3^- or the electrolyte concentration in general are decisive in provoking crystallization. The salts used were NH_4NO_3, $NaNO_3$, NH_4Cl and NaCl. In all cases stoichiometric 0.4 M uranyl nitrate solutions were used to which so much salt was added that a total anion concentration of 1.20

gram ions/l was obtained after the addition of the standard amount of urea. Only in the experiments where NH_4NO_3 and NH_4Cl had been added, crystallization was observed. Even at considerably higher concentrations of $NaNO_3$ or NaCl, no crystallization occurred. Therefore we concluded that the effect studied is specifically caused by the ammonium ion.

2. The influence of the NH_4^+ ion concentration on the carbon dioxide content of the liquid.

There are several mechanisms which might explain why the carbon dioxide concentration depends on the presence of NH_4^+.

a. Any salt will lower the CO_2 concentration of the liquid. However, the influence was a specific one and therefore this salt effect can only be of minor importance. Nevertheless we wanted to know it, and therefore a series of four experiments was carried out which are presented in TABLE V.2.

TABLE V.2 The time delay between precipitation and crystallization for a type III process in the presence of $NaNO_3$ and NH_4NO_3.

Curve in FIG. 43	Nitrate ion concentration (gram ions/l)	Type of precipitate	Initial rate of the CO_2 generation (ml/min)	Time delay P → C (min)
a	0.88 NH_4^+ + 0.32 Na^+	A	8.7	–
b	1.20 NH_4^+ + 0.30 Na^+	–	8.1	44
c	1.20 NH_4^+ + 0.50 Na^+	III + 50% II	8.4	41
d	1.20 NH_4^+ + 0.80 Na^+	II + 20% III	8.3	35

In three experiments (b, c and d) the NH_4NO_3 concentration was chosen such that crystallization into a type III product occurred. The salt effect was studied by the addition of $NaNO_3$. The carbon dioxide curves of these experiments are shown in FIG. 43. It is clear that the salt effect exists: increasing the $NaNO_3$ concentration results in a decrease of the time of delay of crystallization. The shift is into the right direction, to be explained with the change of the carbon dioxide concentration.

b. We have supposed that at least part of the carbon dioxide in the solution is present in the form of uranyl carbonate complexes. The solubility of these complexes might change with the NH_4^+ concentration. Although we are well aware that this effect is exaggerated at a decreased temperature, because of the higher stability of the complex, the solubility of the complex $(NH_4)_4UO_2(CO_3)_3$ was measured at 20 °C as a function of the sodium and ammonium nitrate concentration. The results are shown in FIG. 44. The influence of NH_4^+ and Na^+ ions is strong and in a different direction.

In this figure the uranium and the CO_2 concentration has been plotted. The composition of the solution, however, is not exactly that of $(NH_4)_4UO_2(CO_3)_3$. The experiments were carried out by equilibrating 5 grams of the solid complex salt with 25 ml of an ammonium nitrate or a sodium nitrate solution. The supernatant liquid was analyzed for

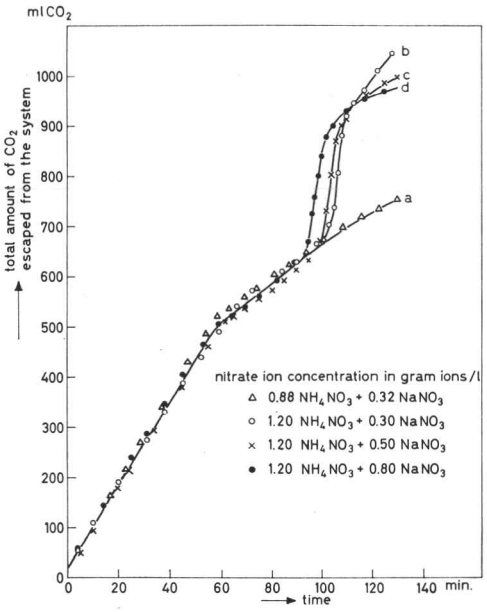

FIG. 43 The influence of NH_4NO_3 and $NaNO_3$ on the CO_2 generation curve.

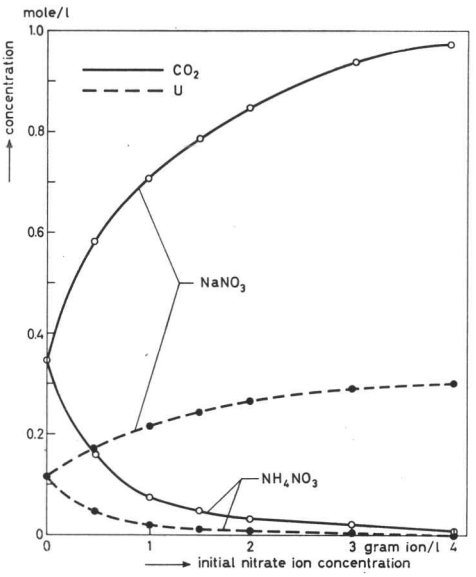

FIG. 44 The concentration of U and CO_2 in saturated solutions of $(NH_4)_4UO_2(CO_3)_3$ in NH_4NO_3 and $NaNO_3$ solutions of 20 °C.

U, CO_2, NH_4^+, Na^+ and NO_3^-. The results are in agreement with the observation of ELOVSKII [55] that the mixed sodium-ammonium salt of the complex has a better solubility than the separate salts. This mechanism might play a role in the crystallization of the amorphous precipitate in a type III process.

c. Although the hydrolysis of urea is very complicated, one might expect that the rate of hydrolysis is influenced by the presence of NH_4^+ ions which are at the same time, an end product. We found that the rate of carbon dioxide generation in a type III process decreases with an increasing ammonium nitrate concentration (see TABLE V.3 and FIG. 45).

Separate experiments * were carried out to measure the rate of hy-

* The valuable assistance of Mr. G. J. C. HAVERKORT for these experiments is gratefully acknowledged.

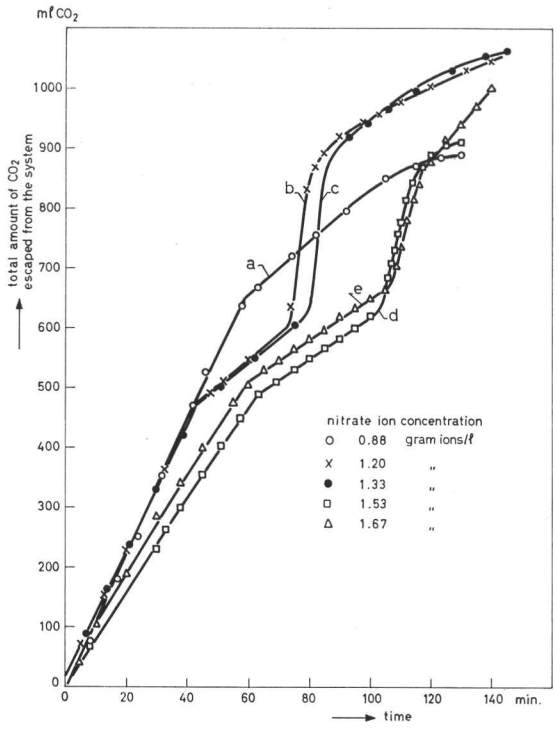

FIG. 45 The influence of the initial ammonium nitrate concentration on the CO_2 generation curve.

drolysis in a pure urea-water-HNO_3–NH_4NO_3 system and in the same system with $NaNO_3$ at 95 °C. To this purpose 100 ml of a NH_4NO_3 or a $NaNO_3$ solution were heated to 95 °C and 50 ml of a hot urea solution containing 50 grams of urea per 100 ml, were added. The pH of the solution was adjusted to 4.00 by the addition of nitric acid and kept at that pH with an automatic pH-stat apparatus.* The solution was stirred at a constant rate. Both the rate of carbon dioxide evolution and the rate of addition of nitric acid to maintain the pH at 4.00 were recorded. The method and the apparatus were calibrated before. The results are shown graphically in FIG. 46. There is some scatter which we attribute to small fluctuations of the reaction temperature. Consequently there is some doubt about the exact position of both lines especially about the presence of an extra inflection in the curve of the NH_4NO_3, but it is

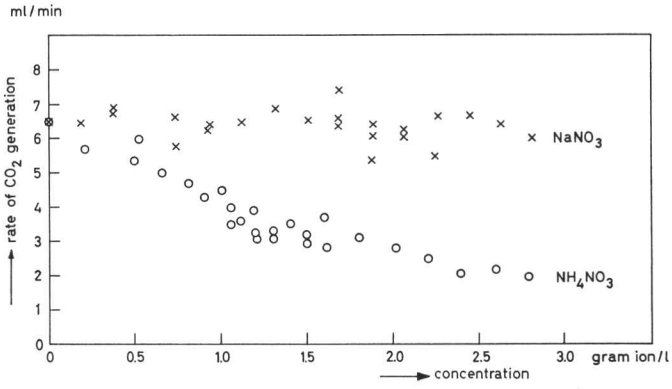

FIG. 46 The rate of hydrolysis of urea in NH_4NO_3 and $NaNO_3$ solutions at 95 °C. Total amount of urea: 25 grams in 50 ml solution.

* The apparatus was a Titrigraph of the Radiometer Company at Copenhagen. This automatic titrator can be used to keep a system at a constant pH by automatic additions of a suitable solution (pH-stat). The amount added is recorded versus time.

clear that the sodium nitrate exerts no influence on the hydrolysis of the urea, whereas this is certainly and strongly the case with ammonium nitrate. We believe that the carbon dioxide content of the liquid is mainly determined by this third mechanism.

All the results presented above seem to fit the following hypothesis:

Through the hydrolysis of urea, CO_2 and NH_3 are formed. The NH_3 is partly taken up by the dissolved uranium ions during hydrolysis, forming ammonium ions. Additionally another part is used to increase the pH of the solution. The less uranium is taken up by hydrolytic reactions the more ammonia is available to increase the pH.

The presence of carbon dioxide or carbonate in the solution can block the hydrolysis of uranium, because it can form uranyl carbonate complexes in a competing reaction. During the process the amount of NH_3, hence the NH_4^+ ion concentration gradually increases through the hydrolysis of urea. This increase causes a decrease of the carbon dioxide concentration of the liquid. Consequently the hydrolysis of initially blocked uranyl ions can start. If this reaction starts fast enough, it will cause a decrease of the pH which is partly compensated by the evolution of carbon dioxide from the amorphous precipitate. Then again UO_2^{++} groups become available for further hydrolysis. When the rate of hydrolysis decreases, the pH increasing effect of the ammonia generation will predominate again and the pH rises sharply. At that point all the uranium is present as a crystalline solid, provided that the pH decreases far enough to expel all the carbon dioxide from the precipitate.

The explanation given above, however, proved to be incomplete for understanding some additional results which were obtained in studying the influence of the NH_4^+ concentration on the time of delay of crystallization.

The arguments that the crystallization is hindered by an interference with carbon dioxide, are convincing. On these grounds one would expect that an increase of the NH_4^+ concentration will favour the crystallization and decrease its time of delay. This expectation, however, is contrary to our results above a certain ammonium concentration. In TABLE V.3 and FIG. 45 the results are collected of a series of standard experiments in which the ammonium nitrate concentration is varied at a constant stirrer amplitude of 1.5 mm.

With an increasing ammonium ion concentration the type of product changes from A to III and thereafter an increasing amount of type II is found. The rate of hydrolysis of the urea seems to decrease in the same order, whereas the time of delay increases. It is this last result which is somewhat surprising. In FIG. 47 the time of delay of these experiments has been plotted versus the ammonium nitrate concentration as curve a. The same tendency was found

TABLE V.3 The time delay between precipitation and crystallization for a type III process as a function of the ammonium nitrate concentration.

Curve in FIG. 45	Ammonium nitrate concentration (gram ions/l)	Type of precipitate	Initial rate of the CO_2 generation (ml/min)	Time delay P → C (min)
a	0.88	A	11.1	–
b	1.20	III + 9% A	10.4	32
c	1.33	III + 2% II	10.4	36
d	1.53	III + 40% II	8.2	43
e	1.67	II + 15% III	7.8	48

in another case where the amplitude was 2.0 mm (curve b) but which might not be compared with the former curve because of a possible difference in the geometry of the stirrer and thus a possible difference in the rate of carbon dioxide extraction. The conclusion from these experiments seems to be that above a certain value the increase of the ammonium concentration causes a delay of the crystallization. This conclusion was confirmed by another series of experiments with an amplitude of the stirrer of 1.5 mm and under the same standard conditions. Up till an ammonium nitrate concentration of 1.33 moles/l amorphous precipitates were obtained. There the amorphous precipitate contained some type III product, which increased to about 50% at 1.47 moles/l. A further increase of the ammonium ion concentration again resulted in the production of type A precipitates. Above 3 moles/l another crystalline modification, the type IV product, was obtained.

If the phenomena are really caused by concentration changes of the carbon

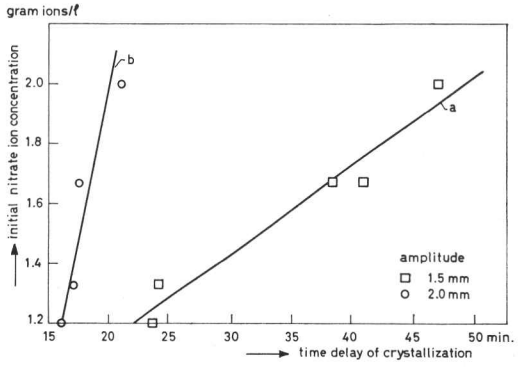

FIG. 47 The influence of ammonium nitrate on the time delay of crystallization in a type III process for two amplitudes of the stirrer.

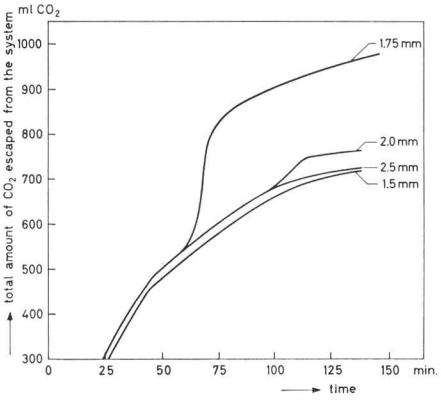

FIG. 48 CO_2 generation curves for different amplitudes of the stirrer. The initial ammonium nitrate concentration is 1.2 moles/l.

dioxide, one must expect that a similar sequence can be obtained by increasing the stirring rate at a constant ammonium ion concentration. A concentration of 1.2 gram ions/l was chosen for one series of experiments. The carbon dioxide curves are presented in FIG. 48. They seem to support the last results mentioned above, in that crystallization occurs in an intermediate region. It should however, be stated clearly that in other experiments a decrease of the time of delay was found with an increase of the intensity of the stirring, without inversion. The reason of this variation in behaviour is not yet clear. It might be that an important parameter of the system has not yet been recognized as such.

A first tentative conclusion is that the crystalline type III product may occur somewhere in the midst of the amorphous region. An indication of this fact was already found in TABLE IV.2 and FIG. 26 where at an increased intensity of the stirring the type I and II products on either side of the amorphous region are accompanied by the type III compound.

On the other hand there are some cases where the type II product occurs in the region between the types A and III. An example of that behaviour is found in TABLE IV.4 where an increase of the carbon dioxide pressure in a type III process results first in a type II and then in a type A product. The same might hold for the results in TABLE V.3, taking into account that a further increase of the ammonium ion concentration leads to the formation of an amorphous precipitate as was demonstrated in subsequent experiments.

The question is still open how a decrease of the carbon dioxide concentration can cause the successive transitions A → III → A, leaving the type II product out of consideration for a moment.

In trying to explain this behaviour we have made two suppositions:

1. Even at the high NH_4NO_3 concentrations and the large amplitudes used in our experiments, the liquid contains enough carbon dioxide to form an amorphous material.
2. For a decrease of the pH and the resulting escape of CO_2 from the particles it is necessary to block the hydrolysis of the uranium to quite some extent in order to accumulate both hydrolyzable ions and OH^- ions (increased pH) for a fast reaction on release.

The hypothesis then is, that at a high carbon dioxide concentration the release of blocked uranyl ions for hydrolysis stays slow throughout the process. On the other hand, not enough uranyl ions and OH^- ions can be accumulated during the process when a low carbon dioxide concentration allows only a relatively small amount of uranyl to be blocked. In the intermediate concentration range there might be enough carbon dioxide to block a considerable number of uranyl ions but not enough to prevent the fast hydrolysis when the carbon dioxide concentration decreases further during the process.

V.5 The degree of hydrolysis of uranium

In V.2 and V.3 we described some experiments from which we concluded that the degree of hydrolysis of the uranium in solution is different for a type A and a type III process, even in the region where the amorphous precipitate is formed. It appears that the presence of ammonium nitrate, in one way or another, favours the increase of the pH over the hydrolysis of uranium, thereby creating a hydrolytically unstable situation, which is stabilized by the presence of carbon dioxide. With increasing time there will be a stronger tendency towards return to a hydrolytically stable system by a fast hydrolysis. If now the hydrolysis is deblocked by the decrease of the carbon dioxide content, H^+ ions will be formed at such a rate that they cannot be neutralized by the solution (*e.g.* by carbon dioxide generation), and a decrease of the pH will result. The amorphous precipitate, present in the liquid, contains carbonate groups which prevent its crystallization but which are, at the same time, unstable in a solution of a decreasing pH. Therefore carbon dioxide is driven off and the amorphous particles crystallize into a type III product, which is, as we will see, a $UO_3 \cdot 2H_2O$ with part of the water replaced by NH_3. The effect of a carbon dioxide overpressure might then be, that the hydrolysis of the uranyl ions is further suppressed by a competing reaction of uranyl carbonate complex formation.

Let us now consider the situation in a type III process, just before crystallization occurs. The solid material consists of amorphous $UO_3 \cdot 2H_2O$ particles containing carbonate groups, attached to the UO_2^{++} groups. When we suppose that the carbonate is mainly present as $UO_2(CO_3)_2^{2-}$, the conversion of this compound into $UO_3 + CO_2$ requires $2H^+$ ions per atom of uranium. These H^+ ions are taken up from the liquid. The decrease of the pH itself occurring at the crystallization, represents a negligable increase of the H^+ ion concentration and is accordingly neglected here.

In the liquid the uranium is present in a partly hydrolyzed, but still soluble form. Dissolved uranyl carbonate complex is not taken into account although small amounts will still be present. The partly hydrolyzed uranium compounds provide H^+ ions on completing their hydrolysis into UO_3. Sutton [54] proposed a scheme of hydrolysis in which hydrolysis and polymerisation occur simultaneously giving rise to a sequence which he writes as follows:

$$UO_2^{2+} \rightarrow U_2O_5^{2+} \rightarrow U_3O_8^{2+} \rightarrow U_3O_8(OH)^+ \rightarrow U_3O_8(OH)_2$$

and possibly leading to uranates by a further increase of the number of OH^- groups.

It is evident that during the precipitation, the number of H^+ ions which can be produced by the complete hydrolysis of the still dissolved uranium, decreases continuously. At the same time the total amount of complex uranyl carbonate groups in the precipitate increases. Beyond a certain point the

number of potential H^+ ions in the liquid will be too small to convert all the amorphous precipitate into a carbon dioxide free product and the residual type A precipitate will be found admixed in the final type III product. This has been ascertained experimentally. The percentage of the type A precipitate increases with an increasing time of delay between the precipitation and the crystallization. Simultaneously, the amount of carbon dioxide generated from the system and the drop in pH, decrease. (See *e.g.* FIG. 41). As these results are in good agreement with the proposed mechanism, one could try to estimate the mean degree of hydrolysis of the uranium in solution. This estimate can be made when one knows how much amorphous precipitate of a known carbonate content can be converted completely into a carbonate free product by the residual uranium in solution.

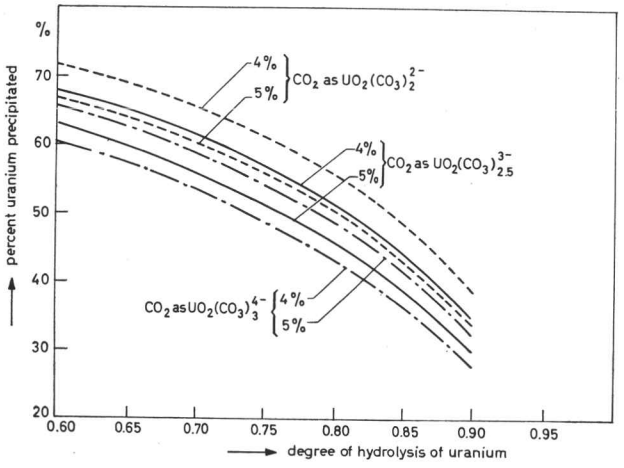

FIG. 49 Percentage uranium, precipitated as type A product, which still can crystallize at different degrees of hydrolysis of the residual dissolved uranium.

In FIG. 49 the degree of hydrolysis of uranium in solution is shown, which is necessary to crystallize all the precipitated amorphous uranium. The curves relate to two different carbonate contents and to three different mean compositions of the complex. The mean degree of hydrolysis is expressed in the ratio of the hydroxyl groups present to the hydroxyl groups required for a complete hydrolysis. From reliable measurements, where amorphous precipitate is still found in the end product and where the total amount of precipitate at the point of crystallization is known, one arrives at a mean degree of hydrolysis of 0.70–0.75 for the dissolved uranium. In terms of the series of compounds given by SUTTON [54] this would mean that a mixture of $U_3O_8^{2+}$ (degree of hydrolysis = 0.67) and $U_3O_8(OH)^+$ (degree of hydrolysis = 0.83) is present in the solution. The ion $U_2O_5(OH)^+$ which is proposed by some other investigators has a degree of hydrolysis of 0.75 and it would therefore also be acceptable from the above estimate.

One should, however, take into account that the possible presence of ions with a lower degree of hydrolysis might require the simultaneous presence of ions with a still higher degree of hydrolysis.

V.6 Conclusion

Although a better understanding has been obtained of some aspects of the type III preparation, not all the experimental results could be combined into a clear hypothesis. This might be due to the fact that one of the essential parameters in the process was not recognized as such. On the other hand it might well be that under the prevailing experimental conditions not all parameters could be controlled to such an extent as would be necessary for dependable and comparable results. A rigid standardization of all conditions is required for a good reproducibility. This causes great difficulties in the case of a reproducible geometry of the stirrer and the vessel and thus of the stirring pattern. We feel sure, that small variations in those conditions influence the results strongly, especially in the case of the type III production. The occasional appearance of the type II material in the type III product seems to confirm this.

CHAPTER VI

SOME HYDROLYTIC PHENOMENA OF URANYL SALT SOLUTIONS

VI.1 Introduction

Our investigations about the formation of a type III product in the urea process have been strongly supported by incidental studies of the reaction between a uranyl salt solution and ammonia or alkali at room temperature. This has already been indicated in CHAPTER V. Additionally, in the compilation of the X-ray data obtained for the identification of the different products in the urea process in CHAPTER VII, reference will be made to similar experiments. For these reasons it seemed appropriate to collect in this chapter some typical experiments concerning the hydrolytic polymeric behaviour of uranyl salts * at room temperature. It has not been our intention to study this fascinating subject extensively. Nevertheless, interesting observations could be made, which might initiate more fundamental studies. Some of the results which we obtained between 1957 and 1959 have been confirmed by others in the mean time. However, as we arrived at our conclusions independently, this work will be reported here and compared with those later publications thereafter.

In this chapter it will be shown that at room temperature the hydrolytic-polymeric reactions of the uranyl ion are extremely slow. Consequently the normal titration curves published, do not represent true equilibrium states. This is evident from the observation that the pH of a partially neutralized uranyl nitrate solution decreases steadily towards the equilibrium value on waiting. Depending on the degree of hydrolysis, this process may take from one hour to a few months time.

In accordance with this conclusion is the fact that the first precipitate in a stoichiometric uranyl nitrate solution can form even before half an equivalent of ammonia has been added per mole of uranium, whereas in the literature a value of $^5/_3$ equivalents is given under non-equilibrated titration conditions. In contradiction with published results [54] it could be demonstrated that under these titration conditions the point of precipitation depends on the concentration of the uranyl ion, as one would expect.

When more ammonia is added to a uranyl salt solution than 0.5 equivalents

* In this chapter the whole sequence of hydrolytic and polymerisation reactions between the UO_2^{++}ion and the precipitate is called a hydrolytic-polymeric reaction. The dissolved ions of this series are all referred to as uranyl ions.

per mole of uranium a decrease of the pH with time can be observed, accompanied by a slow precipitation. This decrease is caused by hydrolytic reactions of the uranyl ions. It may take place in a few steps, each of which shows a simultaneous increase of the amount of precipitate.

Ammonium ions have a specific influence on the hydrolytic-polymeric phenomena described above. This is evident when one considers the difference in behaviour of a uranyl salt solution titrated with NaOH (or KOH) and with NH_4OH. The influence of NH_4NO_3 on the rate of decrease of the pH in a partially neutralized uranyl nitrate solution leads to the same conclusion.

Lastly, the influence of carbon dioxide on the hydrolytic processes in a uranyl nitrate solution will be discussed in this chapter. It will be shown that if sufficient CO_2 is present, the pH of the system rises slowly whilst CO_2 escapes, and that subsequently the decrease of the pH starts, which was described above.

Most of the phenomena described here, can be understood from hydrolytic-polymeric considerations. A tentative explanation for some other observations will be given.

VI.2 Survey of available literature

In this paragraph a survey will be given of all relevant literature which was available for our investigations. More recent publications will be discussed in comparison with our results further on.

The reaction between a uranyl nitrate solution and ammonia was studied by TRIDOT [20] by means of potentiometric and conductometric measurements. He concluded that at 1.5 equivalents of NH_4OH per mole of uranium, precipitation starts, the product being $UO_3 \cdot xH_2O$. The precipitation is complete at 2 equivalents of alkali. At 3 equivalents $(NH_4)_2U_2O_7$ is formed. TRIDOT claims that equilibrium was reached in his experiments, which, as we know, is not true. His concept of the hydrolysis is very simplistic and it is not concerned with the mechanism itself. Extensive studies of the hydrolytic reactions of UO_2^{2+} by a number of authors in the years before 1958, led to the conclusion that the hydrolysis is accompanied by polymerization. MACINNES and LONGSWORTH [56] found indications for the species $UO_3 \cdot UO_2^{2+}$. FAUCHERRE [57] gave evidence for the existence of the same ion, designating it as $(UO_2OH)_2^{2+}$. SUTTON [54, 58] made an elaborate study of the hydrolysis of the uranyl ion. He used uranyl perchlorate and NaOH solutions for cryoscopic, conductometric, potentiometric and spectrophotometric measurements. As a result he proposed a sequence of hydrolytic-polymeric ions:

$$UO_2^{2+} \rightarrow U_2O_5^{2+} \rightarrow U_3O_8^{2+} \rightarrow U_3O_8(OH)^+ \rightarrow U_3O_8(OH)_2 \rightarrow U_3O_8(OH)_3^-$$

etc. Such a sequence would account for the occurrence of uranium both in

cationic and in anionic form. SUTTON made an estimate of the equilibrium constants involved in this sequence. In the uranyl perchlorate titrations a slight drift of the pH was observed in the flat region of the curve, when about 2 equivalents of NaOH have been added per mole of uranium. He states however, that equilibrium is reached within 30–60 seconds in his procedure (a successive addition of 1 ml portions of NaOH solution to 10 ml of a uranyl perchlorate solution of the same molal strength, at room temperature). Furthermore, besides an inflection corresponding with the stoichiometric uranyl salt (due to the presence of free acid in his uranyl solutions) two other inflection points were found. In these inflection points 1.67 and 2.33 equivalents of NaOH had been added per mole of UO_2^{2+} for all curves obtained with uranyl solutions of concentrations between 0.1 and 0.001 M. These inflection points are supposed to mark the formation of $U_3O_8(OH)^+$ and $U_3O_8(OH)_3^-$ respectively, according to SUTTON's hypothesis. To our opinion this is in disagreement with the author's calculated concentrations of the various ionic species for a 0.01 M uranyl perchlorate solution as a function of the amount of NaOH added. These concentrations are presented in a graph in the same publication. It shows that at a OH^-/UO_2^{2+} ratio of 1.67 less than 15% of the uranium in solution is present as $U_3O_8(OH)^+$ and at 2.33 only 40% in the form of $U_3O_8(OH)_3^-$. The maximum amounts of $U_3O_8(OH)^+$ and $U_3O_8(OH)_3^-$ in this graph are found at ratio's of 1.27 and 1.79 respectively.

Similarly, AHRLAND [59] concluded that polymers are formed during the hydrolysis of U(VI), although he suggested the additional formation of UO_2OH^+. AHRLAND's data have been reevaluated a few years later by AHRLAND, HIETANEN and SILLÉN [60] according to SILLÉN's "core and links" theory [61]. The conclusion of this team was that the phenomena observed fit into the core and links theory and that polynuclear compounds of that type with the formula $[UO_2\{(OH)_2UO_2\}_n]^{2+}$ occur in partially hydrolyzed uranyl salt solutions. No definite conclusion was reached about the maximum value of n as the method could not distinguish between an infinite series of hydrolytic products and a series limited by a maximum of $n = 3$ or $n = 4$. The authors preferred the infinite series as there were no arguments for the stability of a very short series of polymeric species.

KRAUS and NELSON [62] made a comparative study of the hydrolytic behaviour of uranium and the transuranic elements. They found a hysteresis effect in the titration curve of a uranyl perchlorate solution with alkali. The curve for a titration of a uranyl salt solution with alkali differed considerably from that of alkali with uranyl salt. This effect was wrongly attributed to a slow depolymerization of the precipitate in the "downscale" titration. With an ultracentrifuge they could isolate compounds from the clear liquid which might be polymeric ions. Later KRAUS [63] presented a more detailed concept of the

same subject. He supposed that the precipitates consist of solid solutions with a varying composition, instead of simple stoichiometric compounds. At the moment when precipitation occurred after the addition of sufficient alkali, the pH decreased abruptly. This behaviour was attributed to a sudden change in structure of the U(VI) polymers, *e.g.* a transition from chains to sheets.

HEARNE and WHITE [64] admit that in solutions containing added alkali or an excess of uranium trioxide polymeric species containing three or more uranium atoms occur most probably. They point out, however, that the situation might be different in stoichiometric uranyl salt solutions. They come to the conclusion that in the latter case their results can be explained by the presence of the monomeric $UO_2(OH)^+$ and the dimeric $UO_3 \cdot UO_2^{2+}$ ions.

VI.3 Preliminary experiments

VI.3.1 The titration of a uranyl nitrate solution with ammonia

For a better understanding of the experiments reported further on in this chapter a description will be given here of some basic observations during the titration of a uranyl nitrate solution with ammonia.

When an ammonia solution is added carefully to a well stirred solution of stoichiometric uranyl nitrate, initially a dark yellow precipitate is formed on each addition. This precipitate, however, dissolves on stirring. Slowly the colour of the solution changes from light yellow to a much darker shade indicating the formation of hydrolytic polymers. At a certain point a lasting precipitate is formed and the pH which started to increase shortly before, levels off again. This precipitation starts before 2 equivalents of NH_4OH have been added per mole of uranium and it is complete by the time when this

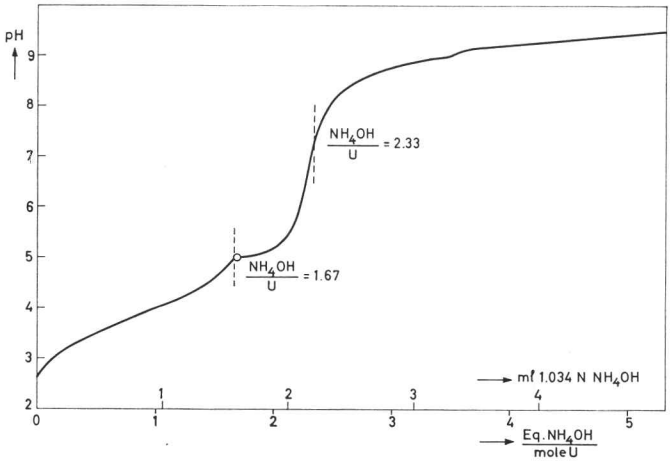

FIG. 50 Titration curve of 20 ml 0.0487 M uranyl nitrate solution with 1.034 N ammonia at a rate of 0.2 ml per minute.

ratio is about 2.33. The pH rises sharply then and a change in the colour of the precipitate towards orange may be noted. In FIG. 50 the curve of the pH versus added ammonia is given for a titration of 20 ml of a 0.0487 molar stoichiometric uranyl nitrate solution with 1.034 N ammonia, the ammonia being fed to the uranyl nitrate solution at a rate of exactly 0.2 ml per minute. The point of visible precipitation has been marked with a circle. If a uranyl nitrate solution is titrated which contains free acid, an additional inflection is found in the curve at the point of stoichiometry.

Early in 1957 we found that the pH of a uranyl nitrate solution, neutralized with ammonia until a lasting precipitate formed, decreased slowly when no further ammonia was added. More important was the observation that the same also occurred in a clear solution just below its point of precipitation. The decrease of the pH was accompanied by the slow formation of a precipitate. A new fuel preparation process was developed on this principle, which essentially is a precipitation from homogeneous solution. By the addition of solid ammonium sulphate the decrease of the pH could be enhanced and a better particle form could be obtained. This "sulphate process" was shortly described in CHAPTER I. Furthermore it appeared that a very definite concentration of ammonium nitrate in the uranyl nitrate solution could retard the precipitation during the neutralization with ammonia.

Shortly afterwards we found the decrease of the pH which occurs in the preparation of a type III product in the urea process (CHAPTER V). This has been the incentive to study more elaborately the hydrolytic behaviour of the uranyl ion at room temperature, in parallel with the urea process.

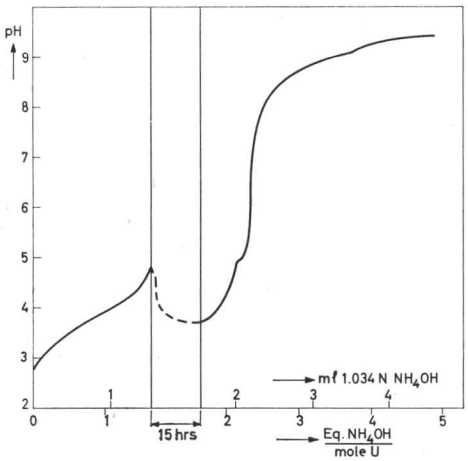

FIG. 51 Interrupted titration of 20 ml 0.0487 M uranyl nitrate solution with 1.034 N ammonia at a rate of 0.05 ml per minute.

VI.3.2 The decrease of the pH in the precipitation point

When a uranyl nitrate solution is titrated slowly with ammonia a slight drift of the pH is observed near the point of precipitation. As soon as the precipitation starts, this decrease of the pH continues for one or more hours, when no ammonia is added any more. When the titration is then continued a curve of the pH versus ml ammonia is obtained as shown in FIG. 51 for 20 ml of a 0.0487 molar uranyl nitrate solution being titrated with 1.034 N ammonia at a rate of

0.05 ml per minute. The first conclusion to be drawn is that part of the normal titration curve (FIG. 50) is unstable especially the first part where a lasting precipitate is present and shortly before that point. It is clear that no true equilibrium exists there during the titration and it is strange that this was not noted in previous investigations.

A further point is, that although the first lasting precipitate in the experiment of FIG. 51 is formed at a pH of 4.88, it can exist at a considerably lower pH (less than 3.70). During the decrease of the pH even further amounts of this precipitate are formed. However, during each preceding addition of ammonia to the system a precipitate was formed which dissolved in the liquid at pH's equal to those where a precipitate was present during the decrease of the pH. This proves that the precipitate formed before the point of precipitation is of a different type and nature than in that point. We suppose that the first compound is stable under conditions of a high pH as it is formed around droplets of ammonia entering the liquid.

On the other hand, if precipitates formed in the precipitation point are stable at a considerably lower pH, one may suppose that such a precipitate is stable also before the precipitation point. If so the occurrence of low hydrolytic reaction rates or a temporary blocking of the hydrolytic polymeric reaction has to be considered.

A method to track down such a phenomenon might be the use of seeding experiments.

VI.3.3 Seeding of a partially hydrolyzed uranyl nitrate solution

A first attempt to see whether seeding a partially neutralized clear uranyl nitrate solution causes precipitation, was made in the following way:

50 ml of a 0.1 M stoichiometric uranyl nitrate solution was titrated at 20 °C with 0.1 N ammonia at a rate of 5 ml per minute. Readings of the pH were taken at regular intervals. The resulting curve of ml versus pH is shown as curve a in FIG. 52. Next, the same experiment was repeated except that after the addition of 30 ml of ammonia a small amount of precipitate was introduced. This precipitate was obtained from a similar system by adding ammonia until precipitation occurred (pH = 4.85), and leaving the system to equilibrate by further precipitation with a decrease of the pH. The precipitate thus obtained (at a final pH = 4.07) was isolated by centrifugation and used for the above experiment. The titration curve of the seeded system is given as curve b in FIG. 52. In comparing curves a and b it is clear that seeding has resulted in a relative decrease of the pH during the rest of the precipitation. The effect, though significant, is not sensational. This has to be attributed to the extremely low reaction rate, which cannot compensate the further addition of ammonia.

Therefore, a more sensitive experiment was carried out, to determine

accurately at what point of the curve precipitation could start. With the same uranyl nitrate and ammonia solutions and the same conditions of the titration rate and the temperature of the previous experiments, eight solutions were composed, thus representing eight points of curve a in FIG. 52. Each sample was immediately divided into two parts. The first one was taken for a determination of the uranium content. To the second (21 ml) 1.4 grams of the seed material mentioned above was added, after which the system was stirred for 10 minutes. The uranium concentration of the clear supernatant liquid was then determined again.

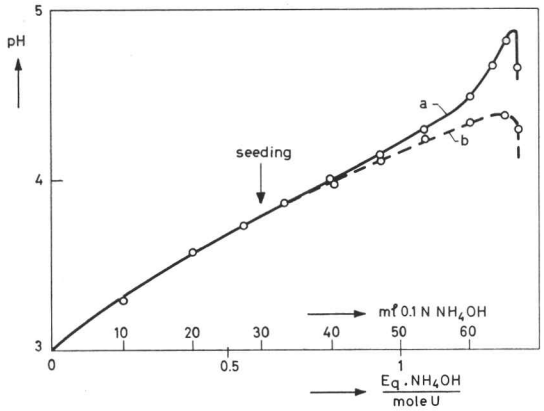

FIG. 52 The influence of seeding on the titration curve of 50 ml 0.1 M uranyl nitrate with 0.1 N ammonia at a rate of 5 ml per minute.

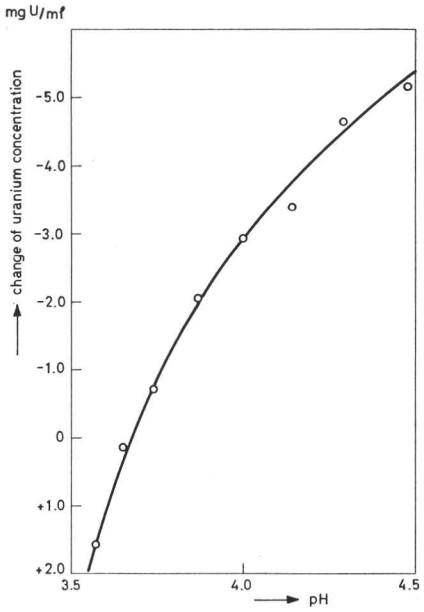

FIG. 53 Changes of the uranium concentration by seeding a 50 ml 0.1 M uranyl nitrate solution, partially neutralized with 0.1 N ammonia.

In FIG. 53 the increase $\Delta[U]$ of the uranium concentration for these experiments has been plotted versus the pH of the system before seeding. Although there is some scatter of the data, the results prove that at a pH = 3.65 neither dissolution nor growth of the seed material occurs. Above this pH the uranium concentration in the solution decreases and thus the amount of precipitate increases. Therefore the limit of pH = 3.65 is considered to be the value above which the system can precipitate under the prevailing conditions. This result is a surprising one when one realizes that the ratio (equivalents of NH_4OH added): (moles of uranium) is slightly below 0.5. This means that the mean degree of hydrolysis of the uranyl ion is less than 25%, whereas about 80% is reported for a normal titration in literature. In a similar solution which was

stored at room temperature for several months, no precipitation was observed. This again points to extremely low reaction rates.

VI.3.4 Spectrophotometric measurements

One of the techniques used by SUTTON [54] for his investigations of the uranyl hydrolysis is spectrophotometry. He observed that in the region between 3800 Å and 4700 Å the light absorption of a uranyl perchlorate solution first increases with increasing alkali content until the first inflexion in the titration curve (1.67 OH^- per uranium). Thereafter a decrease of the absorption occurs although no precipitate is formed, and then the absorption increases slowly again. SUTTON ascribes the first increase of the optical density of the solution to oxygen bridging, thus to the reaction series

$$UO_2^{2+} \rightarrow U_2O_5^{2+} \rightarrow U_3O_8^{2+}$$

The subsequent decrease of the optical density is interpreted as the competing process of hydroxyl ion addition. It marks the formation of

$$U_3O_8(OH)^+ \rightarrow U_3O_8(OH)_2 \rightarrow U_3O_8(OH)_3^- \quad \text{etc.}$$

Unfortunately this conclusion is in contradiction with FIG. 7 of the same publication where it is shown that, according to SUTTON's calculations, at the moment when the maximum of the optical density is reached, already more than 50% of the uranium is present as $U_3O_8(OH)_3^-$, whereas no $U_3O_8^{2+}$ is left. Nevertheless one may conclude that the initial increase of the optical density, followed by a decrease indicates the progression of the hydrolytic process in the uranyl solution.

This technique was therefore selected to see in how far the processes of precipitation were similar to hydrolytic reactions.

The apparatus used was a quartz spectrophotometer * with quartz cells. The cell length was 10 mm. Readings were taken at intervals of 50 Å between wavelengths of 4000 and 5000 Å, the bandwidth having been chosen between 4.7 and 9.0 Å respectively. The curves thus obtained for the optical density versus the wavelength are less detailed than those published by SUTTON. Nevertheless the results are unambiguous.**

The uranyl solutions were prepared in the following way: 97.4 ml of a uranyl nitrate solution 0.03 M in uranium and containing 0.054 gramions of nitrate per litre were weighed into a cilindrical vessel. Then 66.7 ml of water was added and various amounts of a 0.26 N ammonia solution at a rate of 2 ml per minute. The solution was then centrifuged to remove any solid matter and

* This spectrophotometer was a Unicam SP 500, made by Unicam Instruments Ltd., England.

** Recently a theoretical interpretation of the uranyl salt spectrum has been given by MCGLYNN and SMITH [65]. A discussion is out of the scope of this thesis.

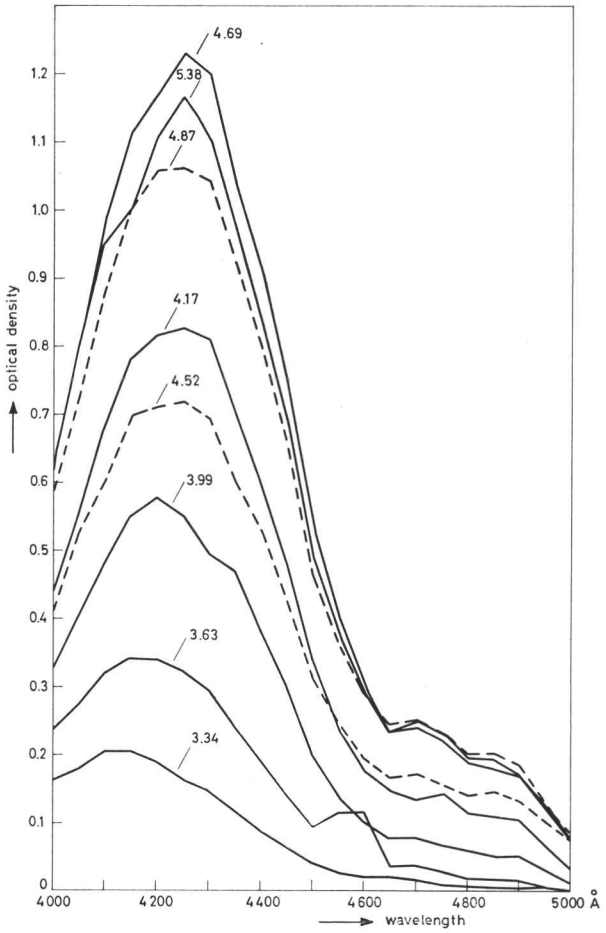

FIG. 54 Extinction of a 0.03 M uranyl nitrate solution at different pH's after the addition of 0.26 N ammonia.

the pH and the optical density were determined. The supernatant liquid of the sample to which just enough ammonia had been added that precipitation occurred (pH = 5.38), was measured again after 40 and 60 minutes.

FIG. 54 shows a set of curves for different uranyl nitrate: ammonia ratio's and thus different pH (drawn lines). The broken lines represent changes in the sample of pH = 5.38 which occurred on waiting. As the pH of this sample decreased gradually, the curve of pH = 4.87 is taken 40 minutes after preparing the sample and the curve of pH = 4.52 still 20 minutes later.

There is an increase in the optical density as the ammonia content increases. This reaches a maximum at a pH = 4.69, where the OH^-/U ratio is about one. Shortly before the precipitation occurs in the system the optical density starts to decrease with increasing ammonia content. At the point of precipitation this decrease goes on even when no more ammonia is added to the system. The decrease of the optical density is faster than the decrease of the uranium concentration. Conclusively it was taken that the changes occurring in such a system near the precipitation point and more particularly the decrease of the pH with time, are caused by slow hydrolytic reactions in the solution. Obvious though this seems now, this was not clear at that time.

VI.4 Measurements with an automatic titrator *

One of the conclusions of the previous investigations was that it is extremely difficult to obtain reproducible results from titrations of a uranyl nitrate solution with ammonia. Especially when very definite additions of ammonia had to be made for measuring variations in the rate of decrease of the pH, largely differing results were sometimes obtained. A careful control of the temperature alone proved to be insufficient. However, from the experiments described above it could be concluded that there was a strong influence of the waiting time. Consequently the rate of adding ammonia to the uranyl nitrate solution should be rigidly standardized for all the experiments. This could not sufficiently be achieved with a hand-controlled burette. Therefore an automatic titrator was chosen for some more refined measurements. All measurements described further on in this chapter were carried out with this instrument.** In normal use for automatic titrations the apparatus is equipped with a proportionally dosing system. The alternative of unintermittent actuation of the burette was chosen for our experiments to assure a high degree of reproducibility.

With this instrument the whole content of a burette (0.5, 2.5 or 5.0 ml) can be fed into the system very regularly in a period varying between 6 and 2000 minutes. The titrant is introduced under the surface of the liquid through a very thin polyethylene capillary.

The solutions of uranyl salt and titrant were made under absolute exclusion of carbon dioxide and the stocks were connected directly to the titration vessel by glass tubing with suitable valves. Syringe burettes *** were used for dosing the uranyl salt solutions. The glass titration vessel itself was pressed against the rubber gasket of the Teflon cover plate. This plate contained holes for the electrodes, a stirrer, the burette tip and the filling capillary for the uranyl solution. Nitrogen freed of carbon dioxide was fed into the titration cell for flushing and to prevent entering of carbon dioxide.

Initially, experimental difficulties were encountered in that even before a lasting precipitate appeared, a solid formed at the tip of the burette thus leading to inhomogeneity of the system and discontinuities in the measured

---

* The valuable assistance of Mrs. J. E. DE BRUIN–NOOTHOUT and of Miss J. H. Bos for these investigations is gratefully acknowledged.

** This apparatus, made by Radiometer (Denmark) consisted of a TTT 1 Titrator, a SBR 2 Titrigraph and a SBU 1 Syringe burette. This assembly can be used for thermostated, automatic potentiometric titrations and for measurements where a system has to be kept at a constant pH by automatic titration (pH stat). Measurements can be carried out under a controlled atmosphere. A normal self compensating mV recorder can be attached for any registration of the pH with time although most of the measurements can be carried out with the Titrigraph recorder.

*** The burettes were made by Metrohm A.G., Switzerland.

curves. This could be prevented by placing the stirrer very close to the tip of the burette. The problem of solids falling out on the glass electrode and in the capillary of the calomel electrode was controlled by checking the pH of the system at the end with a clean electrode.

From the preliminary results described above one may expect that the titration curves can be rather complicated. There are several independent phenomena which might influence the shape of those curves. First there is the slow rate at which the hydrolytic-polymeric reactions take place. Consequently no true equilibrium might be reached in any of the titrations described. Secondly, the hydrolytic-polymeric phenomena might be different depending whether hydrolysis takes place by dilution or by increasing the alkali content. It seems likely that the tendency to polymerize is different for both cases, thus influencing the specific species of hydrolyzed ions. Lastly the system is complicated by the occurrence of different solid compounds as will be demonstrated in CHAPTER VII. The transition of *e.g.* $UO_3 \cdot 2H_2O$ into $UO_3 \cdot {}^1/_3 NH_3 \cdot {}^5/_3 H_2O$ causes a relative decrease of the pH whereas no true hydrolytic reaction takes place. Studying these phenomena quantitatively did not fit the frame of this work, nor was all the apparatus available which should be used in support of the titration work. Nevertheless we thought that even a superficial understanding of the phenomena might help in the interpretation of the urea process, especially in the formation of the type III product. Additionally it seems appropriate to report at least part of the work here, because the methods might be of help in studying the uranyl hydrolysis by other means.

VI.4.1 Titration curves

a. General considerations

Before the actual titration measurements a few preliminary experiments were carried out to check the reproducibility of the measurements and the influence of dilution and carbon dioxide. Generally the reproducibility of the curves was good. In certain pH regions there was considerable scatter in the results, but further work revealed that the shape of the curves was extremely sensitive for small variations of the chemical conditions in those regions.

The influence of the dilution was important because some uranyl salt solutions were obtained by dilution of a concentrated stock solution. On dilution the pH of a uranyl nitrate solution rose at once. During the next 48 hours no change of the pH was detected nor did the titration curves shift. It was therefore assumed that either no further hydrolytic changes took place in the solution or that such changes were extremely slow and would not show up in the experiments. Although the solutions and the titration cell were kept free of carbon dioxide, it was important to know the influence of carbon dioxide

from the air on the titration curve. Therefore two curves were compared, both of a 0.0487 molar uranyl nitrate solution titrated with 1.045 N ammonia, one under carbon dioxide free conditions, the other after 5 hours contact with air and titrated without flushing the titration vessel with nitrogen. Between pH = 4.5 and 9 a slight shift of the second curve towards a lower pH could be observed. Although the difference was of minor importance it was too large to ensure good reproducibility. Thus carbon dioxide was rigidly excluded in all the measurements unless the influence of carbon dioxide was studied.

It has been stated above that the overall hydrolytic-polymeric reactions of uranyl nitrate are slow. Therefore it is interesting to measure titration curves with the rate of titration as the only variable. FIG. 55 shows a set of curves

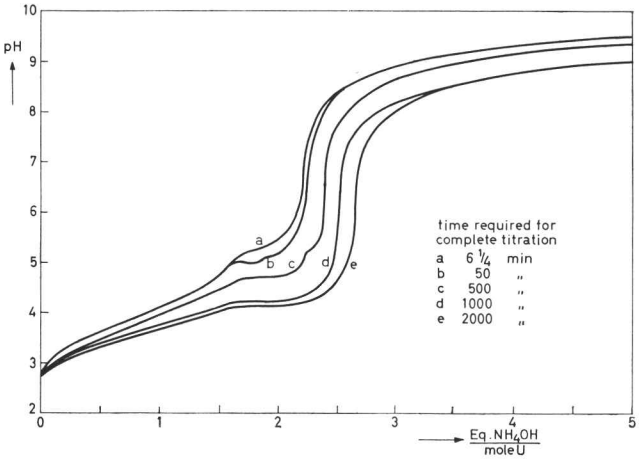

FIG. 55 Influence of the rate of titration of 10 ml 0.0487 M uranyl nitrate with 1.045 N ammonia.

obtained by titrating 10 ml of a stoichiometric 0.0487 molar uranyl nitrate solution with 1.045 N ammonia. The total time of titration has been $6^1/_4$, 50, 500, 1000 and 2000 minutes respectively. It is clear that the rate of hydrolysis is competing with the rate of titration. This is most significant in the middle part of the curves where precipitation occurs. At $6^1/_4$ minute (curve a) the titration is faster than the hydrolysis, and no decrease of the pH is observed. At 50 minutes (curve b) the titration predominates in the first part of the curve, where (as will be shown later) the rate of hydrolysis is low. In the middle however, a decrease of the pH occurs indicating a rather fast hydrolysis. The other curves do not show this decrease. It should be stressed that in none of these curves equilibrium is reached. This is evident from separate equilibration experiments and from the fact that even after a 2000 minutes titration a decrease of the pH occurs. The extra inflection which has developed in curve c

disappears in slower titrations. The same has been found in similar sets of curves of other uranyl concentrations. For 0.0487 molar uranyl nitrate it is found in a measurement of 500 minutes (FIG. 55), whereas for 0.0974 and 0.182 molar solutions the same shape occurs with experiments carried out in 1000 and 2000 minutes respectively. The inflection might mark the presence of a certain hydrolytic species or a certain composition of the precipitate. It is interesting to note that such an inflection and thus the occurrence of a certain ionic or solid species can be developed by choosing the right titration rate. Similar results will be given for other curves. For titration times considerably longer than 2000 minutes a 0.0487 molar uranyl nitrate solution shows another inflection at the upper end of the steep rise of the pH. At a molar strength of 0.10 this inflection occurs in a titration of 2000 minutes and at 0.196 molar it develops in experiments taking from 500 minutes on upwards. This sequence is just the reverse of the first one.

The observation that during a slow titration a decrease of the pH can occur shortly after the beginning of the precipitation, needs some further comment. A similar result had been obtained by KRAUS and NELSON [62], who found a sudden decrease of the pH in the precipitation point, which they attributed to a change in structure of the precipitated solid.

TROMBE [66] reported such an increase in acidity for a $Nd(NO_3)_3$ solution neutralized with gaseous ammonia. Although no explicit interpretation is given of this phenomenon, the author suggests that it is caused by an abrupt transition of the precipitate from a colloidal state into a flocculated one or even into a crystal.

HUFFERMAN [67] describes a neutralization of a $FeCl_3$ solution with gaseous ammonia and she too observed a decrease of the pH in the titration curve. Her explanation is, that an unstable iron complex is formed, which decomposes suddenly. We repeated the experiment and we feel sure that the decrease of the pH is caused by hydrolytic phenomena. Our results with uranyl nitrate solutions were confirmed by the results of SANDERSON, DIBBEN and MASON [18], whose work was only declassified at 1959. They also attributed the decrease of the pH to hydrolysis.

BRUSHILOVSKII [68] studied the hydrolysis of uranyl perchlorate by the titration with NaOH, using times up to four days. His data again confirmed our observations.

Recently CORDFUNKE [69] repeated part of our work with uranyl nitrate and ammonia. He carried out his experiments at 40 °C to enhance the equilibration of his solutions. The results were in complete agreement with our measurements at room temperature. From his titration – equilibration curve it can be seen that the titration curve starts to depart from the equilibrium at a ratio of $OH^-/U = 0.5$ shortly before precipitation occurs. Although there is

no reference in this publication about the concentrations used, it is interesting to note that in our experiments seeding could initiate a precipitation at a ratio of $OH^-/U = 0.5$ in a 0.1 M uranyl nitrate solution titrated with 0.1 N ammonia.

There seems to be a good agreement about the occurrence of a decrease of the pH during titrations under certain conditions. The explanations, however, differ, and to our opinion, no completely satisfactory interpretation has been given yet. The decrease of the pH cannot be caused by the same hydrolytic sequence which causes the precipitation in the solution, because the rate of hydrolysis increases with the increase of the OH^- concentration, according to the mass law. Under no circumstances could this give rise to a decrease of the pH as long as the OH^- is fed into the system at a constant rate.

Consequently, another mechanism must be responsible for the phenomenon. Either a reaction which has been blocked, like in the case of the type III product (CHAPTER V), or a new reaction of which one of the reactants was not available before.

We believe that this reactant is the crystal surface of the precipitate formed. To explain this we must look somewhat further into the question of the mechanism of the hydrolytic-polymeric reactions. There are a few assumptions to be made first:

1. it is rather unlikely that dissolved uranyl ions occur in the system which have a higher charge than +2, especially because any positive charge can be decreased very rapidly by hydrolysis, which is effected by a proton donation. This is generally agreed in literature.
2. polymerization in the solution can only occur to a certain degree above which precipitation occurs. Let us suppose for the discussion that the monovalent trimeric ion presents the last step before the precipitation.

These assumptions do not influence the principle of the hydrolytic scheme, and therefore they are not too important.

The hydrolysis of the uranyl ion could then be presented by the following scheme, in which a horizontal arrow indicates a proton donation and a vertical one a polymerization *:

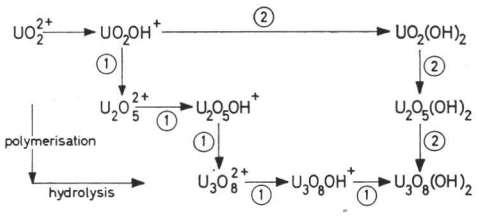

* In this scheme the normal notation which is used in the literature has been applied. Further on in this chapter a notation will be presented which is in agreement with the modern theories of complex chemistry and which provides a better understanding of the reactions in question.

Of course the sequences 1 and 2 represent extremes, and in reality all species may occur simultaneously. Reactions like $U_2O_5OH^+ \rightarrow U_4O_{11}^{2+}$ have not been presented because they result in nucleus formation or in precipitation according to the second assumption. To our opinion the sequence 1 is predominant at high uranyl ion concentrations when the increase of the pH is effected by the addition of alkali. (In CHAPTER VII called "alkaline hydrolysis".) The sequence 2 has a better chance in diluted systems, where the meeting chance necessary for polymerization is much lower than for the hydrolysis. ("Hydrolysis by dilution".) It seems important to note, in this respect that dilution promotes depolymerization in the solution.

Furthermore we expect that the +1 ions predominate in alkaline hydrolysis because the polymerization is expectedly slower than the hydrolysis, which is effected by proton donation by one of the water molecules attached to the uranyl group, to one of the surrounding water molecules. This is not in agreement with most conclusions in literature.

When we suppose that the precipitation of the uranium from a uranyl solution by the addition of alkali occurs along a sequence of the type 1, a uranyl group has to pass through several reactions before the first precipitate is formed. Thereafter, however, the solid surface of the precipitate can act as a reactant, in that polymerization takes place with smaller ions from the sequence, so that some reactions may be bye-passed. This second polymerization mechanism however does not suffice to explain the decrease of the pH, unless the hydrolytic reactions are enhanced also. We believe that the proton donation of the groups "adsorbed" onto the surface is faster because of the crystal forces of the underlying crystal. These allow a higher surface charge and they direct the different groups attached to the uranyl ions. This will be explained in somewhat more detail further on, on the basis of the structure of those groups.

Experimental evidence for the above hypothesis can be derived from experiments similar to that of FIG. 53, where partly hydrolyzed solutions were seeded with a crystalline precipitate. The pH of such a solution, containing U and OH^- in a mole ratio of *e.g.* $OH^-/U = 0.7$ changes hardly in the course of several days, indicating that the reactions are extremely slow. However, when one seeds an identical solution, as was done in the experiment of FIG. 53, nearly 10% of the dissolved uranium precipitated in 10 minutes. Thereby a corresponding decrease of the pH was observed. It is hardly conceivable that at this low mean degree of hydrolysis so much uranium was present near to precipitation. It seems acceptable to state that ions like UO_2OH^+ and $U_2O_5OH^+$ have been attached to the surface directly.

If this hypothesis holds, one would expect similar phenomena for other elements, provided that critical parameters like the concentration and the rate of titration are well chosen. The results cited above, which were obtained

for iron [67] and for the rare earths [66] are considered to be further proof for this hypothesis.

Some thought should be given now to the true configuration of the ions partcipating in such hydrolytic-polymeric reactions, in order to understand the hypothesis in more detail.

When we consider the reactions leading to a decrease of the pH in a titration curve, immediately after the precipitate has started to form, several bridging mechanisms can be taken into account during the polymerization. It seems likely that the ions thus formed show a strong resemblance with the lattice of the precipitate on which they are fixed. This precipitate is, in principle the so called $UO_3 \cdot 2H_2O$, which should be written as $UO_2(OH)_2 \cdot H_2O$. Part of the H_2O can be replaced by NH_3 with minor distortions of the lattice. The lattice is pseudo hexagonal and consists of layers of the composition $UO_2(OH)_2$, in which the U is found between two layers of oxygen. Six OH groups surround the UO_2^{2+} in a hexagonal puckered ring. The H_2O (and the NH_3) are found between the oxygen layers of two subsequent $UO_2(OH)_2$ sheets [70]. In FIG. 56 the structure of one $UO_2(OH)_2$ layer is shown.

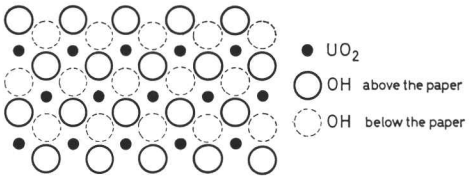

FIG. 56 Configuration of a $UO_2(OH)_2$ layer in the $UO_3 \cdot 2H_2O$ crystal.

It is clear that the UO_2 groups are linked by hydroxyl bridges, as has been the basic concept of SILLÉN's "core and links" theory [61]. The occurrence of OH bridges in the precipitate is the first argument for the hypothesis that those bridges occur also in the polymeric ions in the solution near the precipitation point.

A second argument comes from the theory of complex chemistry. In a non-complexing, strongly acidic solution the UO_2^{2+} ion carries six water ligands. For our discussion this configuration will be written as A in the sequence:

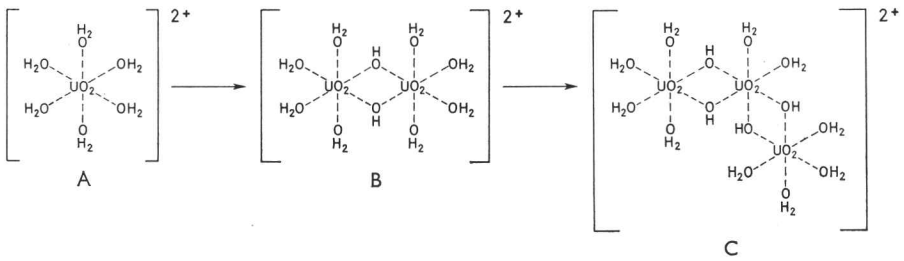

It seems unlikely that two of such ions combine into a dimer. At an increasing pH however the H_2O ligand tends to loose a proton, thus forming an OH

ligand. Two of such uranyl ions might then combine in the way which is represented in B, so that OH bridges are formed, similar to those in the precipitate. The normal notation of this ion is $U_2O_5^{++}$. It might also be represented by a formula like $[UO_2(OH)_2UO_2]^{2+}$. In both cases the water ligands have been omitted. At an increasing pH the transition of another water ligand into OH decreases the charge of the ion and a third uranyl group might attach itself, most probably in an asymmetric position such that configuration C is obtained.

This ion is equivalent with $U_3O_8^{++}$ or $[UO_2(OH)_2UO_2(OH)_2UO_2]^{2+}$. In SILLÉN's notation it is written as $[UO_2\{UO_2(OH)_2\}_2]^{2+}$.

Under strongly alkaline conditions the OH bridges may change further into oxygen bridges. This, however, has not to be considered around the point of precipitation of uranium.

In the same way as has been described above other ligands such as NO_3^- and CO_3^{2-} may be attached to the uranyl groups.

From the above it is clear that in this concept attaching an ion and more particularly a polymeric ion to the crystal surface of the precipitate requires the removal of several protons at the same time. If linking starts across a water ligand a H_3O^+ ion will easily be removed from the two ions. We believe that linking a polymeric ion to the crystal surface is facilitated by the similarity of their structure and by the directing forces in that crystal surface. Thus, "adsorption" of polymeric uranyl ions will result in a fast increase of the H^+ ion concentration of the liquid: the crystal surface enhances the hydrolysis of adsorbed uranyl ions.

It might be usefull to compare the explanation of the decrease of the pH given above with that of TROMBE [66] who suggests that it is provoked by the transition of the precipitate from a colloidal into a flocculated or a crystalline state. This result is in agreement with our hypothesis if the transition of the precipitate is really one from a non oriented (amorphous) state into an oriented (crystalline) state. Adsorption of uranyl groups onto the non oriented solid could not enhance the hydrolysis similarly. There is, of course the possibility that she has observed a flocculation of the initial colloidal precipitate. When this precipitate was amorphous, there is, however a good chance that crystallization starts somewhere in the same pH region. Flocculation of a hydrated metal oxide depends, to our opinion, largely on its hydrolytic behaviour, and there are arguments that the same might hold to some extent for the crystallization of the amorphous precipitate. In that case both phenomena are more or less caused by changes in the structure of polymeric ions and of the solid surfaces in the system, which are both a consequence of the changing hydrolytic conditions. One might say that according to the classical chemistry the hydrolysis is complete when the cations have their equivalent number of OH^- groups. In terms of the modern notation used above this means that all

links between the uranyl groups are OH bridges. On the acid side some OH ligands will become OH_2 ligands, thus providing a positive charge to the surface, which may lead to peptization, on the alkaline side a further proton will be split off from an OH bridge and the link becomes an oxygen bridge, which renders the surface negative. Nearing the pH where the hydroxyl groups are stable, means at the same time lowering the surface charge of the precipitate and accommodating the configuration of the ions to that of the final UO_3 hydrate crystal. This of course will lead to flocculation and it may provoke crystallization. Therefore there seems to be no essential disagreement between the different facts. However, the decrease of the pH can only be explained with the hypothesis presented above, which at the same time explains the simultaneous effect of flocculation and suggests the possibility of crystallization.

b. The influence of the uranyl nitrate concentration

A second variable which might be important is the concentration of the uranyl nitrate solution. SUTTON [54] asserts that all his titration curves of uranyl perchlorate with NaOH show an inflection at exactly a ratio $OH^-/U = 1.66$ independent of the concentration. FIG. 57 gives a set of curves for five

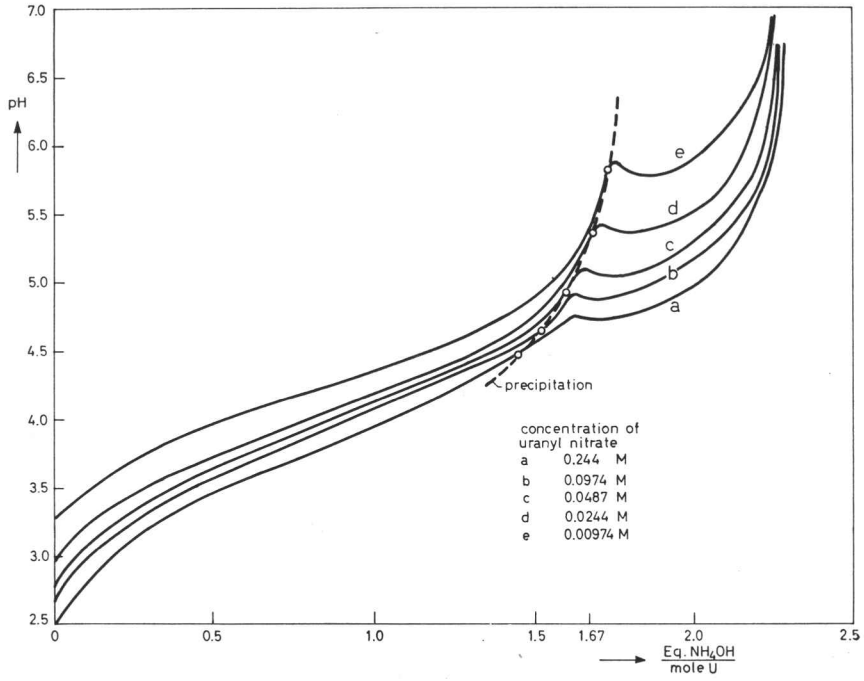

FIG. 57 Influence of the uranium concentration on titrations with 1.045 N ammonia. The ammonia has been added at a constant rate of 0.21 equivalents NH_4OH per mole uranium and per minute.

different uranyl nitrate concentrations ranging from 0.0097 to 0.2435 molar. The rate of titration has been chosen such that the complete titration of each of the curves would have taken 25 minutes. The volume of uranyl nitrate and the size of the burette have been selected to cause the same increase of the OH^-/U ratio per unit time, which is 0.21 OH^-/U per minute. The curves are therefore completely comparable to one another and they show what happens when various amounts of water are added to 4 ml of a 0.2435 molar uranyl nitrate solution on titration with 1.945 N ammonia at a constant rate. As one might expect, the point of precipitation shifts to higher OH^-/U ratios on dilution. These points of precipitation are the intercepts of the broken line in the graph with the titration curves. Furthermore the point of precipitation comes nearer to the point of decrease of the pH when the uranyl solution is diluted.

c. The influence of the anion

Uranyl nitrate may form anionic complexes on hydrolysis. Therefore studies of the hydrolytic behaviour of the uranyl ion are generally carried out with uranyl perchlorate, the titrant being NaOH.

We made two measurements of titration curves with 0.0487 molar uranyl perchlorate and 1.045 N ammonia. The time of titration was $6^1/_4$ and 200 minutes respectively. Comparison with the matching uranyl nitrate curves shows that only a shift of a few percent of the curve towards higher NH_4OH/U ratio's occurs in the case of the perchlorate. This is in accordance with the strongly acidic character of perchloric acid.

d. The influence of the titrant

Titration of 0.0487 molar uranyl perchlorate or – nitrate solutions with NaOH gives curves which are rather alike those obtained with ammonia, except for the fact that the pH rises to a higher level at the end of the precipitation. The higher dissociation constant of NaOH compared with that of NH_4OH is responsible for this increase.

e. The influence of ammonium nitrate

Ammonium nitrate plays an important role in the formation of a type III product in the urea process (CHAPTER V). It is important to know in how far the hydrolytic reactions of U(VI) in solution are influenced by the presence of ammonium nitrate. Therefore titration curves with a time of 200 minutes were measured for 10 ml of a 0.0487 molar uranyl nitrate solution to which 10, 100, 500 and 1000 mg of NH_4NO_3 had been added. The titrant was 1.045 N NH_4OH. The initial pH of the solution decreases slightly with an increasing NH_4NO_3 content. In the same order it decreases at the end of the titration. This seems to be caused by the acidic nature of NH_4NO_3. The curves show the

normal shape, the precipitation point is found at a constant NH_4OH/U ratio. No significant influence of NH_4NO_3 was evident from these curves. For higher uranyl concentrations (0.5 to 2 molar) this NH_4OH/U ratio in the precipitation point decreases to below unity.

f. The influence of the stoichiometry

A variable related with the NH_4NO_3 content is the nitrate deviation from stoichiometry in the initial uranyl nitrate solution. Three curves were measured at rates of 25 minutes, the uranium concentration of the starting solution being 0.0487 molar, the nitrate 0.081, 0.097 and 0.154 gram ions per litre respectively. In the case of over-stoichiometry *i.e.* in the presence of free acid, the normal titration curve is preceded by the titration of the free acid, thus giving rise to an extra inflection point for the free acid. For understiochiometric uranyl nitrate the curve is accordingly shorter. Except for a slight influence of the NH_4NO_3 the curves are identical for the rest.

We are well aware of the objection that in the work described above an arbitrary choice has been made, especially as far as the time of titration is concerned. Other titration rates might reveal effects which were not found in our experiments. Consequently the conclusions are very preliminary. However, it appeared to us that studying the decrease of the pH in a partially hydrolyzed system provided a much more sensitive means for detecting the influence of certain parameters than the titration curves. Here again the objection will be that the field has been explored rather superficially. The aim of this work has been to track down certain phenomena which might be related with the urea process. A more complete study, fascinating though it is, did not fit into our program.

VI.4.2 Changes of the pH in closed systems

A uranyl nitrate solution which is titrated with alkali at a reasonable rate can not reach equilibrium during a titration at room temperature. Consequently, when the addition of alkali is stopped the system will change towards equilibrium. In this chapter such a system is called a closed system from the moment that the titration stops.

a. The rate of titration

In the foregoing it has already been mentioned that after the addition of ammonia the pH of a uranyl nitrate solution decreases slowly. The rate of decrease may depend on a variety of conditions, but it certainly will depend on the deviation from equilibrium and thus on the rate at which the titrant has

been added. Therefore in the first series of experiments 10 ml portions of a 0.0487 molar uranyl nitrate solution were titrated with 0.778 ml of 1.045 N ammonia at different rates. With this amount of ammonia the decrease of the pH was complete within a few hours for all the curves. The time necessary for the addition of ammonia was 7.8, 15.6, 62 and 156 minutes (FIG. 58 curves a through d respectively). Thereafter the pH was recorded. In FIG. 58 these recordings are given without the curve of the preceding titration. In accordance

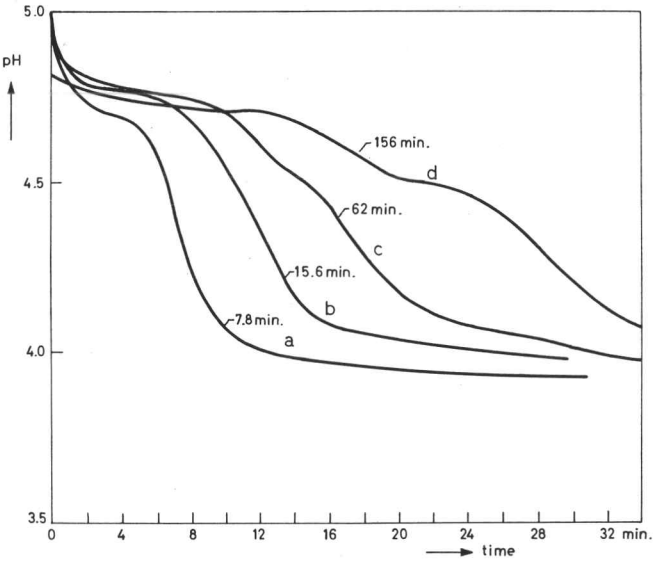

FIG. 58 Decrease of the pH after the addition of 0.778 ml 1.045 N ammonia to 10 ml 0.0487 M uranyl nitrate at different rates.

with the fact that the hydrolysis proceeds further during titration at a low rate of addition, the starting pH for the decrease and the rate of decrease are lower for the lower rates of titration. Roughly the decrease takes place in two steps, the first level being near 4.75 pH and the second one near 3.90 pH. For slower titrations however a third level is developed at about 4.50 pH, indicating another step in the hydrolytic sequence. The occurrence of this level will not only depend on the titration rate, but also on the total amount of ammonia added to the system, the uranyl nitrate concentration and the temperature. This could not further be investigated.

b. The stepwise decrease of the pH

The occurrence of several steps in the decrease of the pH is most probably due to the presence of more species of hydrolytic U(VI) ions in the solution, which precipitate after several hydrolytic reactions, most probably complicated by polymerization. There might be, however, another explanation of the curve,

in which the first decrease is due to some supersaturation effect. This decrease might *e.g.* cause a change in the electric double layer of the solid and the system might shift towards a new equilibrium. In that case one could expect that the stepwise decrease does not occur when the system is kept rigourously at the pH which is reached at the end of the titration. Curve c from FIG. 58 is shown in FIG. 59 as curve a. In the same figure the total amount of 1.045 N ammonia which is needed to prevent the decrease of the pH in an identical experiment

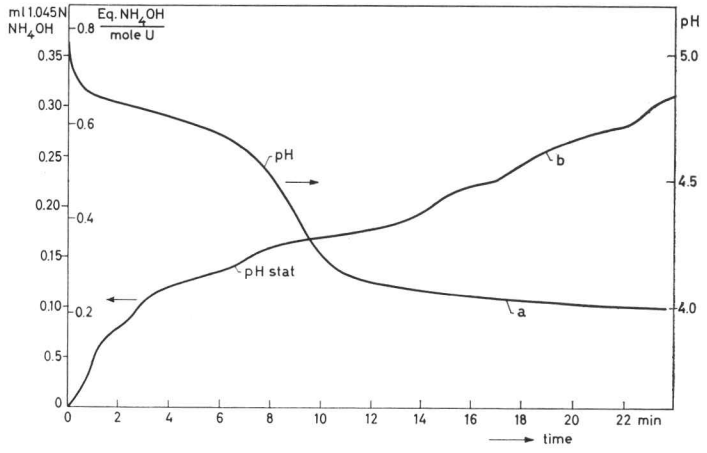

FIG. 59 Decrease of the pH of a closed system compared with the rate of addition of ammonia to keep the system at its initial pH (10 ml 0.0487 M uranyl nitrate, 0.778 ml 1.045 N ammonia).

is plotted versus time. The number of levels has increased. They are not provoked by the operation of the automatic titrator, but they seem to represent true phenomena in the liquid. These phenomena have been complicated of course by the intermittent addition of ammonia to keep the pH constant and by the dilution effect. Thereby superposition of several titration curves may have occurred.

A few things should be kept in mind in comparing both curves. The first is that by keeping the pH at the initial high value, a higher driving force is present for the hydrolytic reactions than in a closed system. One expects therefore that the pH stat curve will be shorter and that only the first part of it represents the total of the other curve. Secondly, one should try to compare the pH of one curve with ml NH_4OH of the other. Only an estimate can be made here, because nothing is known about the buffering capacity of the changing system. If the system, after the decrease of the pH would have the same buffering action as during the last part of the titration, which precedes the decrease, the total amount of ammonia used in the pH stat curve would

suffice to raise the pH of the closed system to its starting pH value of 5.05. This seems reasonable. One should then be aware of the fact that whereas the pH stat curve is on a linear scale, the pH decrease curve is on a logarithmic scale with respect to the H^+ production or the NH_4OH consumption. This means that in the first five minutes the ammonia take up is higher than the H^+ production of the other curve. This again indicates that the pH stat curve is essentially shorter in the first part, than the pH decrease curve. Estimated by comparison again with the titration curve, the NH_4OH taken up in the pH stat experiment would compensate the pH decrease in the other case after about 13 minutes.

c. The rate of precipitation

If hydrolytic reactions cause the stepwise decrease of the pH in a closed system, this might appear in measurements of the rate of precipitation of uranium in such a system.

To 200 ml of a 0.0487 molar uranyl nitrate solution 15.29 ml of 1.045 N ammonia was added in 20.9 minutes (this rate being equal to that of the foregoing experiments). Of the resulting solution 15 ml samples were taken at intervals. The liquid was centrifuged in one minute and 10 ml of the supernatant liquid were taken for the determination of the uranium concentration. In these measurements it was supposed that all solids were removed in the centrifuging procedure because a very clear liquid was obtained. On the other hand precipitation during centrifuging was neglected.

The results both of the concentration and the pH measurements with time are given in FIG. 60. It is evident that a decrease of the pH is accompanied by

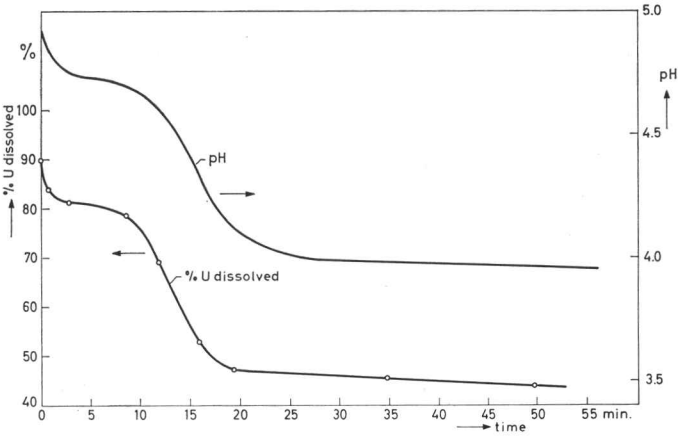

FIG. 60 The rate of precipitation of uranium in a closed system and the simultaneous decrease of the pH (10 ml 0.0487 M uranyl nitrate, 0.778 ml 1.045 N ammonia).

a simultaneous increase of the precipitation rate. This seems to be a further proof of our theory.

d. The influence of the OH^-/U ratio *

The rate of decrease of the pH depends largely on the total amount of ammonia added. One might expect that this rate increases with an increasing ammonia content, when added at the same rate. This view, however, does not hold for a sequence of reactions with different reaction rates. By increasing the amount of ammonia the reaction rate of a certain hydrolytic or polymeric step will be increased to such an extent that the reaction becomes instantaneous and thus

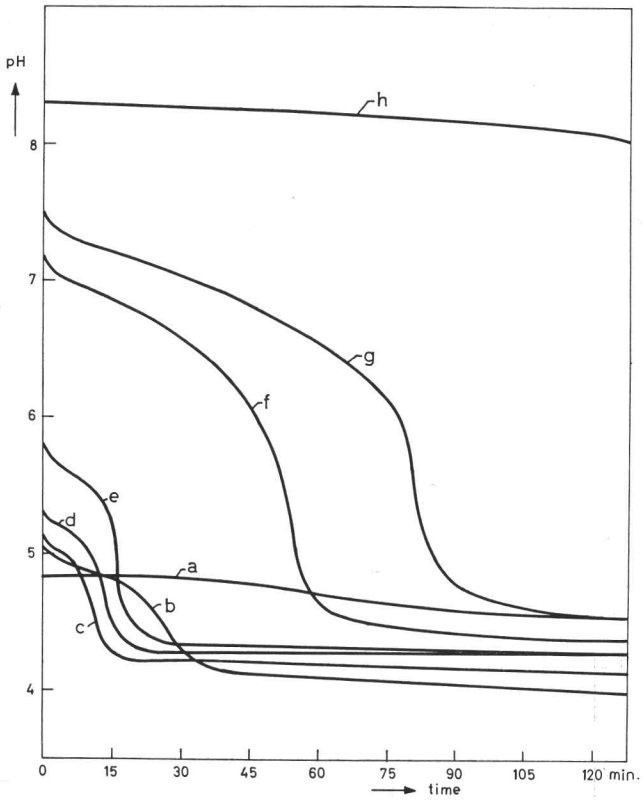

FIG. 61 The rate of decrease of the pH of 10 ml 0.0487 M uranyl nitrate, titrated with different amounts of 1.045 N ammonia.

invisible in the pH decrease diagram. There the next, slower reaction will become visible as a pH decrease of initially slower rate. This might be the explanation for a series of experiments with 0.0487 and 0.0974 molar uranyl nitrate solutions. The results of both series were essentially the same. Only the

* The valuable assistance of Mr. H. KERSTEN in these experiments is gratefully acknowledged.

experiments with 0.0487 normal uranyl nitrate are reported here. The experiments were carried out as follows: 10 ml of a 0.0487 molar uranyl nitrate solution were titrated with 1.045 N ammonia at a rate of 0.1 ml per minute. At a certain pH the addition was stopped and the pH was measured versus time. Twenty seven of such curves were measured between a pH of 4.56 and 8.30. Eight of them are shown in FIG. 61, which will be used to demonstrate the results. In this graph it is shown that at a low pH, curves are obtained with a very low initial rate of decrease of the pH (curve a), because the driving force for hydrolysis is still small. With increasing amounts of ammonia the pH starts to decrease faster (curves b and c), then it becomes slower again (curves d to h). In fact the same cycle of increase and decrease of the rate with which the pH falls is repeated once between the curves c and d. However, for the sake of readibility of the graph these curves have been omitted. The same result is found for the 0.0974 molar solution.

This alternating behaviour of the system to decrease fast and slowly in pH, should show up in the complete titration curve itself. The modulations, however, may be very small in most cases. The method of measuring the decrease of the pH with time seems therefore much more accurate.

In relation with the decrease of the pH occurring during the formation of a type III product one might conclude that a uranyl nitrate system of gradually increasing ammonia content shows a varying tendency to decrease its pH. Of course the results cannot be applied to the conditions of the urea process directly. We believe however that crystallization of the amorphous precipitate into a type III product occurs in such a region of fast decrease of the pH.

e. The influence of the concentration

The influence of the concentration has been measured also, be it for only one

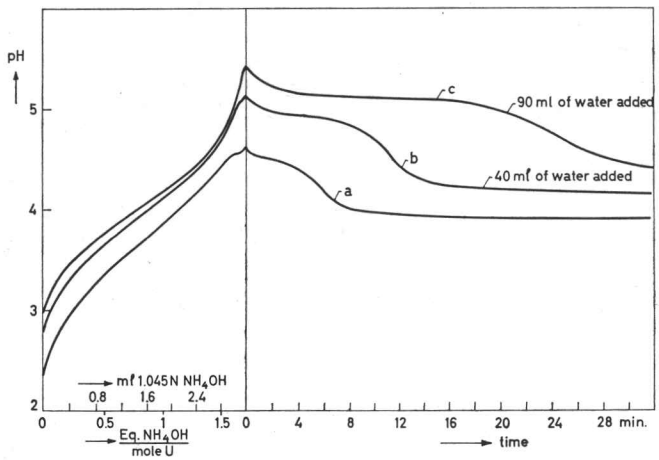

FIG. 62 Influence of the dilution on the rate of decrease of the pH (10 ml 0.196 M uranyl nitrate, 3.20 ml 1.045 N ammonia)

ammonia content. After the results just mentioned it needs no further comment that the data of this experiment depend strongly on the amount of ammonia added.

The measurements were carried out with a 0.196 molar uranyl nitrate solution. To 10 ml of this solution 3.20 ml of 1.045 N ammonia was added at a rate of 0.1 ml per minute. Then the pH was recorded as a function of time. FIG. 62 shows the results for the 0.196 molar solution itself (curve a) and for two experiments where 40 and 90 ml of water had been added (curves b and c respectively). The conclusion of this graph is clear: for the same amounts of uranium and ammonia the pH decrease is slowest for the most dilute system. The driving force for the hydrolysis appears to be the lowest in that case.

f. The influence of the titrant

In the urea process it was found that sodium ions had much less the tendency to provoke the transition A → III than ammonium ions. It is therefore important to see whether NaOH behaves differently from NH_4OH in a pH decrease curve. The main problem is: How does one compare those two titrants? One might add ammonia and NaOH either up to the same pH or in the same amounts. From the results presented in FIG. 61 it is evident that the choice may be rather critical. There might even be a third criterion which has escaped our attention. For lack of further indications we compared the pH decrease curves of 10 ml of a 0.0487 molar uranyl nitrate solution, titrated with either 1.045 N ammonia or NaOH at a rate of 0.1 ml per minute both to the same pH and with the same amount of 0.820 ml. FIG. 63 gives the results for

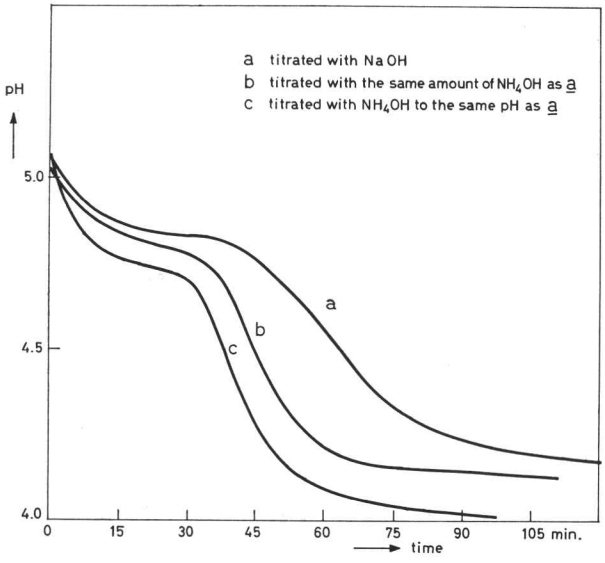

FIG. 63 Influence of the titrant on the rate of decrease of the pH (10 ml 0.0487 M uranyl nitrate, 1.045 N ammonia or NaOH).

uranyl nitrate with NaOH (curve a), with the same amount of NH_4OH (curve b) and with ammonia to the same pH as with NaOH (curve c). Similar results were found for a 0.0974 molar solution. The results indicate that the tendency towards a decrease of the pH is in this case much smaller for NaOH than for NH_4OH both when the amount of titrant added and when the starting pH are considered to be the decisive parameter.

g. The influence of carbonate ions

Hitherto we considered systems which were kept free of carbon dioxide. In the urea process this carbon dioxide plays an important role and it is self-evident that the influence of carbon dioxide on such measurements as described above, should be considered. Carrying out titrations in the presence of carbon dioxide or with carbon dioxide containing ammonia is very unsatisfactory because carbon dioxide escapes from the system in a nearly uncontrollable way. No good reproducibility could be obtained. This is mainly due to the stirrer (inhomogeneity and extraction of carbon dioxide), to the liquid – air interface (turbulence of the liquid, flushing of the gas) and to the measuring electrodes (gas bubbles in the liquid). It was far more interesting to see how carbon dioxide affects the decrease of the pH after the addition of ammonia. To this end an open titration vessel was used in which 15 ml of a 0.0487 molar uranyl nitrate solution was titrated with 0.990 ml of 1.1614 N ammonia containing carbon dioxide up to a molarity of 0.3. The titrant was made up of two solutions, one 1.1614 N ammonia and the other 1.1614 N in ammonia and containing 0.4 mole CO_2 per litre. They were mixed to the required CO_2 content. Depending on the amount of carbon dioxide which remained in the liquid, a certain pH was reached, which varied between 4.20 and 4.90 .The amount of ammonia was such that for curve a in FIG. 64, which was measured in the absence of CO_2, no precipitate had been formed at the end of the titration. However, as soon as the system contained carbon dioxide there was a precipitate. The higher the carbon dioxide content, the lower the starting pH and the more precipitate had been formed.

The curve without CO_2 shows the normal pH decrease with two levels, one at about 4.75, the other at 3.9. The same holds for curve b, representing a system with a very low CO_2 content. For the curves c through f, where the starting pH is lower than 4.75 due to a higher CO_2 content, the pH starts to rise until about the first level, then the pH decreases in two steps to the lower level. During the rise of the pH carbon dioxide is slowly leaving the system. This accounts for the fact that the system with the lowest pH and thus the highest CO_2 content, needs most time to reach its maximum. The correctness of this statement could be proved by measuring the rate of escape of carbon dioxide during the rise of the pH and by changing its chance of escape. When the

titration vessel is closed such that no CO_2 escapes, there is an increase of the pH of the system, but even after a few days no decrease takes place. It appears therefore that carbon dioxide interferes with the hydrolytic reactions, probably by the formation of $UO_2(CO_3)_3^{4-}$ ions and solid $(NH_4)_4UO_2(CO_3)_3$. The precipitate present after the addition of NH_4OH and CO_2 in these experiments consisted at least largely of this compound. On the other hand an enhanced extraction of CO_2 from the system by stripping the liquid with nitrogen causes

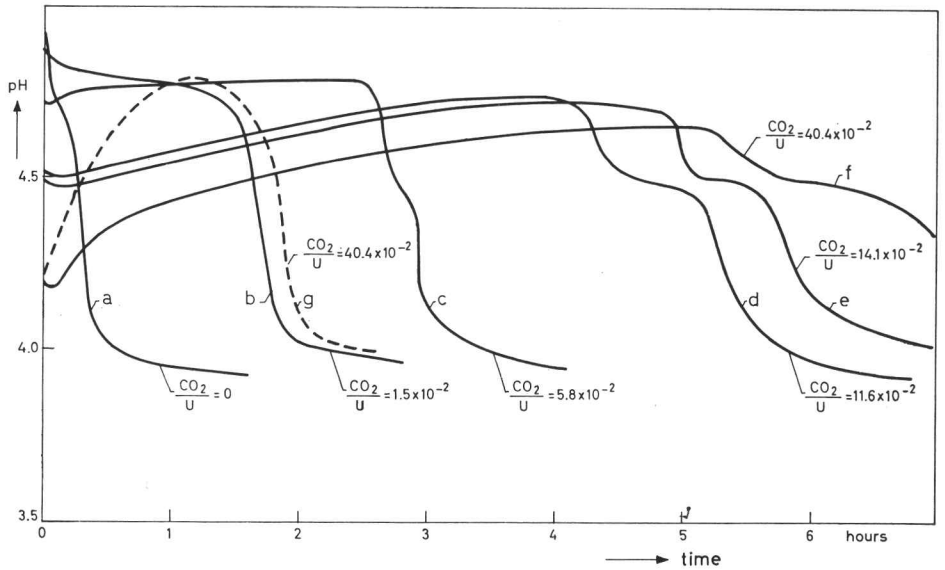

FIG. 64 Influence of the amount of CO_2 on the changes of the pH in a closed system (15 ml 0.0487 M uranyl nitrate, 0.990 ml 1.1614 N ammonia).

the pH to rise fast, as is the case in the dotted curve (g). Extraction by evacuation with a water jet pump did not work because after some time above the liquid a stagnant layer of CO_2 had formed which was not swept away and which had enough relative pressure to stop further escape of CO_2 from the liquid.

From the graphs it can be seen that the pH of CO_2 containing systems with an initial pH lower than the first level, starts to decrease slightly before it rises. The reason of this phenomenon is uncertain. We believe that it represents a slight hydrolysis as a consequence of the alkali addition. There are further indications that during the rise of the pH some hydrolysis takes place, as one should expect in parallel with the dissociation of the uranyl carbonate complex. The decrease of the maximum pH with time for the different curves could be understood that way. Additionally, when the system would reach, by

the expulsion of the carbon dioxide, a state which was identical for all curves, why would the decrease differ so much? We have seen that the intermediate level generally develops with time, that is to say with progressing hydrolysis, and it is therefore likely that hydrolysis has proceeded further the more waiting time was required for expelling the carbon dioxide. When air is bubbled through the liquid to enhance the escape of CO_2, the maximum pH becomes higher and the decrease of the pH proceeds in one step (compare f and g in FIG. 64).

h. The precipitation rate in carbonate containing systems

During the rise of the pH in carbonate containing systems, the precipitate present at the end of the titration dissolves partially. This was demonstrated in an experiment the results of which are shown in FIG. 65. In 64 minutes

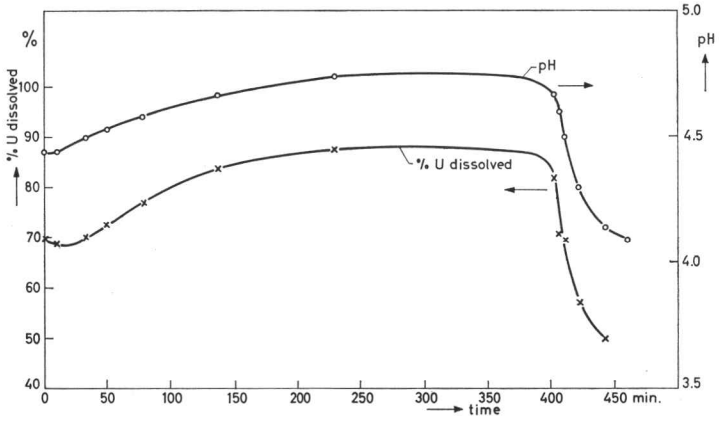

FIG. 65 Changes of the pH and the uranium concentration in a partially hydrolyzed carbonate containing system (200 ml 0.0487 M uranyl nitrate, 12.71 ml 1.1614 N ammonia).

12.71 ml of 1.1614 N ammonia, containing at the same time 0.192 moles of CO_2 per litre were added to 200 ml of a 0.0487 molar uranyl nitrate solution. Subsequently the concentration of the solution was measured with time in the same way as for the curve of FIG. 60. The pH was recorded during the whole process. The resulting curves show clearly that whereas 30% of the uranium was precipitated at the end of the titration, more than half this amount dissolved during the rise of the pH. The initial slight decrease of the pH shows up as a short precipitation, most probably due to hydrolysis.

The results obtained lead to the conclusion that during the addition of carbon dioxide containing ammonia a precipitate is formed consisting of ammonium uranyl carbonate and the normal precipitate obtained with am-

monia. Directly after the addition the hydrolysis still predominates as it does after a CO_2 free titration. Thereafter carbon dioxide starts to escape from the system and the complex ammonium uranyl carbonate dissolves slowly. The UO_2^{++} originating from this reaction starts to pass through the hydrolytic sequence towards precipitation. When the carbon dioxide content becomes low enough the influence of the hydrolysis of the U(VI) becomes larger than that of the CO_2 escape and the pH starts to fall. Thereby the rest of the CO_2 is removed and the system is dominated by the hydrolytic reactions, leading it to equilibrium at a lower pH. During this last part, the according precipitation occurs.

CHAPTER VII

X-RAY DIFFRACTION DATA AND STRUCTURAL RELATIONSHIPS

VII.1 Introduction

In this chapter all available X-ray data of the different compounds obtained in the urea process will be presented. Details of their preparation are included because only part of them has been discussed in the previous chapters. We feel sure, that a more systematic investigation will result in the detection of additional compounds. This, however, has not been the aim of the present work and we have restricted ourselves considerably.

The X-ray diffraction patterns were used for identification of products and only incidentally a structure analysis was carried out. A remarkable similarity of some patterns gave rise to a closer investigation of some related products obtained by other procedures such as titration of uranyl nitrate solutions with ammonia, or treating UO_3 hydrate with liquid or gaseous ammonia. The situation proved to be extremely complicated by the occurrence of different series of compounds in parallel. From this work strong indications were found that many of the so called "ammonium diuranates" are essentially UO_3-hydrates-ammoniates. The picture might be further complicated by the presence of NH_4^+ groups, when the existence of uranic acid is accepted.

VII.2 The compounds of the urea process

In the course of our experiments concerning the urea process, six different compounds were found with great certainty. In some cases it might be doubted whether another single compound was present or a mixture of identified compounds. Such cases are not included in this review.

The compounds prepared by the urea process are indicated by A (for the amorphous product) and by Roman numerals I to V.

VII.2.1 Method of preparation

The six compounds described in this part of the chapter have been prepared in the following way:

A. The amorphous precipitate is the main subject of this thesis, and its method of preparation has been nominated the "standard procedure". As for further products reference will be made to this standard procedure,

it will be described here shortly again: 100 ml uranyl nitrate solution, containing 40 millimoles of uranium and 132 milligram ions of nitrate, with a pH of about 2.7 (ammonia being used for raising the pH) is heated to 95 °C. Than, 50 ml of a hot urea solution (containing 25 grams of urea) is added under vigourous stirring with a vibrational or rotational stirrer (see CHAPTER II). In about one hour the precipitation starts, and it is complete in another hour. The precipitate is then isolated by rapid filtration, washing with cold water and drying with acetone.

I. This product can be obtained when the urea content in the standard procedure is lower than 10 to 13 grams. The duration of the process is thereby increased accordingly. It should be kept in mind for this and for the following products that the intensity of stirring influences the process, as has been shown in CHAPTER IV. Consequently, the exact limits of the chemical conditions depend to some extent on this parameter.

II. When, in the standard procedure, the urea content is above 35 grams, a type II product is obtained.

III. This product is prepared with a standard procedure in which the nitrate ion concentration of the starting solution is increased to more than 1.8 gram ions per litre by the addition of nitric acid or ammonium nitrate.

IV. This compound has been prepared by increasing the nitrate ion concentration of the starting solution to above 3.5 gramions per litre. This nitrate ion concentration can be decreased somewhat, provided that the urea content is decreased also. The same product was obtained in an experiment where hexamethylene tetramine was used as the ammonia donor instead of urea: 100 ml of a uranyl nitrate solution containing 40 millimoles of uranium and 82 milligram ions of nitrate were heated to 70 °C and a solution of 12 grams of hexamethylene tetramine in 50 ml of water was added. Some precipitate was formed at once. This was dissolved by adding some nitric acid and the final precipitation was carried out in the same way as with urea. A third method was to boil a type II product in an ammonium nitrate solution: 4 grams of a type II product were boiled for one hour with 16 grams of ammonium nitrate in 100 ml of water. The solids were filtered, washed with water and with acetone and dried. Some type III product was also present.

V. The type V material could be produced either by carrying out the standard procedure at an increased temperature (104–108 °C), or at an increased intensity of the stirring. By applying a stirrer with an extreme shear rate (*e.g.* an Atomix Mill) the same product could be obtained at 95 °C.

VII.2.2 X-ray diffraction diagrams

The X-ray diffraction diagrams of the five crystalline products are listed in TABLES VII.1 through VII.5 The diagrams were taken with a Philips diffractometer * and a recorder, the dispersion of the registration being 1 inch per 1 °Θ and the speed 1 °Θ per 2 minutes. The radiation was CuKα.

TABLE VII.1 X-ray diagram of type I product.

d	I	d	I
7.38	VS	2.431	W
5.04	VW	2.299	W
3.65	VS	2.266	VW
3.53	S	2.152	W
3.19	VS	2.133	W
3.03	W	2.041	W
2.95	VW	2.007	W
2.668	VW	1.965	M
2.537	M		

TABLE VII.2 X-ray diagram of type II product.

d	I	d	I
7.88	VS	3.77	W
6.16	W	3.47	W
5.13	VS	3.29	S
4.29	W	3.12	W
3.97	S	2.551	W
3.82	W	2.369	W

In FIG. 66 strongly reduced diagrams are shown of the type A, I and III products respectively. The identification of some of these products will be discussed further on.

VII.2.3 Chemical composition

The mean chemical composition of the six compounds listed under VII.2.1 is given in TABLE VII.6. In evaluating the results of the analysis it should be borne in mind, that slight variations were observed in all cases. It is doubtful whether the result of the analysis fits a single compound. The possibility should be considered, that the particles have an inhomogeneous texture, due to the fact that the successive layers of the particle are formed in a solution of slightly changing composition. On the other hand, considerable amounts of a compound may be present in such a way that it is not detected in the X-ray diagrams. In some cases a urea content of 10% in the solid could not be detected, nor did it influence the diagram of the main compound. This might indicate that this urea was randomly incorporated in the polymeric uranyl-hydroxyl-water skeleton.

VII.2.4 Discussion of results

The different products which were prepared by variants of the urea process can be classified according to their X-ray diagrams into six types. Within each of

* Type PW 1010.

TABLE VII.3 X-ray diagram of type III product.

d	I	d	I
7.63	VS	2.593	M
3.79	VS	2.524	M
3.60	W	2.058	M
3.56	W	1.965	W
3.25	M	1.888	W
3.21	M		

TABLE VII.4 X-ray diagram of type IV product.

d	I	d	I
7.57	S	2.593	M
3.74	S	2.104	M
3.64	S	2.045	M
3.52	W	2.023	M
3.26	S	1.973	W
3.19	W		

TABLE VII.5 X-ray diagram of type V product.

d	I	d	I
7.57	VS	2.593	W
3.77	M	2.544	W
3.59	M	2.510	W
3.47	M	2.041	W
3.24	M	1.969	W
3.15	M		

TABLE VII.6 Composition of the products obtained in the urea process.

Type of product	Specific condition in the preparation	Chemical Analysis					Mean Composition			
		% U	% CO_2	% NH_3	% NO_3^-	% urea	mole CO_2 / mole U	mole NH_3 / mole U	gr.ionNO_3^- / mole U	mole urea / mole U
A	standard	68.5	4.6	2.2	–	~1	0.36	0.44	–	0.05
I	reduced urea content	73	<0.1	1.7[5]–1.9	–	<0.5	–	0.34–0.36	–	–
II	increased urea content	57	<0.1	–	–	27	–	–	–	2.0
III	incr. nitrate ion content	73	<0.1	1.6–1.7[5]	–	<0.2	–	0.31–0.34	–	–
IV	high nitrate ion content	73	–	1.8	2.8	<0.1	–	0.35	0.15	–
V	increased temperature	73	<0.4	1.8	–	2.8	–	0.35	–	0.15

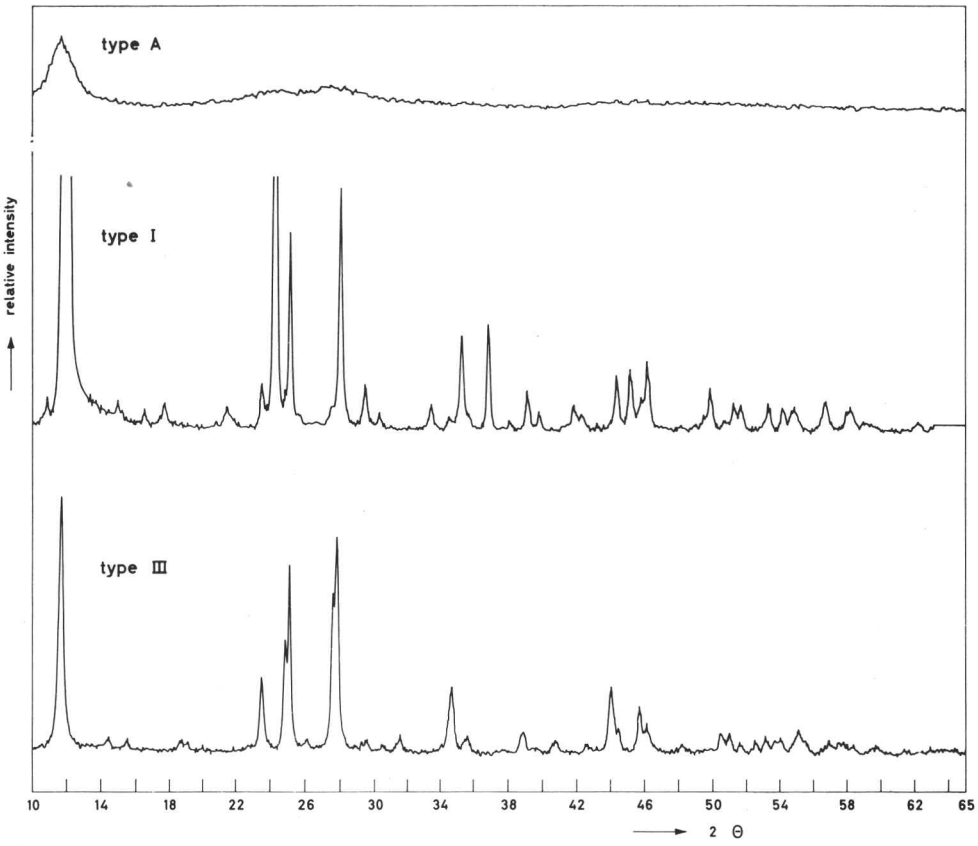

FIG. 66 X-ray diffraction diagrams of the type A, I and III products.

these categories slight variations of the cell parameters are found, thus giving rise to a great number of different X-ray patterns. Apart from those of the amorphous and the type II products, the X-ray patterns indicate pseudo hexagonal orthorhombic structures which show a great resemblance with that of $UO_3 \cdot 2H_2O$ [71].

There are two compounds which contain a rather constant amount of urea: II and V. We consider those as specific for the urea process. The type II compound contained more than 25% of urea and could be identified with the later published urea uranate of GENTILE [49].*

The formula was given as $H_2UO_4 \cdot 2CO(NH_2)_2$. The type V compound contains about 2.8% urea. It is likely that the amorphous precipitate is also typical for the urea process.

* The compound has been described again recently by DEMBINSKY [72].

Three sequences of products were found by varying the standard procedure:

1. With an increasing nitrate ion concentration the sequence

   $$A \rightarrow III \rightarrow IV$$

   is obtained.

2. When the urea concentration increases, the successive products are

   $$I \rightarrow A \rightarrow II$$

3. A third series can be obtained by decreasing the CO_2 content of the liquid. This is either effected by increasing the temperature (*cf.* FIG. 32) or by increasing the intensity of stirring. In the order of a decreasing carbon dioxide content the products

   $$A \rightarrow III \rightarrow II \rightarrow V$$

   were obtained.

From these sequences the conclusion can be drawn that there are several competing processes:

1. Incorporation of carbonate in the precipitate under complex formation with the uranyl group, versus carbon dioxide escape from the system.
2. The reaction of $UO_3 \cdot 2H_2O$ derivatives with urea, leading to the formation of a type II and possibly even a type V product.
3. Reactions of UO_3 hydrate like products with ammonia or ammonium ions.

The influence of ammonium nitrate is very complex. We found that ammonium reduces considerably both the rate of hydrolysis of urea and the carbon dioxide concentration of the liquid. Furthermore it might take part in the reactions by the formation of basic salts and decrease the rate of hydrolysis of uranyl nitrate.

The type III product might be the crystalline form of the amorphous precipitate in those cases where carbonate groups do not prevent its crystallization.

Further investigations are necessary to detect the true relations between the above mentioned sequences.

VII.3 Similar products prepared by other procedures

VII.3.1 The reaction products of a uranyl nitrate solution and ammonia

In trying to identify the different products of the urea process, precipitates were investigated which had been obtained by the reaction of ammonia with a uranyl nitrate solution. Several methods were used:

1. slow addition of aqueous ammonia to a uranyl nitrate solution;
2. very rapid addition of the ammonia;
3. slow simultaneous addition of uranyl nitrate and gaseous ammonia to a uranyl nitrate-ammonia system of the right pH in such a ratio that the pH was kept constant;
4. slow reaction of gaseous ammonia with a uranyl nitrate solution.

We found no influence of the method of precipitation on the type of product obtained as far as the X-ray diffraction pattern was concerned. At high reaction rates products of poor crystallinity and containing more impurities, were obtained. The fourth method yielded precipitates free of nitrate. This was taken as an indication that no occlusion had occurred and that the material was pure.

Uranyl nitrate solutions 0.14, 0.40 and 0.59 molar in uranium were treated with 1 N ammonia solutions. The precipitates were filtered and washed free from mother liquor very rapidly with water. Below a pH of 9.5 three different compounds could be isolated, all of which have closely related orthorhombic lattices. They were nominated α, β and γ in the order of increasing pH.

α. This compound was the first lasting precipitate produced in the clear solution. It was isolated at a pH below 3 after a very slow reaction. The X-ray diffraction pattern is identical with that of the type IV product.

β. In the pH region between 3 and 8.5 a second compound was obtained, the X-ray diffraction pattern of which is identical with that of a type III product. The α-compound is completely converted into the β-compound while the pH is raised.

γ. Above a pH of about 8.5 the structure of the precipitate changes again into that of the third compound. Its X-ray diffraction pattern is the same as that of a type I product.

The chemical composition of these three products is given in TABLE VII.7. The results agree fairly well with those of the corresponding products in TABLE VII.6.

TABLE VII.7 Composition of the α-, β- and γ-compound.

Compound	% U	% NH_3	% NO_3^-	mole NH_3/mole U	gram ion NO_3^-/mole U
α	72	1.5	2.9	0.30	0.16
β	73	$\leqslant 1.7^5$	–	$\leqslant 0.33$	–
γ	73	$> 1.7^5$	–	> 0.33	–

No investigation was made of compounds occurring at a pH above 10.

From TABLE VII.7 it can be seen that it is difficult to assign a certain composition to the β- and γ-compound. The transition $\beta \rightarrow \gamma$ occurs at a mole ratio $NH_3:U = 1:3$. As we found the composition of the β-compound always close to this ratio, whereas the γ-compound might have an ammonia content considerably in excess of this value, we are inclined to appoint to the β-compound a composition with the mole ratio 1:3 for $NH_3:U$. This has been confirmed by CORDFUNKE [69] recently.

It could be shown, that the criterion whether at a certain uranium concentration an α-, a β- or a γ-compound is formed, is given by the pH exclusively and not by the NH_4^+ or the NO_3^- content. The addition of ammonium nitrate does not cause the transformation $\beta \rightarrow \gamma$ below the pH transition point, whereas β is formed back from γ on lowering the pH below this point. It is interesting to compare these results with what was known at the time in literature.

Authors [20, 54] largely agreed on the occurrence of at least two compounds in the system described, a UO_3 hydrate and $(NH_4)_2U_2O_7$ [73]. Additionally there might be, under special conditions, and at an even higher pH, a compound $(NH_4)_2UO_4$. None of the structures belonging to these compounds is in agreement with that of the three compounds reported here. The ammonium uranate could certainly not have occurred in our system under the prevailing conditions, nor is it likely that the pH was increased far enough to obtain the diuranate. Only in one case – a slow reaction of gaseous ammonia with a uranyl nitrate solution at 95 °C – did we succeed in isolating a product which, most probably, is identical with the $UO_3 \cdot 2H_2O$ investigated by DAWSON and coworkers [71].

VII.3.2 The reaction products of UO_3 dihydrate and liquid ammonia

According to WATT [73], one of the methods to prepare $(NH_4)_2U_2O_7$ is to treat uranyl nitrate hexahydrate crystals with liquid ammonia. The product which we obtained from this procedure was micro crystalline and very impure. For reasons which will be discussed later on in this chapter, one of the conclusions of the experiments described above, was that the ammonia containing compounds were derived from $UO_3 \cdot 2H_2O$ by replacing part of the water by NH_3.* As liquid ammonia is strongly dehydrating we hoped to obtain a compound with a high ammonia content by treating $UO_3 \cdot 2H_2O$ with liquid ammonia. The disadvantage of the low reaction temperature was accepted in these experiments.

* This idea was put forward by Dr. P. B. BRAUN of Philips Laboratories (Eindhoven), who executed the X-ray work for the preceding experiments.
Later, the X-ray investigations were carried on by Ir. T. MARKESTEIN of our laboratory.

The starting material was produced by electro-dialysing an aqueous suspension of a type A product until it was free from electrolyte. The product thus obtained consisted of pure, crystalline $UO_3 \cdot 2H_2O$, with the structure given by DAWSON *et al* [71]. Ammonia gas was dried over solid NaOH and liquified in a condenser cooled by a solid carbon dioxide-acetone mixture. The UO_3 dihydrate was treated 5 to 10 times with fresh amounts of liquid NH_3, and dried by slow evaporation of the residual NH_3. The resulting compound had a hexagonal structure and contained about $^2/_3$ moles of NH_3 per mole of uranium. Subsequent treatments with water or dry NH_3 gas showed that a continuous region of hexagonal structures exists and that in this region the increase of the ammonia content causes a decrease of the lattice parameter. By washing the above compound with water and drying it in air a hexagonal compound δ was obtained with subcell parameters a = 4.09 Å and c = 7.50 Å. In this case part of the hexagonal compound had been converted into the β-product. When, on the other hand it was treated with dry gaseous ammonia, another hexagonal compound ε was prepared with subcell parameters a = 4.03 Å and c = 7.12 Å. This was initially considered to be the upper limit of the hexagonal region. The composition of the β-, δ- and ε-compound, as determined by chemical analysis, are

β. $UO_3 \cdot {}^5/_3 H_2O \cdot {}^1/_3 NH_3$

δ. $UO_3 \cdot {}^3/_2 H_2O \cdot {}^1/_2 NH_3$

ε. $UO_3 \cdot {}^4/_3 H_2O \cdot {}^2/_3 NH_3$

A surprising effect was, that the NH_3 content of the compounds within the hexagonal region could change very fast, thereby causing a rapid shift of the lines during the registration of the X-ray diagrams. The peaks remained sharp during these transitions. This phenomenon became an experimental problem in later stages of the investigations, especially for samples with a high ammonia content.

The X-ray diffraction patterns of the compounds δ and ε are given in the TABLES VII.8 and VII.9.

TABLE VII.8 X-ray diagram of δ-ammoniate.

d	I	d	I
7.10	VS	2.377	W
3.57	S	2.020	W
3.50	S	1.965	W
3.14	S	1.941	W
2.495	M	1.757	W

TABLE VII.9 X-ray diagram of ε-ammoniate.

d	I	d	I
7.50	VS	2.507	W
3.77	S	2.045	M
3.55	S	1.973	W
3.21	S	1.798	W
2.575	M		

VII.3.3 The reaction products of UO_3 dihydrate and gaseous ammonia at room temperature

From the experiments described under VII.3.2 it became clear, that a rather fast reaction might be expected between gaseous ammonia and $UO_3 \cdot 2H_2O$. The UO_3-dihydrate was therefore exposed to a dry gasstream of ammonia diluted with nitrogen or air, freed from carbon dioxide. The partial pressure of the ammonia was controlled by bubbling the nitrogen through a diluted ammonia solution and drying the gas over solid NaOH. The ammonia content of the gas was measured by an automatic titration assembly which determined the total amount of NH_3 versus time, and a flowrator. The sample was well stirred by vibrating the round bottom sample container in a vertical direction with a Vibromischer. In this way an intimate contact of the gas with all particles was assured.*

Two samples of UO_3 dihydrate were tested: the first one has been described above, the second was prepared by the reaction of U_2O_7 with water at room temperature. As the former sample proved to be much more reactive, it was chosen for further experiments.

In the course of these experiments it appeared, that the partial pressure of the ammonia gas was of hardly any influence on the composition of the end product. However, the lower the partial pressure of the ammonia, the longer it took to reach a certain composition. In one respect, the ammonia content of the gas was important: when a too high ammonia pressure was used, the sample heated itself to well above 100 °C and lost extra water, which was not replaced in further stages of the process. Therefore it was important to increase the ammonia content in the gas gradually.

With ammonia contents of the solid approximately between 1.0 and 1.7% by weight a new orthorhombic compound ζ was obtained. Around 1.7% a trifling but definite shift of the lines occurred, resulting in another compound

TABLES VII.10 X-ray diagram of ζ-ammoniate.

d	I	d	I
7.27	W	2.868	W
5.07	M	2.537	W
3.74	W	2.476	W
3.52	M	2.036	W
3.43	M	1.978	W
3.40	W	1.957	W
3.19	M		

TABLES VII.11 X-ray diagram of η-ammoniate.

d	I	d	I
7.27	W	2.850	W
5.07	M	2.530	W
3.74	W	2.457	W
3.52	M	2.032	W
3.40	M	1.973	W
3.38	W	1.957	W
3.17	M		

* The valuable assistance of Mr. J. H. PENNINGS for these experiments is gratefully acknowledged.

η, again with an orthorhombic structure. The X-ray pattern did not change with NH_3 contents increasing to well above 3%. Then a hexagonal compound was obtained fitting in the continuous region between the compounds δ and ε. By further reaction with dry pure NH_3 gas a hexagonal compound was obtained of the same type as the ε-compound but with a still smaller c-parameter: a = 4.03 Å, c = 7.07 Å. The ammonia content of that sample was 0.8 NH_3 per U. For the time being, this compound was nominated θ. The X-ray diffraction diagrams of the ζ-, η- and θ-compounds are shown in TABLES VII.10, VII.11 and VII.12.

TABLE VII.12 X-ray diagram of θ-ammoniate.

d	I	d	I
7.03	VS	2.362	W
3.53	S	2.020	W
3.50	S	1.956	W
3.14	S	1.940	W
2.472	M	1.754	W

VII.3.4 Discussion of results

The field, discussed in this part of the chapter had not been explored before, except for the compound called ammonium diuranate. Our results certainly are of a rather preliminary nature, but they provide, besides some tentative conclusions, a first orientation to a more systematic investigation. An attempt will be made here to point out why such differing and confusing results might have been obtained in our experiments and which conclusions have been reached for the moment.

In the results described above there are two arguments which induced the concept that at least part of the compounds found are UO_3–hydrates-ammoniates instead of ammonium uranates:

1. The resemblance of the structures α through θ with $UO_3 \cdot 2H_2O$ is remarkable. The orthorhombic lattices in this series are pseudo-hexagonal and all differences between the lattices can be explained by the occurrence of minor distortions and shrinkage of one lattice. When the $UO_3 \cdot 2H_2O$ is really a dihydrate, the similarity can only be understood when NH_3 can replace part of the water in the lattice.
2. The exchange of NH_3 with H_2O is reversible and proved to be so fast that it is a strong argument for the existence of UO_3 ammoniates in which the ammonia is not present as an ammonium ion, but as the easily removable NH_3.

On these grounds we proposed to write the pure UO_3–NH_3–H_2O-compounds not as ammonium uranates, but in the form $UO_3 \cdot (2-x)H_2O \cdot xNH_3$.

Independent measurements of the infra-red absorption spectra of similar compounds by DEANE [74] confirmed our hypothesis in so far that no NH_4^+ was found. Nevertheless, the interpretation of the X-ray diffraction patterns in view of structural relationships may be poor, because the pattern is mainly determined by the reflections of the heavy uranium atoms and nothing can be deduced concerning the positions of the light atoms. Neutron diffraction might shed some light on this question. The same holds for results obtained by GARNER [75], who also came to the conclusion that in a similar compound NH_3 could replace hydration water. She investigated a compound of the approximate composition $UO_3 \cdot 1^3/_4 H_2O \cdot {}^1/_4 NH_3$ and with the same X-ray pattern as our type III product.

CORDFUNKE [69] recently reinvestigated the system starting from the pure components UO_3–H_2O–NH_3 in water at 40 °C in order to avoid the presence of nitrate. He found the compounds $UO_3 \cdot 2H_2O$, β and two hexagonal ones which are well within the region between δ and ε. This seems to be in good agreement with our results. Although there is some discrepancy about the lattice parameters of the hexagonal compounds, the formula's attributed to the three ammonia containing compounds of CORDFUNKE are the same as those of our compounds β, δ and ε respectively. In view however of our further results, we believe that several series of UO_3–H_2O–NH_3 compounds may occur. This may depend on the system which is investigated, whether it is liquid or dry, and on the presence of nitrate. It might be that the hexagonal compounds found in the system investigated by CORDFUNKE comprise only an incidental selection in a much wider region of hexagonal compounds prepared in a different way. It is remarkable in this respect that, whereas we found a one phase hexagonal region between δ and ε, CORDFUNKE states that he found that his system is a two phase one between the two hexagonal compounds.

The γ compound which we found as a type I product in the urea process and as γ in the reaction between uranyl nitrate and ammonia solutions is not found in the pure UO_3–NH_3–H_2O system, although it does not contain nitrate itself. It might therefore be that the compound can only be formed in the presence of nitrate ions. When one now compares the β- and γ-compounds with those obtained by the reaction of dry ammonia gas with $UO_3 \cdot 2H_2O$ at room temperature it is interesting to note that the transistion $\beta \rightarrow \gamma$ takes place at the same U/NH_3 ratio of 3 as that of the transformation $\zeta \rightarrow \eta$. One might conclude therefore that $UO_3 \cdot 2H_2O$ is different or behaves differently in dry and liquid systems, or that a possible "astoichiometry" of the compounds causes the slight differences in structure. As to the first point: the true nature of the UO_3 dihydrate is still the subject of many investigations.

DELL [76] investigated several samples of $UO_3 \cdot 2H_2O$. Although the X-ray diagrams were identical, he observed marked differences in the infra-red ab-

sorption spectra, depending on the way of hydration. GENTILE [49] believes that he found proof for the uranate structure $H_2UO_4 \cdot H_2O$ because a urea uranate can form. DAWSON and coworkers [71] considered it to be a normal dihydrate and DEANE [74] is in favour of the formula $UO_2(OH)_2 \cdot H_2O$. More variations have been proposed but for our considerations these are not essentially different from the above ones. We believe that the formula given by DEANE represents the actual situation in the lattice. This would then consist of uranyl groups to which OH^- groups are attached, and additionally water molecules. A description of this lattice has been given in CHAPTER VI.

Arguments for this concept may be drawn from the following considerations:

1. DEANE [74], SCHWARZMANN [77] and PORTE [78] came to the conclusion that in the $UO_3 \cdot 2H_2O$ which they investigated, both OH^- groups and water are present.
2. We found that the exchange of NH_3 with H_2O in $UO_3 \cdot 2H_2O$ becomes extremely difficult after less than 1 mole of H_2O has been exchanged per mole of uranium. This might indicate that the true composition is $UO_2(OH)_2 \cdot H_2O$ in which the uranyl groups are linked into large polymers via OH bridges.
3. $UO_3 \cdot H_2O$ does not contain free water [77, 79] and accordingly we could not introduce NH_3 into the lattice. This last observation was confirmed independently by DELL [80].

Conclusively there are indications that the formula of a stoichiometric UO_3-hydrate-ammoniate should be written as

$$UO_2(OH)_2 \cdot (1-x)H_2O \cdot xNH_3$$

If one now supposes, in accordance with the scheme presented in CHAPTER VI, that the H atoms of the OH group can be split off as a proton, the oxide has the acidic properties expressed in the formula of GENTILE. The number of parameters in the UO_3–H_2O–NH_3 system has now increased considerably:

1. H_2O may be exchanged with NH_3.
2. H^+ may be exchanged with NH_4^+.
3. The total number of molecules $NH_3 + H_2O$ may deviate from 2. This was called astoichiometry above.

The difference between the compounds in a liquid and in a dry system might be caused by the first two parameters and even the special influence of nitrate might be ascribed to this effect. The third parameter has certainly been of influence in our experiments with dry gaseous ammonia. A compound $UO_3 \cdot (2-x)H_2O \cdot xNH_3$ is in equilibrium with a certain combination of pressures of H_2O and NH_3. When one lowers one of these pressures a defiency of the corresponding component (H_2O or NH_3) in the compound will occur

and it seems very unlikely that this defiency is completely compensated by an increase of the second component. One must expect that deviations occur from a total of two molecules (H_2O+NH_3) per molecule of uranium. The complete series of samples prepared by the reaction of dry ammonia gas with $UO_3 \cdot 2H_2O$ may be deficient in H_2O for this reason. A direct method for determining the water content of the samples is under development. The results presented here are considered to be preliminary and a more systematic investigation has started.

The problem to be solved first is, whether astoichiometry occurs and if so, whether this influences the structure. To this purpose samples are treated at different partial pressures of water, but at a constant NH_3 pressure.

After this first question has been answered, it can be decided in how far the investigation of the ternary system UO_3(solid)–H_2O(gas)–NH_3(gas) can be simplified. We hope to complete this study by applying thermogravimetry with simultaneous analysis of the decomposition gases.

In interpreting the results of the chemical analysis one should be well aware of the possibility that adsorption of H_2O and NH_3, or condensation of H_2O may occur at the surface or in the pores. It is still doubtfull in how far one can discern completely between this effect and the chemical reaction.

Concerning the products obtained in aqueous systems one might consider the fact that the two processes of hydrolysis and polymerization occur simultaneously. It is generally supposed that the same sequence of ionic species is produced. However it has been argued in CHAPTER VI that expectedly one process will be favoured above the other under certain circumstances. This in turn will lead to ionic species and possibly even solid products which are not identical for the different conditions.

VII.4 Conclusions

The aim of the X-ray work was to try and identify the different compounds obtained in the urea process. We have only partly succeeded there. The type I, III and IV products are identical with the compounds γ, β and α respectively, which are formed by the reaction between uranyl nitrate and ammonia solutions. They are, therefore, not specific for the urea process.

On the other hand the type II and V products are, and the amorphous precipitate probably also.

A remarkable effect of the products obtained in the urea process is, that except for the amorphous and the type II product, all compounds contain about $^1/_3$ mole of NH_3 per mole of uranium. The reason might be sought in the pH at which the process is stopped and which is in the same region as that of the β-compound in the uranyl nitrate-ammonia reaction. This β-compound

has the composition $UO_3 \cdot {}^5/_3 H_2O \cdot {}^1/_3 NH_3$. Because of the great similarity in the X-ray pattern and in the composition it is very likely that all the products discussed, are UO_3–hydrates-ammoniates or variants there from, except for the amorphous and the type II compound.

The relation between the series IV–III–I in the urea process and the corresponding α–β–γ in normal titrations is not yet understood.

From the observations of products obtained along other routes it is evident that the phase relations in the urea process should have been studied without washing these products. Even the very superficial and rapid rinse with cold water, may have changed the composition and the X-ray diagram. Although this gives rise to a certain doubt concerning the work described, it still provides a clear lead for a further investigation as a result of this work. Additionally, we believe that the rough outline given above is still correct.

CHAPTER VIII

THE APPLICATION OF UO_2 FROM THE UREA PROCESS

VIII.1 Introduction

In the INTRODUCTION to this thesis the requirements were listed which should be met in the production of the UO_2 powders for the subcritical assembly and for the high temperature loops.

In this last chapter an account will be given in how far the specifications were met and to what extent the powders were suitable for the development of the KEMA Suspension Test Reactor (KSTR). The experiments themselves fall outside the scope of this thesis. They were carried out by several members of the Reactor Development Group of KEMA.

VIII.2 Powder and process specifications

VIII.2.1 The particle size distribution

The requirements that the particles should be within a size range of 4 to 13 microns was not fulfilled, as 14 weight percent was larger than 13 microns (FIG. 8). However, with the knowledge acquired after the production and described in this thesis, a better product can be prepared.

Starting from the result that for a well designed precipitation apparatus a geometric size distribution is obtained with a standard deviation $\sigma_g = 1.2$, the weight percent of the UO_2 powder above 13 or below 4 microns can be plotted as a function of the d_g of the precipitate.

To that purpose use is made of a log probability grid (FIG. 67) in which the integrated size distribution is represented by a straight line. The slope of this line depends on the standard deviation σ_g, whereas the geometric mean diameter d_g is found at the 50% value. A set of parallel lines has been drawn, all having of course the same standard deviation $\sigma_g = 1.2$. On the vertical axis the diameter of the precipitate particles is plotted. The horizontal dotted lines at 5.7 and 18.6 microns represent final UO_2 sizes of 4 and 13 microns respectively. From this graph the percentage of the final UO_2 fuel which has a size smaller than 4 microns (the undersize fraction) or larger than 13 microns (the oversize fraction) can be read for any d_g value of the precipitate. Four examples have been drawn in the graph. They constitute the size distributions with under- and oversizes of 1 and 5%.

The under- and oversize fractions, taken from this graph can be plotted

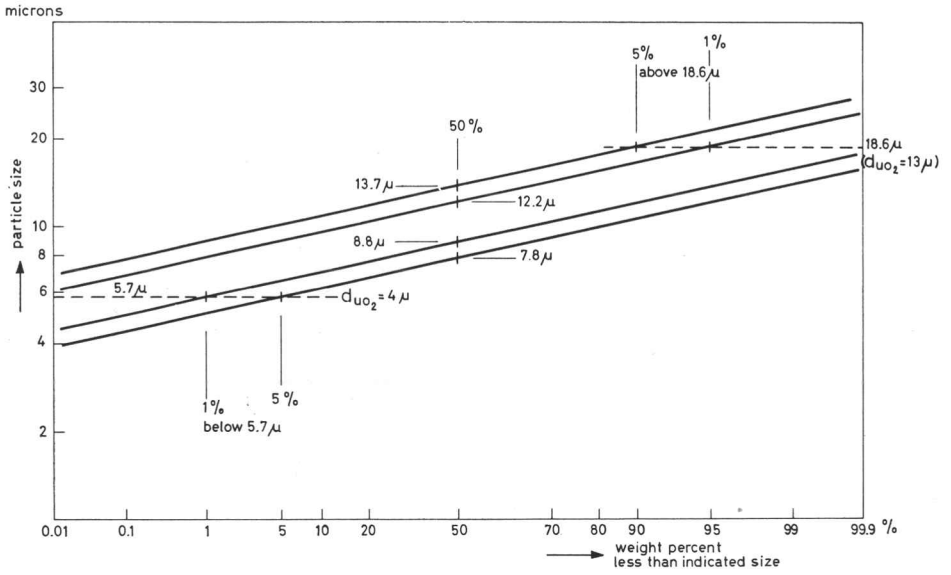

FIG. 67 Oversize and undersize of amorphous precipitates with $\sigma_g = 1.2$ for different values of d_g. The required size interval is 4 to 13 microns for the dense UO_2.

versus the mean diameter d_g of the precipitate, as has been done for $\sigma_g = 1.2$ and $\sigma_g = 1.3$ in FIG. 68. For example with a $d_g = 11$ microns and $\sigma_g = 1.3$, 0.6% of the UO_2 powder has a size below 4 microns, whereas 2.4% is larger

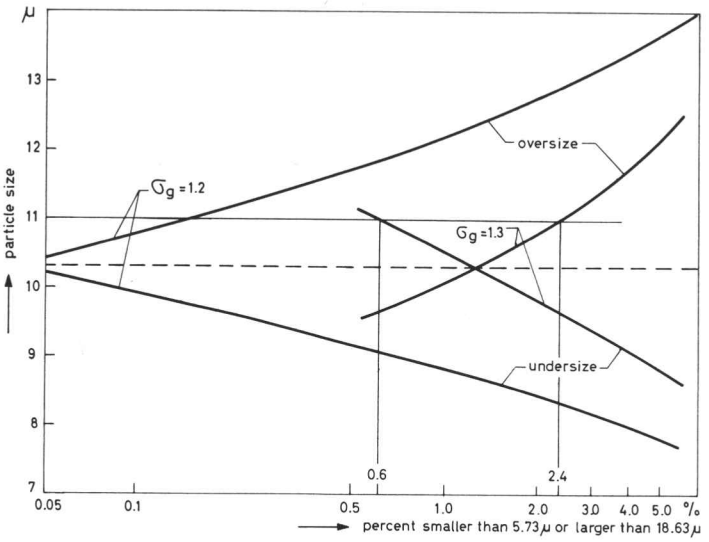

FIG. 68 Undersize and oversize for the 4 to 13 microns region as a function of the mean diameter and the standard deviation.

than 13 microns. This has been indicated in the graph by thin lines. For $\sigma_g =$ $= 1.2$ any d_g value between 8.8 and 12.2 microns results in a UO_2 powder with less than 1% by weight outside the specified limits. The best d_g value would of course be

$$d_g = \sqrt{d_{\max} \times d_{\min}} = \sqrt{5.73 \times 18.6} = 10.3 \text{ microns}$$

In II.4.1 it was shown that with a vibrational stirrer with an amplitude of 2 mm a precipitate with a $d_g = 12.8$ microns and a $\sigma_g = 1.2$ could be produced under standard conditions. From FIG. 68 it is concluded that in that case about 2 weight % of the resulting UO_2 powder is above 13 microns and that the amount below 4 microns is negligibly small. Powders with a better size distribution can be prepared when a still lower value for d_g is obtained. Two processes might be applied to achieve this purpose: either the urea process with an enlarged amplitude of the stirrer and a carbon dioxide overpressure for preventing crystallization, or the sulphate precipitation process (described in I.4.2) which yields smaller particles than the urea process. This process has the additional advantage of the very low σ_g value of 1.13.

In a similar way as described above a more general graph has been drawn (FIG. 69) for the weight percentage of the powder within the particle size limits of $d_{\min}$ and $d_{\max}$ as a function of the ratio $d_{\max}/d_{\min}$. The values indicated again hold for the optimal case where

$$d_g = \sqrt{d_{\min} \times d_{\max}}$$

This means that undersize and oversize constitute the same percentage of the powder. The vertical line at $d_{\max}/d_{\min} = 3.25$ indicates the size limits (4 and 13 microns) required for the UO_2 powder in the subcritical assembly.

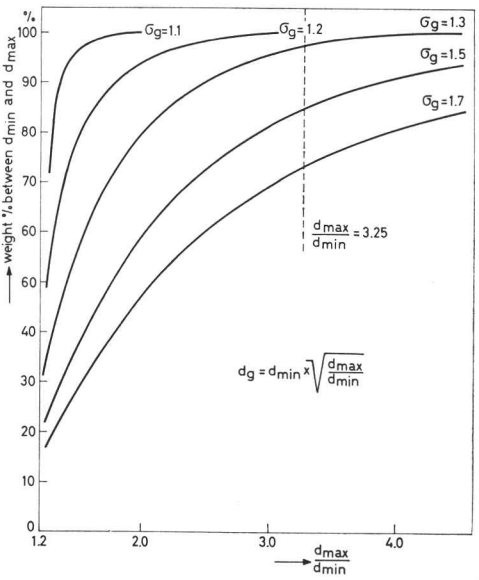

FIG. 69 The weight percent of a powder with a geometric size distribution, which falls within the size limits $d_{\min}$ to $d_{\max}$ as a function of the ratio $d_{\max}/d_{\min}$.

Although the size of the UO_2 powder was not within the limits indicated, the fuel was accepted for the subcritical assembly. As will be seen further on, the size range of this powder proved to be a better one afterwards for the near

critical experiments than the fuel ultimately chosen for the KSTR for several experimental reasons.

VIII.2.2 The particle shape

The amorphous precipitate obtained in the urea process consists of particles which are not spherical. Their cauliflower like habit is preserved during subsequent treatments of reduction and sintering (FIG. 70 a and b respectively). It

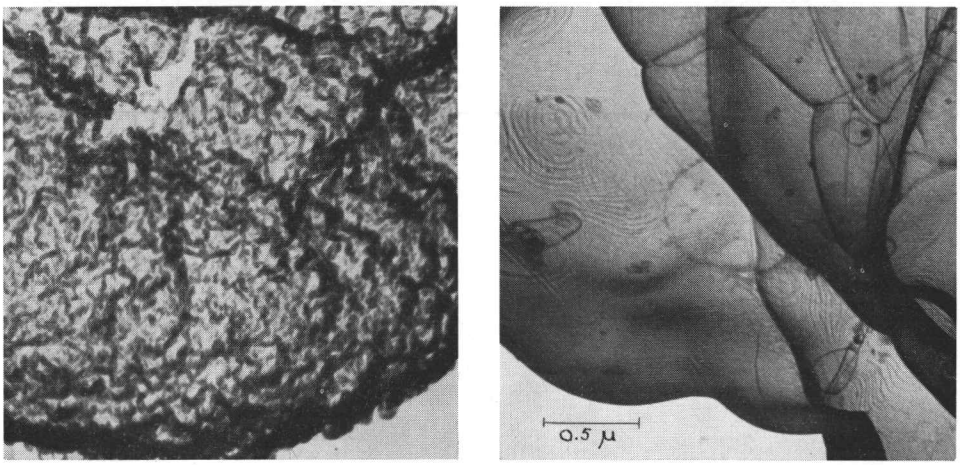

FIG. 70 Electron micrographs of (a) amorphous precipitate and (b) sintered UO_2 from the urea process.

can be seen, however, from these electron micrographs that the sintered material has a smooth surface and shows no sharp crystal edges. Due to this smoothness, the erosion caused by suspensions of this UO_2 in water was low as will be shown further on.

VIII.2.3 The specific surface area

The specific surface area of a powder of spherical, non porous UO_2 particles (density 10.6) of the given size distribution is about 0.05 m^2/gram. For the powder used in the subcritical experiment this specific surface area, as calculated from the adsorption isotherm of methane at the temperature of liquid nitrogen (B.E.T.-method) was, according to the specification, less than 0.1 m^2 per gram. The relatively small difference between the theoretical and the measured specific surface area is mainly caused by the cauliflower like nature of the particles surface.

VIII.2.4 The "strength" of the particles

It is very difficult to define the "strength" of a particle to be used in a circu-

lating suspension in a sensible way by simple physical parameters. In the reactor circuit the particles are mainly exposed to impact and grinding wear as soon as they break through the boundary layer. The strength of the particles in this respect proved to be good as will be discussed under VIII.3 and VIII.4.

VIII.2.5 Caking properties of the suspension fuel

No caking was observed in our loops under flocculating conditions. Temperatures up to 250 °C and flow velocities up to about 10 m/sec were used. At increased temperatures a hydrogen overpressure was chosen to prevent oxidation of the UO_2. It is our opinion that the two most important conditions for provoking caking seem to be the presence of fines in the caking material and of slightly soluble compounds, which can undergo recrystallization. If these fines are produced from the fuel at a sufficiently high rate, caking might occur when the other conditions are favourable.

VIII.2.6 Process specifications

The process, as it was applied, furnishes an extremely reproducible product of a narrow, controllable size distribution, whithout a size separation and without recycle. The precipitation yield is better then 99.5%. The process is simple and can easily be carried out remotely controlled. The main problem in the production was the sintering step, as the material exhibited such favourable sintering properties that the particles showed a strong tendency to form sintered agglomerates even at relatively low temperatures. This difficulty could be overcome by transporting the material slowly through a vibrating tube during sintering or by admixing 30–40% of already finished, and thus "inert" product.

VIII.3 The application of the UO_2 suspension fuel in the subcritical assembly *

The UO_2 powder, the preparation of which is the main subject of this thesis, proved to be an excellent fuel material for the subcritical reactor [9] and until recently it was used for all the experiments carried out with this assembly [81, 82].

With these experiments it could be demonstrated that very stable and safe reactor conditions can be established and that a rather ideal distribution of particles can be obtained under well defined conditions. The solids concentration of the circulating suspension can be kept extremely constant (*i.e.* within a few tenths of a promille) during extended periods of time.

The UO_2 powder, having a geometric size distribution with $d_g = 10.6$

* The experiments with the subcritical assembly were carried out by Dr. J. A. H. KERSTEN and his collaborators.

microns and $\sigma_g = 1.2$ (FIG. 7), afterwards proved to be a good choice for the subcritical reactor for two reasons:

a. In the reactor the range of the fission fragments in UO_2 was measured, because no reliable data were available. This can only be done when not all the fission fragments leave the particles, and thus when the particles are larger than the range of the fission fragments. This proved to be the case with the UO_2 powder from the urea process.

b. The settling velocity of the fuel particles in the liquid is an important factor in the kinetic behaviour of the reactor, as could be shown in other near critical experiments. The particle size of the ultimate fuel should be about 5 microns in order to have a good recoil separation effect. The settling velocity of such particles in water at 250 °C is comparable with that of 10–15 micron particles in water at room temperature.

Near critical experiments were carried out both with colloid chemically unstable and stable suspensions. Above a pH of about 8 the UO_2 suspension is colloid chemically stable and it has a negative surface charge. Below a pH = 7 the suspension is colloid chemically unstable and therefore it can flocculate. However, at a pH = 4.5 it becomes slightly less unstable due to the formation of some positive surface charge. A complete stability, however, is not reached at that point. Initially, the stabilization was brought about by the addition of ammonia because this can easily be removed from the fuel suspension. After a one thousand hours running period in the subcritical assembly a fast decrease of the pH was observed. This appeared to be due to dissolution of copper from the bronze impeller of the pump, forming a complex positive copper-ammonia ion which caused the negative suspension to become colloid chemically unstable. Flocculation in the reactor core was then observed. The difficulty was overcome by the use of NaOH.

The attrition of the particles was low. During 1500 running hours at a linear velocity of approximately 5 meters per second in the main tubing, about 1% of fines, with a size below 0.5 microns, had formed. The size distribution of the fuel, however, did not change markedly. The total neutron dose of the UO_2 particles was much too low to cause any fragmentation by fission products.

The experiments carried out with the UO_2 in the subcritical reactor are described now.

VIII.3.1 Reactor kinetic experiments [81, 82]

Their purpose was to study the influence of the colloid chemical stability of the suspension, the average flow velocity and the flow distribution in the reactor vessel on the neutronic stability and on the temperature coefficient of the system. The results are irrelevant for this thesis.

VIII.3.2 Measurement of the range of fission fragments in UO_2 [3, 83] *

When a fission occurs inside a particle of the suspension, the fission fragments will leave the particle and enter the liquid if the distance of the fissioned nucleus to the surface of the particle is less than the range of the fragments in the fuel material. The percentage of the fission fragments which is withheld in the solid phase is called the retention, and therefore a high fission recoil separation effect is identical with a low retention. As the range of a fission product depends on its mass and on the material in which it moves, it will be clear that the retention in a certain fuel particle is a function of the particle size and of the mass number of the fission fragment.

When, however, the fuel particles are approaching each other, there is an increasing chance that a fission fragment, ejected from one particle, has enough residual kinetic energy to enter another one, thereby causing an increase of the retention. For this reason, flocculation of the suspension and unfavourable flow conditions were avoided in the reactor core during the experiments. These were carried out with a neutron source in the reflector of 10^8 neutrons/second and a multiplication factor of the system of approximately 100. With an irradiation time of three hours, sufficient activity could be accumulated to make a radiochemical analysis of the fission products. Yttrium, the lanthanides and iodine were chosen as representatives.

When these experiments started it was assumed that the range of the fission fragments in UO_2 was about 10 microns, as was stated in literature [6], and a high separation yield was expected. The retention of the UO_2 powder, as calculated for the given size distribution [4], should be 1.5% for yttrium and 10% for the lanthanides. Instead 10% was found for yttrium, 25% for iodine and 44% for the lanthanides. From these figures ranges of 8.0, 5.6 and 4.2 microns could be calculated for the respective fission fragments [3]. These values, differing largely from the values generally reported [84, 85], are, however, in close agreement with those of BELLE and JONES [86] which came to our knowledge later.

For the calculation of the ranges, the UO_2 particles were assumed to be dense spheres with a diameter equal to the

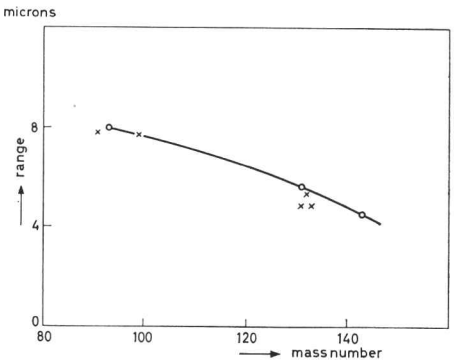

FIG. 71 Range of the fission fragments in UO_2 as a function of their mass number.

* The range measurements were carried out by Ir. T. MARKESTEIN, Drs. TH. VAN DER PLAS and their collaborators.

Stokes diameter of the actual particles. We believe that this assumption introduces only minor deviations. The ranges are given in FIG. 71 as a function of the mass number. The circles refer to the KSTR experiments, whereas the crosses represent the results of BELLE and JONES [89].

VIII.3.3 Measurement of the competitive adsorption of fission products on carbon *

The behaviour of the fission fragments which have left their UO_2 particle can be very complicated. Depending on their chemical nature they may be adsorbed onto the fuel surface or onto the wall of the suspension system. As it could be demonstrated that at 250 °C such adsorbed fission products adhere very strongly to the fuel surface, a simple separation of these products from the fuel will be impossible. It was therefore proposed [5] to introduce an easily removable adsorbing surface to compete with the fuel. Active carbon was chosen for this purpose. In a colloid chemically stable system it can be separated from the fuel by passing the suspension through a hydrocyclone. The carbon is thus transported with the water through the overflow, whereas the thickened fuel suspension forms the underflow.

The measurement of the distribution of adsorbed fission products between the fuel and the carbon can only be carried out after an irradiation. The reason is that most fission fragments initially formed are very unstable such that they change by a sequence of radioactive decays through a series of largely differing elements. Type, place and time of adsorption will therefore depend on the fission process, the decay sequence and the respective chemical and physicochemical properties of the isotopes formed, and on the specific properties of the adsorbing surfaces.

The subcritical reactor seems to be a perfect tool to carry out these investigations, even though the results will not be applicable at once at high temperature. Separate experiments have been carried out to this purpose with the described UO_2 fuel and carbon. This has led to unexpected results, which now are understood on the basis of the ionic and the colloid chemical charges in the system.

VIII.4 The behaviour of the UO_2 suspension in high temperature loops **

Many rheological and mechanical investigations at reactor temperature and pressure (250 °C and 60 atmospheres) are required for the design of the KSTR.

---

* These measurements were carried out by Drs. TH. VAN DER PLAS, Ir. T. MARKESTEIN and their collaborators.

** The technological experiments with the UO_2 suspensions were carried out by Dr. H. A. KEARSEY, Ir. F. W. VAN DER BRUGGHEN, Ir. A. SPRUYT and their collaborators.

These experiments and tests are carried out in stainless steel circuits in which suspensions are circulated under reactor conditions (except for the irradiation). In the loops the pressurization is achieved with hydrogen. From those technological experiments general experience is gained in handling suspensions. Furthermore technical data are obtained for the erosive properties and the attrition of the suspension. These data depend strongly on the geometry and the dimensions of the loop, on the flow velocity and on the size, shape and hardness of the fuel particles.

The phenomena by which the fuel particles decrease in size are breakdown by impact with the wall or the impeller of the pump, and by grinding forces between the particles mutually or between a particle and the wall. It is evident, that the mass of the fuel particles plays an important role. The mass of a UO_2 particle, produced with the urea process is roughly ten times that of an ultimate $UO_2 \cdot ThO_2$ fuel particle, produced with the sol-gel process.* Additionally the smoothness of the surface was considered to be better in the latter case. Therefore we thought that the use of the UO_2 particles in the loop would yield less favourable results than could be obtained with the spherical $UO_2 \cdot ThO_2$ fuel.

Comparative runs, however, with both fuels in toroids with a radius of 65 mm and an inner diameter of 8 mm, at 250 °C and with linear velocities of 6 m/sec showed that under flocculated conditions erosion of the stainless steel by the $UO_2 \cdot ThO_2$ particles occurred and that this erosion ten to twenty times higher was than that by the UO_2 particles [88]. Electron micrographs then showed that the surface of the $UO_2 \cdot ThO_2$ particles is rough and sometimes covered with small crystals. We suppose therefore that the roughness and possibly the greater hardness of the $UO_2 \cdot ThO_2$ powder accounts for this large difference.

The main circuit of one loop contains 12 kg of UO_2 of the same size distribution as in the subcritical assembly, dispersed in 27 liter of water. The suspension can easily be manipulated and a careful adjustment of the solids concentration is possible with the aid of a storage vessel and a hydrocyclone. In 3000 running hours at full concentration and with linear flow velocities of 4 m/sec in the main tubing under flocculated conditions, no caking was observed in the system. After this period about 4% of the fuel had a particle size below 2 microns and a slight shift in the size distribution towards smaller sizes indicated a preferred wear of the largest particles [89].

The overall erosion of the 347 stainless steel circuit was very low and well within acceptable limits for a reactor. Additionally, extremely severe erosion was observed in places of bad hydrodynamic design in the rotating pump.

---

* This process has been developed in our laboratory by Ir. H. S. G. Slooten [87].

An interesting observation was made on the fuel particles after an extended circulation time. The particles were partially covered with a thin oxide layer originating from the stainless steel walls.* This layer showed ferro-magnetic properties. The curiepoint (450 °C) indicated that the magnetic material might be a nickel-chromium ferrite [90]. It could be shown by toroid experiments that the particles were partially covered with bare metal after the oxide layer had been removed from the tube wall by erosion, and that oxidation of the non-magnetic metal by water produced the ferro-magnetic compound. Accordingly, hydrogen was found in the gas phase after runs at 250 °C. The attractive forces between the coated particles are strong and polarized, and they bring about a flocculation into a very specific open structure. The technical consequences of this effect are not yet clear.

A direct test [89] of the erosivity of the UO_2 suspension as a function of the flow velocity in a straight tube was carried out in a high pressure, high temperature loop (250 °C, 60 atm.). The suspension was pumped through a conical section of stainless steel tube in which the linear flow increased from 2 to 20 meters per second. Along the wall longitudinal strips were replaced by a soft metal. After 180 hours of running time the first indication of erosion of the soft metal was observed at that part of the cone where the linear flow velocity had been more than 9.5 m/sec. In 360 hours, this erosion became more severe, but no attack at places of lower velocities was found. The conclusion of these experiments is that in a straight tube erosion can be kept within acceptable limits, provided that a certain critical velocity is not exceeded.

VIII.5 Applicability of the UO_2 from the urea process for ceramic fuel elements

It has been mentioned that the sintering properties of the UO_2 powder from the urea process are excellent and that it compares favourably with the best UO_2 products from other "ADU" processes. One might expect that pellets pressed from such UO_2 will also sinter at comparatively low temperatures in a hydrogen-water vapour atmosphere. However, for producing dense pellets, additional requirements should be fulfilled as will be seen further on.

The high reproducibility of the process would certainly be an advantage in the production of ceramic fuel elements. It means that automatic presses can be fed with a UO_2 powder of constant properties and that readjustments of these presses during the production become superfluous as far as the feed material is concerned. This again warrants a product of constant quality. The powder is, without granulation, free flowing, thereby ensuring easy transport

* These experiments were carried out by Dr. H. A. KEARSEY, Ir. F. W. VAN DER BRUGGHEN and the author.

in furnaces and through feeding devices. For plants to be operated remotely controlled this property is of great importance.

A disadvantage, on first sight, is the narrow particle size distribution. It is unlikely that a dense packing in the powder and thus in the "green" pellet can be attained with a powder consisting of particles of nearly equal size. However, this argument only holds for hard powders which do not disintegrate easily under pressing conditions. For pellet production rather soft powders may be preferred, which are still reactive and which break down under moderate compression. This ensures a high density of the "green" pellet and a good interlock of the individual particles. For the ease of transport these powders should be free flowing. If, however, for one reason or another a UO_2 powder is needed with a high bulk density (*e.g.* for swaged elements) a production process which yields powders of a narrow size distribution in a controllable, wide variation of sizes might be of great help. Powders of different optimum sizes could be blended to yield a "synthetic" powder of maximum tap density.

A few experiments by VERKERK [91] to investigate the applicability of our standard UO_2 powder, previous to sintering, for pellet production were not successfull. This was attributed to the fact that the individual particles did not break down or did not deform under compression to produce a "green" pellet of high density. It seems to us that the production of a sintered UO_2 powder and a sintered UO_2 pellet require UO_2 starting materials with largely differing textures and reactivities. These, however, must depend strongly on the physical and chemical treatments of the precipitate. Recently we found how the porosity and the texture of the UO_2 can be controlled in the reduction step and we believe that a more elaborate investigation will result in a good procedure for preparing UO_2 for pellets with the urea process. The advantage of this process over other ones is the extreme reproducibility of the precipitate and therefore considerable savings will result from a decrease of the number of rejects, provided that the transition from the precipitate to a UO_2 powder with the desired properties can be controlled. We believe that this will not be too difficult.

Another investigation [92] intended to study the use of our standard UO_2 for pellet production seems to be less reliable because the starting material was not identical with ours.

VIII.6 Conclusions

Although it is evident from the data presented in this chapter, that minor improvements could be made to the UO_2 suspension fuel now, it will be clear that the powder produced served its purpose satisfactorily for research and development of the KSTR. Evidently no other UO_2 available at the time or

produced by processes then known would have been suited to our aims so well. We believe on the other hand that, with the present knowledge, better processes can be applied. For the further reactor development, however, there is no direct need for pure UO_2 fuel.

It will also be clear, that the UO_2 which we obtain from the precipitate by reduction with hydrogen is less favourable for pellet production. This, however, may be due to this specific reduction technique which yields a favourable powder for the fuel suspension process. The reproducibility of the precipitate, which is better than in most other processes, is important enough to study the transformation into UO_2 more fundamentally. Preliminary investigations indicate that this transformation might be guided towards the required UO_2 powder. The same holds for the other pure products of the urea process as was shown in two specific cases. Of these the work of the Swedish group [34] was known already for several years. In fact this process formed the basis from which we developed our new variant. The results obtained in our investigations might be applied to the Swedish process in order to attain a higher reproducibility. VERKERK [93] modified our process in so far that he increased all concentrations with 50 percent and that he worked at boiling temperature. From the crystalline product which he obtained, good pellets were produced after reduction, pressing and sintering.

Therefore we consider the urea process, in its many possible variations, well controlled and well understood, to be an excellent starting procedure for the more fundamental investigation of the textural relations between precipitate and reduced UO_2 as a function of different treatments. A wider industrial application of the process for the production of UO_2 pellets then seems indicated.

APPENDIX

ANALYTICAL PROCEDURES

In this appendix the methods of analysis have been collected, which were applied during the investigations described in this thesis. All chemicals used were reagent grade. The volumetric glassware was calibrated.

1 Uranium

The procedure presented here was used for the determination of the uranium content of the different products and of the uranyl salt solutions. Sulphate does not interfere.

Procedure

a. Solid uranium compounds

These are fired at 900 °C without pretreatment, and weighed as U_3O_8. If much organic matter or carbonate is present, the solid is covered in the crucible with a thin layer of desiccated oxalic acid. The temperature of the furnace is only slowly increased to 900 °C then.

b. Uranyl salt solutions

The sample is diluted with water, slightly acidified with 4 N sulphuric acid and boiled to remove any carbonate present. The uranium is then precipitated from the hot solution by the dropwise addition of carbonate free concentrated ammonia. The precipitate is filtered, washed with 0.4 N ammonia, dried and fired in a crucible at 900 °C to U_3O_8.

Reference

C. J. RODDEN, "The analytical chemistry of the Manhattan Project", National Nuclear Energy Series (McGraw-Hill Book Company, Inc., New York 1950) p. 46–47.

2 Carbonate

The procedure described was used for the determination of the carbonate content of solid uranium compounds. A micro modification was applied in a few cases to determine the carbonate content of solutions.

Procedure

The sample is enclosed in a leak tight glass vessel into which an excess of concentrated sulphuric acid is introduced. The carbon dioxide evolved from the sample is taken up in a stream of air which has been freed from carbon dioxide and water. The carbon dioxide is fixed in ascarite as sodium carbonate and the water resulting from the chemical reaction is then bound in desiccated magnesium perchlorate in a second U-tube. The carbon dioxide is determined by weighing the U-tubes.

Reference

G. E. F. LUNDELL, H. A. BRIGHT and J. J. HOFFMAN, "Applied Inorganic Analysis" (John Wiley & Sons, Inc., New York 1953) p. 768.

3 Ammonia

Two procedures were used for the determination of ammonia in uranium containing solids and solutions. The normal method was, to free the ammonia with alkali and distill it for acidimetric titration. In the presence however of urea, this compound hydrolyzes and the resulting ammonia is also determined. It seemed preferable to measure separately the NH_3 and NH_4^+ on the one hand and urea on the other. Therefore an existing method, called the Conway micro-diffusion method, was adapted for uranium compounds. The ammonia again is removed from the sample but at a temperature where urea does not decompose. Potassium carbonate is used for this purpose because it complexes uranium into a rather soluble compound.

Procedure

a. The distillation method

In this well known procedure the liquid to be analyzed is diluted, the solution is made strongly alkaline and the ammonia is distilled off with three fourths of the water into a known amount of standardized sulphuric acid. The ammonia content is determined by back titration with standardized alkali.

If the sample is a solid it is dissolved in water or in the smallest possible amount of acid. The solution is then neutralized and made strongly alkaline.

To improve the escape of ammonia, enough sodium carbonate is added to prevent the precipitation of uranium compounds by the alkali.

b. The Conway micro-diffusion method

The micro-diffusion is carried out in a commercially available Conway dish. This consists of a small thick-walled dish with a concentric inner compartment of lower height.

The sample is weighed into the outer compartment of the Conway dish and dissolved in a small amount of 1 N hydrochloric acid. Into the inner compartment 1 ml of standardized H_2SO_4 is measured. The outer rim of the dish is then greased with a special sealent paste. The solution in the outer compartment is neutralized with some alkali onto the point of precipitation and the liquid is made strongly alkaline with a potassium carbonate solution. The dish is closed immediately with a flat glass plate and swirled to ensure a good mixing in the outer compartment. After some hours all the ammonia has been absorbed by the H_2SO_4 of the inner compartment. The dish is opened and the excess acid of the inner compartment is back titrated in the dish.

The accuracy of the method is better than 1%. It is convenient for large series of analyses.

Reference

C. J. G. Altmann, B. H. J. de Heer and M. E. A. Hermans, Anal. Chem., *35*, 596 (1963).

4 Urea

The procedure described allows the determination of urea in the presence of ammonia and carbonate, but in the absence of carbamide. With xanthydrol urea forms a rather insoluble compound dixanthyl urea according to the reaction

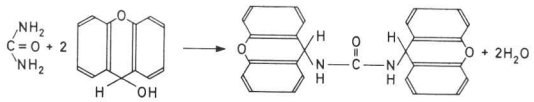

Procedure

3.5 ml methanol are added to a sample containing 5 to 40 mgr. of urea. Then 10 ml of water and 26.5 ml of concentrated acetic acid are used to dissolve the sample. The urea is precipitated immediately to prevent hydrolysis, by the addition of five 1.5 ml amounts of a 10 % xanthydrol solution in methanol. A waiting time of 5 minutes is required between the additions. The precipitate is filtered 60 minutes after the last addition, and washed with 20 ml of a saturated xanthydrol solution in methanol. The precipitate should not be sucked dry until the washing operation has been completed. All the liquid is then drawn off sharply, the residue is dried at 105 °C for one hour and weighed.

Reference

R. Fosse, Z. Anal. Chem., *63*, 80 (1923).

5 Sodium

A few sodium micro-determinations were carried out in uranium containing solutions. The sodium was precipitated as Na–Mg–UO_2-acetate with $6^1/_2$ molecules of water, and weighed as such.

Procedure

To 1 ml of the neutral solution, containing about 0.5 mgr. of Na 8 ml of a magnesium–uranyl–acetate solution is added. This solution consists of 3.2 grams of uranyl acetate, 10 grams of magnesium acetate, 2 ml of concentrated acetic acid dissolved under heating in 50 ml ethylalcohol and 30 ml water. The solution is diluted to 100 ml, filtered after 48 hours and stored in a polyethylene bottle. After the reagent has been added to the sodium containing solution, it is stirred for two minutes, stored at 20 °C for one hour and at 0 °C for at least two hours. The precipitate is filtered off, washed three times with 1 ml of an ice cold saturated solution of Na–Mg–UO_2–acetate in ethyl alcohol and with 1 ml of ether. It is dried at 70 °C.

Reference

C. J. VAN NIEUWENBURG and J. W. L. VAN LIGTEN, „Kwantitatieve Chemische Microanalyse" (D. B. Centen's Uitgeversmaatschappij, Hilversum 1961) p. 54.

6 Nitrate

Two methods have been used here. For low nitrate contents and in the absence of other anions an ion exchange method was used. In all other cases a reduction with the Devarda alloy was applied.

Procedure

a. The ion exchange method

A sample of the solution with a total content of less than 2 milligram ions NO_3^-, is diluted to 10 ml and percolated through a very small cation exchange column with a total exchange capacity of about 20 milligram ions NO_3^-. The cation exchanger is in the H^+ form. Thereafter the column is washed free from acid with 1 l of deionized water. The NO_3^- is determined as the free acid in the total percolate by titration with alkali.

In the case that a solid must be analyzed it is dissolved first in a known minimum amount of standardized acid before dilution.

About seven determinations can be carried out on one column before the exchanger need to be regenerated.

A similar method was developed by BHATNAGAR independently.

b. The reduction method

The sample is dissolved in some sulphuric acid if necessary, diluted and made strongly alkaline as for the NH_3 distillation method. Part of the water and all the ammonia present is distilled off and determined quantitatively if desired. Then the Devarda alloy is introduced which reduces the nitrate to ammonia, which in turn is distilled off and determined by absorption in standardized sulphuric acid.

Reference

D. V. BHATNAGAR, J. Sci. Ind. Res., *16B*, 23 (1957).

7 Sulphate

All the sulphates which had to be analyzed for the work in this thesis were free of other acids. Therefore an ion exchange method was used which is quite similar to the one described for nitrate.

8 Perchlorate

Here again the cation exchange method was used because the samples did not contain other acids.

9 Water

Water was determined in several solid uranium compounds. As uranium interferes with the Karl Fischer reaction, the water was extracted with methanol.

Procedure

From the sample to be analyzed the water is extracted in a dry flask by stirring the sample in absolute methanol for about one hour. A sample is taken then from the supernatant liquid and titrated by the dead stop-end point method with Karl Fischer reagent.

REFERENCES

Reports distributed by the United States Atomic Energy Commission and by the United Kingdom Atomic Energy Authority will be referred to as USAEC-Report and UKAEA-Report respectively. Reports issued by Reactor Centrum Nederland are indicated as RCN.

1. Bruyn, H. de, M. E. A. Hermans, Th. van der Plas, B. L. A. van der Schee and J. J. Went, Proc. 1st Geneva Conf., *3*, 116 (1955).
2. Kreyger, P. J., Th. van der Plas, B. L. A. van der Schee and J. J. Went, Proc. 2nd Geneva Conf., *9*, 427 (1958).
3. Markestein, T. and Th. van der Plas, Reactor Sci. and Techn., *16*, 33 (1962).
4. McDole, C. J., USAEC-Report WCAP-277 (1956).
5. Hermans, M. E. A. and Th. van der Plas, Nucl. Sci. Eng., *2*, 224 (1957).
6. Gardner, D. G., Nucl. Sci. Eng., *6*, 487 (1959).
7. Kitzes, A. S. and R. N. Lyon, Proc. 1st Geneva Conf., *9*, 414 (1955).
8. Jong, K. J. de, J. A. H. Kersten, J. J. Went, H. H. Woldringh and J. J. van Zolingen, Proc. 2nd Geneva Conf., *12*, 525 (1958).
9. Went, J. J., B. L. A. van der Schee, M. van Tol, J. J. van Zolingen and F. J. Schijff, Philips Techn. Rev., *21*, 109 (1960).
10. Gibson, A. R. and L. L. Wassell, Symposium on Reactor Materials, Stockholm (October 1959).
11. Schlechter, M., J. Nucl. Mat., *10*, 145 (1963).
12. Demarco, R. E. and M. G. Mendel, J. Phys. Chem., *64*, 132 (1960).
13. Kuhlman, C. W., USAEC-Report MCW-217 (1949).
14. Kuhlman, C. W., USAEC-Report MCW-215 (1949).
15. Bridge, J. R., C. W. Melton, C. M. Schwartz and D. A. Vaughan, USAEC-Report BMI-110 (1956).
16. Lister, B. A. J. and R. J. Richardson, UKAEA-Report AERE-C/R-1874 (1954).
17. Johnson, J. R. and C. E. Curtis, Proc. 1st Geneva Conf., *9*, 169 (1955).
18. Sanderson, J. R., H. E. Dibben and H. Mason, UKAEA-Report CI-R-15(SCS-R-163) (1959).
19. Boggs, J. E. and Munzir El-Chehabi, J. Am. Chem. Soc., *79*, 4258 (1957).
20. Tridot, G., Ann. Chim. 12e Serie, *5*, 358 (1950).
21. Gelin, R., H. Mogard and B. Nelson, Proc. 2nd Geneva Conf., *4*, 36 (1958).
22. Belle, J., (Westinghouse Atomic Power Division) Private communication (1959).
23. Harrington, C. D. and A. E. Ruehle, Nucl. Sci. Eng. Conf., Chicago (1958). Preprint 65.
24. Brater, D. C. and C. C. Littlefield, USAEC-Report TID-5453 (1956).
25. Argonne National Laboratory, USAEC-Report ANL-5466 (1955).
26. Wett, T. W. and G. W. Tompkin, Chem. Proc., *20*, 82 (1957).
27. Graigner, L., Proc. 1st Geneva Conf., *8*, 149 (1955).
28. Hawthorn, E., L. P. Shortis and J. E. Loyd, Trans. Inst. Chem. Eng., *38*, 197 (1960).
29. Goldschmidt, B. and P. Vertès, Proc. 1st Geneva Conf., *8*, 152 (1955).
30. Anonymous, Proc. 1st Geneva Conf., *8*, 156 (1955).
31. Decrop, J., M. Delange, J. Holder, H. Huet, J. Sauteron and P. Vertès, Proc. 2nd Geneva Conf., *4*, 10 (1958).
32. Hausner, H. H. and R. G. Mills, Nucleonics, *15*, (7), 94 (1957).

33. Harrington, C. D., USAEC-Report TID-7546 (Pt. 2), 369 (1957).
34. Runfors, U., N. Schönberg and R. Kiessling, Proc. 2nd Geneva Conf., *6*, 605 (958).
35. Keller, D. L., Reactor Handbook, Vol. I, Materials (Interscience Publishers, Inc., New York, 1960) p. 304.
36. Johnson, J. R., L. M. Doney, S. D. Fulkerson, A. J. Taylor, J. M. Warde and G. D. White, USAEC-Report ORNL-2011 (1956).
37. Hansen, R. S. and R. E. Minturn, Reactor Sci. Techn., *1*, 126 (1951).
38. Allen, A. L., H. A. Bernhardt, S. Bernstein, R. H. Harrison and E. W. Powell, USAEC-Report K-389 (1949).
39. Millard, W. R. and P. R. Crowley, USAEC-Report ISC-258 (1952).
40. McBain, J. W., The Sorption of Gases and Vapours by Solids (George Routledge & Sons, Ltd., London, 1932) p. 79.
41. Herdan, G., Small Particle Statistics (Elsevier Publishing Company, Amsterdam, 1953).
42. Arenberg, C. A. and P. Jahn, J. Am. Ceram. Soc., *41*, 179 (1958).
43. Traill, R. J., Am. Min., *37*, 394 (1952).
44. Rose, H. E., The Measurement of Particle Size in very fine Powders (Constable & Company., Ltd., London 1953).
45. Telle, O., Tonindustrie Zeitung, *76*, 369 (1952).
46. Telle, O., Chemie-Ingenieur-Technik, *26*, 684 (1954).
47. Hawksley, P. G. W., B.C.U.R.A. Bull., *1951*, 129.
48. Kalshoven, J., Reactor Sci. Techn., *16*, 39 (1962).
49. Gentile, P. S., L. H. Talley and T. J. Collopy, J. Inorg. Nucl. Chem., *10*, 110 (1959).
50. Shaw, W. H. R. and J. J. Bordeaux, J. Am. Chem. Soc., *77*, 4729 (1955).
51. Bullwinkel, E. P., USAEC-Report RMO-2614 (1954).
52. McLaine, L. A., E. P. Bullwinkel and J. C. Huggins, Proc. 1st Geneva Conf., *8*, 26 (1955).
53. Blake, C. A., C. F. Coleman, K. B. Brown, D. G. Hill, R. S. Lowrie and J. M. Schmitt, J. Am. Chem. Soc., *78*, 5978 (1956).
54. Sutton, J., J. Chem. Soc., (1949) S 275.
55. Elovskii, N. N. and A. J. Stabrowskii, Zhur. Neorg. Khim., *6*, 1300 (1961).
56. MacInnes, D. A. and I. G. Longsworth, USAEC-Report MDDC-911 (1942).
57. Faucherre, J., Compt. Rend., *227*, 1367 (1948).
58. Sutton, J., J. Inorg. Nucl. Chem., *1*, 68 (1955).
59. Ahrland, S., Acta Chem. Scand., *3*, 374 (1949).
60. Ahrland, S., S. Hietanen and L. G. Sillén, Acta Chem. Scand., *8*, 1907 (1954).
61. Sillén, L. G., Quaterly Reviews, *13*, 146 (1959).
62. Kraus, K. A. and F. Nelson, USAEC-Report AECD-1864 (1948).
63. Kraus, K. A., Proc. 1st Geneva Conf., *8*, 149 (1955).
64. Hearne, J. A. and A. G. White, J. Chem. Soc., *1957*, 2168.
65. McGlynn, S. P. and J. K. Smith, J. Molec. Spectr., *6*, 164 (1961).
66. Trombe, M., Compt. Rend., *216*, 888 (1943).
67. Hufferman, L., Chem. Weekblad, *48*, 441 (1952).
68. Brushilovskii, S. A., Dokl. Akad. Nauk. S.S.S.R., *120*, 305 (1958).
69. Cordfunke, E. H. P., J. Inorg. Nucl. Chem., *24*, 303 (1962).
70. Debets, P. C. and B. O. Loopstra, J. Inorg. Nucl. Chem., *25*, 945 (1963).
71. Dawson, J. K., E. Wait, K. Alcock and D. R. Chilton, J. Chem. Soc., *1956*, 3531.
72. Dembinsky, W., A. Deptula and B. Volavšek, J. Inorg. Nucl. Chem., *25*, 320 (1963).
73. Watt, G. W., W. A. Jenkins and J. M. McCuiston, J. Am. Chem. Soc., *72*, 2260 (1950).
74. Deane, A. M., UKAEA-Report AERE-R 3411 (1960).
75. Garner, E. V., J. Inorg. Nucl. Chem., *21*, 380 (1961).
76. Dell, R. M. and V. J. Wheeler, Trans. Farad. Soc., *59*, 485 (1963).
77. Schwarzmann, E. and O. Glemser, Z. Anorg. Allgem. Chem., *315*, 305 (1962).
78. Porte, A. L., H. S. Gutowsky and J. E. Boggs, J. Chem. Phys., *36*, 1695 (1962).
79. Aleksandrov, N. M. and L. P. Rodionova, Zhur. Strukt. Khim., *3*, 97 (1962).

80. Dell, R. M., (Atomic Energy Research Establishment, Harwell), Personal Communication.
81. Kersten, J. A. H., J. J. Went and J. J. van Zolingen, Proc. Int. Symp. "Power Reactor Experiments" (IAEA, Vienna, 1962), Vol. I, p. 197.
82. Kersten, J. A. H., Reactor Sci. and Techn., *16*, 15 (1962).
83. Hermans, M. E. A., J. Kalshoven, J. Kuypers, T. Markestein, Th. van der Plas, H. S. G. Slooten and R. G. Sowden, Proc. Int. Symp. "Power Reactor Experiments" (IAEA, Vienna, 1962), Vol. I, p. 225.
84. Barth, F., C. B. von der Decken, A. Claus, H. Reichel and W. R. Ruston, Proc. Int. Symp. „Power Reactor Experiments" (IAEA, Vienna, 1962), Vol. I, p. 155.
85. Nishibori, E.. R. Ueda, S. Yajima, S. Ichiba, Y. Kametnoto and Y. Shiba, Pulvermetallurgie in der Atomkerntechnik (Springer Verlag, Wien, 1962), p. 198.
86. Belle, J. and R. J. Jones, USAEC-Report WAPD-PWR-PMM 904 (1956).
87. Hermans, M. E. A. and H. S. G. Slooten, EAES Enlarged Symposium on "Reactor Materials" (Saltsjöbaden, 1959).
88. Kearsey, H. A. and F. W. van der Brugghen, Unpublished results.
89. Spruyt, A., Unpublished results.
90. Keller, K. J. and F. Schurink, Unpublished results.
91. Verkerk, B. (Reactor Centrum Nederland), Personal Communication.
92. Ainscough, J. B. and B. W. Oldfield, J. Appl. Chem., *11*, 365 (1961).
93. Verkerk, B. and G. H. Brouwer, RCN-2 (1959).

SUMMARY

The KEMA Suspension Test Reactor is intended to be an instrument in which the properties of aqueous suspensions as a nuclear fuel, can be studied. For the development of this KSTR a UO_2 powder was required with very specific properties, in order to carry out a series of nuclear experiments in a sub-critical assembly. The specifications were: a narrow particle size distribution between 4 and 13 microns, a specific surface area less than 0.1 m^2/gram, a smooth surface, a spherical shape and sufficient strength to be applied in a circulating suspension. Preferably a process without recycle should be used.

The arguments for the above specifications and a schematic description of the KEMA Suspension Test Reactor are presented in the INTRODUCTION.

In CHAPTER I the relevant literature about UO_2 preparation techniques is reviewed, both for laboratory methods and for large scale production. The conclusion of this review is that no suitable UO_2 is available commercially, nor has an adequate method to prepare this material been published.

Two methods have been developed: the urea and the sulphate process. The first method was applied to produce the required enriched fuel according to the specifications. The detailed study of this rather complex urea process is the main subject of this thesis. Special emphasis has been given to the preparation of the amorphous precipitate, which was used for the UO_2 production. The sulphate process which yields a better product, but which was developed later, is only briefly mentioned. Its chemistry is less complicated and it is based on phenomena described in CHAPTER VI.

For the near critical experiments to be carried out with the enriched UO_2 fuel, the particle size distribution is of great importance. The light extinction method was used to measure this size distribution. Its principle is explained in CHAPTER II in some detail, as well as its theoretical basis. The size of the particles is derived from a settling velocity according to Stokes law. This is well adapted to the near critical experiments, where generally the settling velocity is more important than the actual dimensions of the particles. The amorphous precipitates which are important for the KSTR all appeared to follow quite closely a geometric size distribution. A simple characterization with a mean diameter and a standard deviation is therefore possible.

The mean particle diameter of the amorphous precipitate proved to be determined by the shear stresses which occur in the system during the precipitation, more particularly at the stirrer. A linear relationship was found between the inverse of the mean particle size and either the stirring rate of a rotational, or the amplitude of a vibrational stirrer. Deviations are found at too low or too high stirrer speeds. The standard deviation of the size distribution of the final precipitate depends on the homogeneity of the mixing in the system. The mechanism by which the stirrer exerts an influence on the mean particle size is the occurrence of colloid chemical flocculation in the system and the limitation of the floc size by the shear rate of the stirrer. This mechanism is called: particle growth by controlled flocculation.

In CHAPTER III it is shown that the chemical conditions have only a slight influence on the mean particle diameter when an amorphous precipitate is formed. At the same time, however, it appeared that apart from this amorphous precipitate several crystalline products could be obtained with the urea process, by varying the chemical conditions. The most important ones are the types I and II (at low and high urea concentrations respectively) and type III (at increased nitrate ion concentrations). Those crystalline products do not contain carbon dioxide, whereas the amorphous precipitate does. The type II product contains 27% urea.

The urea acts as an ammonia donor in the process through its hydrolysis at an increased temperature and at the prevailing pH. At the same time carbon dioxide is formed which is partly incorporated in the amorphous precipitate, but which escapes from the system during the formation of any of the crystalline products. A careful analysis of the amount of carbon dioxide expelled from the system with time, provides useful information about the type of product obtained. A transition of the amorphous into a crystalline product can thus be observed during the process.

The amorphous precipitate is essentially a $UO_3 \cdot 2H_2O$ in which carbonate groups, linked to the uranyl ions are randomly incorporated, together with ammonium or ammonia, hydroxyl groups and water. The carbonate groups prevent the crystallization of the precipitate. Their presence in the precipitate is explained by the incomplete hydrolysis of an intermediate uranium-urea compound. On the same basis the formation of the type I and II products can be understood.

A rather unexpected phenomenon is discussed in CHAPTER IV. The stirring rate and the amplitude of the stirrer proved to exert a "chemical" influence on the process, apart from the above mentioned effect on the mean particle diameter. It is demonstrated that the carbon dioxide content of the liquid

depends on the intensity of the stirring. In the standard procedure, where the amorphous precipitate is obtained, the solution is supersaturated with carbon dioxide. The stirrer can lower this degree of supersaturation by bubble nucleation in a caviation-like mechanism. At this decreased carbon dioxide concentration, the crystalline products are favoured above the amorphous. Consequently, the effect of a high stirring intensity can be counterbalanced by an overpressure of carbon dioxide on the system. The variations in the carbon dioxide content of the liquid are reflected in the composition of the precipitate.

Similarly, in certain cases, an increase of the stirring intensity can be neutralized by a decrease of the temperature, which is, at the same time, an increase of the carbon dioxide content.

One of the crystalline products, the type III compound, forms during the precipitation through a sudden crystallization of initially precipitated amorphous material. Thereby the incorporated carbon dioxide is expelled from the solid. Because these phenomena are, of course, closely related with the stability of the amorphous precipitate, an attempt has been made in CHAPTER V to reveal its chemical background. Although not all experimental data could be fitted into a consistent theory, several reliable conclusions could be drawn. It is shown in this chapter, that the crystallization of the amorphous precipitate occurs during a fast decrease of the pH in the system and that the rate of precipitation increases at the same time. The moment of crystallization of the amorphous precipitate proved to be governed by the NH_4^+ concentration and by the intensity of stirring. Strong arguments were found, that, here again, the carbon dioxide content of the liquid plays an important role. However, not all data fit this hypothesis and there certainly is a parameter which has been overlooked, or which has not been kept constant enough throughout the experiments. An answer can only be derived from additional experiments.

In order to understand the decrease of the pH which was observed under certain conditions in the urea process, quite a series of experiments was carried out to study the hydrolytic behaviour of the uranyl ion at room temperature. The results of these experiments, though not directly related with the urea process, seemed to be interesting enough to present them in CHAPTER VI. It appears that the hydrolytic reactions caused by the addition of ammonia or alkali, are extremely slow. Consequently, the formation of a precipitate is retarded considerably and a decrease of the pH towards its equilibrium value is observed after the addition of ammonia or alkali. This decrease takes place in several steps, each step being accompanied by an increase of the rate of precipitation. It is shown that these observations are caused by hydrolytic phenomena.

A similar decrease of the pH has been observed under certain conditions in a slow titration of a uranyl nitrate solution with ammonia. There the decrease occurs after the appearance of a first colloidal precipitate, and it is followed by an enhanced hydrolysis. A hypothesis is presented to account for the observed phenomena, which at the same time explains similar results with other cations, reported in literature.

The influence of several important parameters on the titration curves of the uranyl ion with ammonia has been reported in this chapter. Similar influences are discussed on the equilibration of a uranyl solution after the addition of ammonia.

In CHAPTER VII the X-ray data have been collected which were obtained during the investigations of the urea process. They consist of the diagrams of the different products and of those diagrams which were found during the identification of the former ones. As a consequence of this identification work the reaction between solid $UO_3 \cdot 2H_2O$ and gaseous NH_3 was studied. A series of compounds were found and strong arguments are presented that the so called "ammonium-diuranate" is essentially a $UO_2(OH)_2$-hydrate-ammoniate, in which water can be replaced by NH_3.

In CHAPTER VIII a discussion is given in how far the initial requirements for the UO_2 fuel could be met. It is shown with the experiments carried out in the subcritical assembly and in technological systems, that important information for the development of the KSTR could be gathered with the UO_2 from the urea process. It can be considered to be a justification of the urea process as it was carried out, and of the investigations to reveal the chemistry behind it. It is argued that the investigations have a wider bearing than the KEMA Suspension Test Reactor.

SAMENVATTING

De bouw van de „KEMA Suspension Test Reactor" (KSTR) heeft ten doel de beschikking te verkrijgen over een apparaat waarin de eigenschappen van waterige suspensies als nucleaire splijtstof onderzocht kunnen worden. Voor een bepaald stadium in de ontwikkeling van deze KSTR was een UO_2 poeder nodig met zeer specifieke eigenschappen, teneinde een aantal nucleaire experimenten te kunnen uitvoeren in een nul-energie opstelling. De vereisten voor dit poeder waren een nauwe korrelverdeling tussen 4 en 13 micron, een specifiek oppervlak kleiner dan 0,1 m^2/gram, een glad korreloppervlak, bolvormige deeltjes en een voldoende sterkte om te kunnen worden rondgepompt in een waterige suspensie. De voorkeur ging uit naar een proces zonder recycle.

De argumenten voor de boven gegeven specificaties alsmede een korte beschrijving van de KSTR vormen het onderwerp van het inleidend hoofdstuk.

In HOOFDSTUK I wordt een overzicht gegeven van de literatuur betreffende bereidingsmethoden van UO_2 poeders, zowel op laboratoriumschaal als technisch. De conclusie van dit overzicht is dat geen UO_2 poeder met de vereiste kwaliteiten in de handel was, noch dat een bereidingsmethode ervoor was beschreven.

Twee methoden werden ontwikkeld, het ureum- en het sulfaatproces. Daarvan werd de eerste methode toegepast voor de produktie van de verrijkte splijtstof volgens de gegeven specificaties. Een enigszins uitgebreid onderzoek van dit vrij ingewikkelde ureumproces vormt het eigenlijke onderwerp van dit proefschrift. Daarbij is het onderzoek gericht op de bereiding van het amorfe neerslag dat werd gebruikt voor de UO_2 produktie.

Het sulfaatproces, dat eerst later werd ontwikkeld, wordt slechts zeer oppervlakkig besproken. Het levert een beter eindprodukt op. De chemie van dit proces is veel eenvoudiger en gebaseerd op een verschijnsel dat in HOOFDSTUK VI wordt beschreven.

De korrelverdeling van de verrijkte UO_2 splijtstof is van het grootste belang voor de experimenten in de nulenergie-reactor. Voor het meten van die korrelverdeling werd gebruik gemaakt van de licht-extinctie-methode. Zowel de meetmethode als de theoretische achtergrond ervan worden in HOOFD-

STUK II uitvoerig beschreven. De deeltjesgrootte wordt bepaald door toepassing van de wet van Stokes op een sedimenterend systeem. Deze methode sluit zeer goed aan bij de nulenergie-experimenten, waar, in het algemeen, de sedimentatiesnelheid van de splijtstofdeeltjes van meer belang is dan hun werkelijke afmetingen. De voor de KSTR van belang zijnde amorfe neerslagen bezitten alle een zuiver geometrische korrelverdeling. Zij kunnen daarom gekarakteriseerd worden door een geometrisch gemiddelde korrelgrootte en een geometrische standaarddeviatie.

Experimenteel bleek, dat de gemiddelde korrelgrootte van het amorfe neerslag wordt bepaald door de afschuifkrachten die gedurende de precipitatie in het systeem, en meer in het bijzonder aan de roerder, optreden. Er werd een lineair verband gevonden tussen het omgekeerde van de gemiddelde deeltjesgrootte en òf het toerental van een roterende roerder, òf de amplitude van een trilroerder. Bij zeer lage of zeer hoge toerentallen traden afwijkingen op.

De standaarddeviatie van de korrelverdeling hangt af van de homogeniteit waarmede het systeem wordt geroerd.

Het mechanisme waarmede de gemiddelde korrelgrootte door de roerder wordt bepaald, is het optreden van een colloïdchemische vlokking in het systeem en een beperking van de grootte van de ontstane vlok door de afschuifkrachten aan de roerder. Dit mechanisme werd genoemd: deeltjesgroei door gecontroleerde vlokking.

In HOOFDSTUK III wordt aangetoond dat er slechts een geringe invloed is van de chemische condities op de gemiddelde korrelgrootte bij de vorming van het amorfe neerslag. Tevens bleek dat naast dit amorfe neerslag enige kristallijne produkten verkregen konden worden met het ureumproces door de chemische condities te variëren. In dit opzicht het belangrijkst zijn de neerslagtypen I en II (respectievelijk bij een verlaagde en een verhoogde ureumconcentratie) en het type III (bij verhoogde nitraatconcentratie). In tegenstelling tot het amorfe neerslag, bevatten de kristallijne produkten geen CO_2. Bovendien bevat een neerslag van het type II 27% ureum.

In het proces vervult het ureum de taak van ammoniak-donor doordat het in het gegeven pH gebied hydrolyseert bij verhoogde temperatuur. Daarbij wordt tevens koolzuur gevormd, dat gedeeltelijk wordt ingebouwd in het amorfe neerslag, maar dat in zijn geheel wordt uitgedreven uit het systeem bij de vorming van een kristallijn produkt. Een analyse van de snelheid waarmede CO_2 uit het systeem wordt ontwikkeld biedt de mogelijkheid tot het verkrijgen van waardevolle informatie omtrent het type neerslag dat gevormd wordt. Op deze wijze kan de overgang tijdens het proces van het amorfe neerslag in een kristallijn terstond worden waargenomen.

Het amorfe neerslag bestaat in wezen uit $UO_3 \cdot 2H_2O$, waarin statistisch verdeeld carbonaatgroepen voorkomen, gebonden aan uranylgroepen, tezamen met ammonium ionen of ammoniak, hydroxylgroepen en water. Het zijn de carbonaatgroepen die de kristallisatie van het neerslag voorkomen. Hun aanwezigheid in het neerslag wordt verklaard door de onvolledige hydrolyse van een intermediaire uranium oxyde-ureum verbinding. Met hetzelfde mechanisme is de vorming van de typen I en II te verklaren.

Een nogal onverwacht verschijnsel vormt het onderwerp van HOOFDSTUK IV. Het bleek, dat het toerental of de amplitude van de gebruikte roerder, behalve het reeds genoemde effect op de gemiddelde deeltjesgrootte, nog een chemische invloed uitoefende op het proces. In dit hoofdstuk wordt aangetoond, dat het koolzuurgehalte van de vloeistof afhangt van de roerintensiteit. Bij het standaardproces, in gebruik voor de bereiding van het amorfe neerslag, is de oplossing oververzadigd aan CO_2. Door de kiemvorming van bellen met een soort cavitatieverschijnsel, kan de roerder de mate van oververzadiging verlagen. Bij een dergelijke verlaagde CO_2 concentratie wordt de vorming van kristallijne neerslagen bevorderd boven die van het amorfe. In overeenstemming met dit beeld, kan het effect van een te hoge roersnelheid gecompenseerd worden door de toepassing van een overdruk van CO_2 op het systeem. De veranderingen van het CO_2 gehalte van de vloeistof worden teruggevonden in de samenstelling van het neerslag.

Evenzo kan in bepaalde gevallen een toename van de roerintensiteit gecompenseerd worden door een afname van de temperatuur, hetgeen wederom overeenkomt met een verhoging van het CO_2 gehalte.

Een van de kristallijne produkten, het type III, ontstaat tijdens de neerslagvorming door een plotselinge kristallisatie van het aanvankelijk amorfe neerslag. Daarbij ontwijkt het in het neerslag ingebouwde CO_2. Omdat dit verschijnsel nauw samenhangt met de stabiliteit van het amorfe neerslag, wordt in HOOFDSTUK V getracht, enig inzicht te verkrijgen in de chemische achtergrond ervan. Hoewel het niet is mogen gelukken alle experimentele gegevens samen te vatten in een duidelijk beeld, kon toch een aantal duidelijke conclusies getrokken worden. In dit hoofdstuk wordt aangetoond, dat de kristallisatie van het amorfe neerslag plaats vindt tijdens een snelle daling van de pH in het systeem en dat dit samenvalt met een verhoogde neerslagsnelheid. Het blijkt, dat het tijdstip waarop de kristallisatie begint, wordt bepaald door de NH_4^+ concentratie en door de roersnelheid. Er werden sterke aanwijzingen gevonden, dat ook hier het CO_2 gehalte van de vloeistof van groot belang is. Het feit, evenwel, dat niet alle resultaten door deze hypothese gedekt kunnen worden, wijst erop dat een belangrijke parameter niet als zodanig is onderkend, of niet

voldoende constant is gehouden in de reeks van experimenten. Een definitief antwoord op deze vraag kan slechts verkregen worden na aanvullende experimenten.

Teneinde een beter inzicht te verkrijgen in de oorzaken van de pH daling, die onder bepaalde voorwaarden in het ureumproces werd waargenomen, werd een vrij uitvoerige reeks metingen uitgevoerd omtrent het hydrolytisch gedrag van het uranylion bij kamertemperatuur. Hoewel de resultaten van deze metingen geen directe relatie bleken te hebben met het ureumproces, leken zij interessant genoeg om ze in HOOFDSTUK VI te verzamelen. Het blijkt, dat de hydrolytische reacties, die door ammonia of alkali worden veroorzaakt, uiterst traag zijn. Dientengevolge wordt de vorming van neerslag aanzienlijk vertraagd, zodat een pH daling naar de evenwichtstoestand wordt waargenomen na de toevoeging van ammonia of alkali. Deze daling geschiedt in enkele stappen, waarbij iedere stap gepaard gaat met een verhoging van de neerslagsnelheid. De waargenomen verschijnselen vinden hun oorzaak in het hydrolytisch gedrag van het uranylion.

Een soortgelijke pH daling werd waargenomen bij een aantal langzame titraties van een uranylnitraatoplossing met ammonia. Daar treedt de pH daling op na het verschijnen van een eerste, colloïdaal neerslag, gevolgd door een versnelde hydrolyse. Een hypothese wordt ontwikkeld, die de waargenomen verschijnselen kan verklaren, alsmede een aantal gelijksoortige resultaten aan andere kationen, bekend uit de literatuur.

De invloed van verscheidene, belangrijke parameters op de vorm van de titratiecurven van uranylionen met ammonia wordt in dit hoofdstuk geschetst. Soortgelijke invloeden op de evenwichtsinstelling van uranyloplossingen na de toevoeging van ammonia, worden eveneens besproken.

In HOOFDSTUK VII zijn de Röntgendiffractiegegevens verzameld die werden verkregen bij de bestudering van het ureumproces. Zij omvatten de diagrammen van de verschillende produkten en de diagrammen die een rol speelden bij de pogingen om de eerstgenoemde te identificeren. Als gevolg van onderzoekingen bij deze identificatie, werd de reactie tussen vast $UO_3 \cdot 2\,H_2O$ en gasvormig NH_3 bestudeerd. Daarbij werd een reeks van nieuwe verbindingen gevonden. Tevens bleken er sterke argumenten te bestaan voor de bewering, dat het zogenaamde „ammonium diuranaat" in feite een $UO_2(OH)_2$-hydraat-ammoniakaat is, waarin water vervangen kan worden door NH_3.

In HOOFDSTUK VIII wordt onderzocht in hoeverre werd voldaan aan de eisen, gesteld aan de UO_2 splijtstof. Aangetoond wordt, dat de experimenten, die met dit UO_2 werden uitgevoerd in de nulenergiereactor en in de technologische

circuits, een belangrijke bijdrage hebben geleverd tot de ontwikkeling van de KSTR. Het hoofdstuk kan worden beschouwd, als een rechtvaardiging van het ureumproces en van het onderzoek dat eraan werd verricht. Daarbij wordt betoogd, dat deze onderzoekingen een grotere draagwijdte hebben dan alleen de KEMA Suspension Test Reactor.

CURRICULUM VITAE

De schrijver van dit proefschrift werd op 27 september 1923 te Brunssum (L.) geboren. Aan het St. Joseph College te Sittard volgde hij de eerste drie jaren van de Gymnasium-β opleiding, die werd voortgezet te Rolduc, waar hij in 1941 het eindexamen aflegde. Vervolgens studeerde hij aan de Technische Hogeschool te Delft, waar hij, met een onderbreking van zes jaren door oorlogsomstandigheden, in januari 1953 het diploma van scheikundig ingenieur behaalde. Zijn afstudeer-onderwerp, de textuur van silicagel, werd bewerkt onder leiding van Prof. Dr. J. H. DE BOER.

Sinds 1953 is hij in dienst van de N.V. KEMA te Arnhem, waar hij in de Euratom-RCN-KEMA Reactorontwikkelingsgroep medewerkt aan het Suspensie Reactor Project.

STELLINGEN

I

De kennis omtrent de invloed van procesvariabelen bij de bereiding van sinterbaar UO_2 op de textuur en de reactiviteit van dit produkt en de invloed van deze textuur en reactiviteit op het pers- en sintergedrag van tabletten is onvoldoende om een goede produktie van deze tabletten te waarborgen.

II

In verband met de verschillende mate van schadelijkheid van SO_2 en SO_3 in de lucht dient de analyse zodanig te worden uitgevoerd, dat de resultaten separaat kunnen worden opgegeven.

Vereinigung der Grosskesselbesitzer e.V., Mess- und Analysenverfahren zur Prüfung der Luftverunreinigung durch Feuerungsanlagen (Vulkan-Verlag Dr. W. Classen, Essen, 1962).

III

Met het door Kok voorgestelde elektroforese mechanisme voor de elektrische doorslag van vloeibare diëlektrika zijn snelle doorslagverschijnselen niet op bevredigende wijze te verklaren.

Kok, J. A., Electrical breakdown of insulating liquids (Philips Technical Library, 1961)
Vos, J. C. de en J. Vermeer, The International Conference on Large Electric Systems, 18th Convention, 1960 (C.I.G.R.E., Parijs, 1960) Vol. II nr. 226

IV

Het als „hindered settling" beschreven sedimentatie-verschijnsel is een bijzonder geval van thixotropie.

Orr, C. en J. M. Dallavalle, Fine particle measurement (The MacMillan Company, New York, 1959)
Mysels, K. J., Introduction to colloid chemistry (Interscience Publishers inc., New York, 1959)

V

Uit het feit dat Stouthamer bij het centrifugeren van het reactiemengsel van oliezuur en waterstof in aanwezigheid van koperoleaat, geen neerslag ver-

krijgt, kan geenszins tot de afwezigheid van colloidaal koper worden geconcludeerd.

STOUTHAMER, B., dissertatie Delft (1964)

VI

Hoewel de wereldvoorraad aan fossiele brandstoffen de toepassing van kernenergie voor elektriciteitsproduktie niet op korte termijn noodzakelijk maakt, is uitstel van de ontwikkeling van reactoren voor de produktie van kunstmatige splijtstoffen onverantwoord.

VII

De toepassing van hydrazine als corrosiebestrijder voor ijzer is aan zekere beperkingen gebonden, die onvoldoende onderkend worden.

FREIER, R. K., Der Maschinenschaden, *36*, 50 (1963).
IPENBURG, K. VAN, 3e Congrès de la Fédération Européenne de la Corrosion, Brussel, 1963 en Electrotechniek, *41*, 455 (1963)

VIII

De algemeen gebruikte grootheid MWD/ton als kwaliteitswaardering voor splijtstofelementen is slechts in beperkte mate hanteerbaar voor de economische evaluatie van de splijtstofcyclus. Daarenboven is deze grootheid misleidend bij overwegingen betreffende de grondstofsituatie van splijtstoffen.

IX

De bewering van VAN DE WEERDT, dat zijn gesulfideerde nikkelkatalysator een oppervlaktelaag van Ni_3S_2 bezit, is niet door zijn experimenten bewezen.

WEERDT, W. J. VAN DE, dissertatie Delft (1963)
COENEN, J. W. E., dissertatie Delft (1958)

X

De juistheid van de opvatting, dat bij een breuk in de bekleding van een UO_2 element in een kernreactor, gekoeld met water, nagenoeg geen verspreiding van uranium in het koelwater optreedt, kan op goede gronden in twijfel worden getrokken.

BELLE, J., Uranium dioxide: properties and nuclear applications. (Naval Reactors, Division of Reactor Development, United States Atomic Energy Commission, 1961)
SLOOTEN, H. S. G. en R. G. SOWDEN, Nature, *198*, 369 (1963)